

---

# 3 Mechanics

The mechanics of materials deal with stresses, strains, and deformations in engineering structures subjected to mechanical and thermal loads. A common assumption in the mechanics of conventional materials, such as steel and aluminum, is that they are homogeneous and isotropic continua. For a homogeneous material, properties do not depend on the location, and for an isotropic material, properties do not depend on the orientation. Unless severely cold-worked, grains in metallic materials are randomly oriented so that, on a statistical basis, the assumption of isotropy can be justified. Fiber-reinforced composites, on the other hand, are microscopically inhomogeneous and non-isotropic (orthotropic). As a result, the mechanics of fiber-reinforced composites are far more complex than that of conventional materials.

The mechanics of fiber-reinforced composite materials are studied at two levels:

1. The micromechanics level, in which the interaction of the constituent materials is examined on a microscopic scale. Equations describing the elastic and thermal characteristics of a lamina are, in general, based on micromechanics formulations. An understanding of the interaction between various constituents is also useful in delineating the failure modes in a fiber-reinforced composite material.
2. The macromechanics level, in which the response of a fiber-reinforced composite material to mechanical and thermal loads is examined on a macroscopic scale. The material is assumed to be homogeneous. Equations of orthotropic elasticity are used to calculate stresses, strains, and deflections.

In this chapter, we look into a few basic concepts as well as a number of simple working equations used in the micro- and macromechanics of fiber-reinforced composite materials. Detailed derivations of these equations are given in the references cited in the text.

### 3.1 FIBER–MATRIX INTERACTIONS IN A UNIDIRECTIONAL LAMINA

We consider the mechanics of materials approach [1] in describing fiber–matrix interactions in a unidirectional lamina owing to tensile and compressive loadings. The basic assumptions in this vastly simplified approach are as follows:

1. Fibers are uniformly distributed throughout the matrix.
2. Perfect bonding exists between the fibers and the matrix.
3. The matrix is free of voids.
4. The applied force is either parallel to or normal to the fiber direction.
5. The lamina is initially in a stress-free state (i.e., no residual stresses are present in the fibers and the matrix).
6. Both fibers and matrix behave as linearly elastic materials.

A review of other approaches to the micromechanical behavior of a composite lamina is given in Ref. [2].

#### 3.1.1 LONGITUDINAL TENSILE LOADING

In this case, the load on the composite lamina is a tensile force applied parallel to the longitudinal direction of the fibers.

##### 3.1.1.1 Unidirectional Continuous Fibers

Assuming a perfect bonding between fibers and matrix, we can write

$$\varepsilon_f = \varepsilon_m = \varepsilon_c, \quad (3.1)$$

where  $\varepsilon_f$ ,  $\varepsilon_m$ , and  $\varepsilon_c$  are the longitudinal strains in fibers, matrix, and composite, respectively (Figure 3.1).

Since both fibers and matrix are elastic, the respective longitudinal stresses can be calculated as

$$\sigma_f = E_f \varepsilon_f = E_f \varepsilon_c, \quad (3.2)$$

$$\sigma_m = E_m \varepsilon_m = E_m \varepsilon_c. \quad (3.3)$$

Comparing Equation 3.2 with Equation 3.3 and noting that  $E_f > E_m$ , we conclude that the fiber stress  $\sigma_f$  is always greater than the matrix stress  $\sigma_m$ .

The tensile force  $P_c$  applied on the composite lamina is shared by the fibers and the matrix so that

$$P_c = P_f + P_m. \quad (3.4)$$

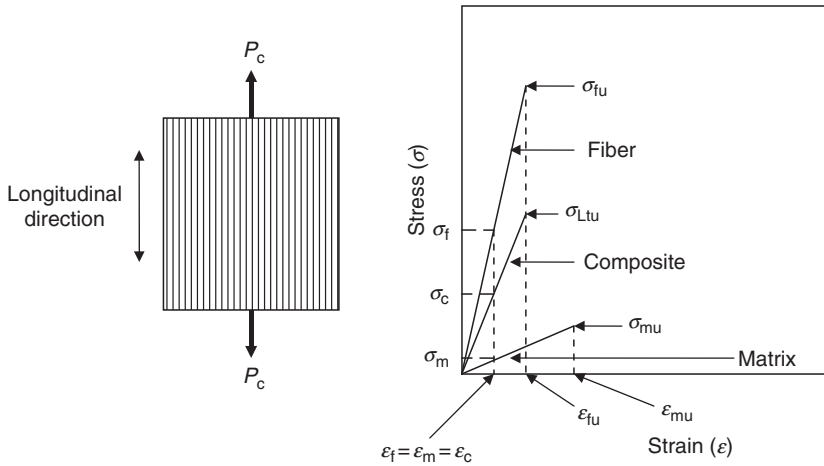


**FIGURE 3.1** Longitudinal tensile loading of a unidirectional continuous fiber lamina.

Since force = stress  $\times$  area, Equation 3.4 can be rewritten as

$$\sigma_c A_c = \sigma_f A_f + \sigma_m A_m$$

or

$$\sigma_c = \sigma_f \frac{A_f}{A_c} + \sigma_m \frac{A_m}{A_c}, \quad (3.5)$$

where

- $\sigma_c$  = average tensile stress in the composite
- $A_f$  = net cross-sectional area for the fibers
- $A_m$  = net cross-sectional area for the matrix
- $A_c = A_f + A_m$

Since  $v_f = \frac{A_f}{A_c}$  and  $v_m = (1 - v_f) = \frac{A_m}{A_c}$ , Equation 3.5 gives

$$\sigma_c = \sigma_f v_f + \sigma_m v_m = \sigma_f v_f + \sigma_m (1 - v_f). \quad (3.6)$$

Dividing both sides of Equation 3.6 by  $\epsilon_c$ , and using Equations 3.2 and 3.3, we can write the longitudinal modulus for the composite as

$$E_L = E_f v_f + E_m v_m = E_f v_f + E_m (1 - v_f) = E_m + v_f (E_f - E_m). \quad (3.7)$$

Equation 3.7 is called the *rule of mixtures*. This equation shows that the longitudinal modulus of a unidirectional continuous fiber composite is intermediate between the fiber modulus and the matrix modulus; it increases linearly with increasing fiber volume fraction; and since  $E_f > E_m$ , it is influenced more by the fiber modulus than the matrix modulus.

The fraction of load carried by fibers in longitudinal tensile loading is

$$\frac{P_f}{P_c} = \frac{\sigma_f v_f}{\sigma_f v_f + \sigma_m (1 - v_f)} = \frac{E_f v_f}{E_f v_f + E_m (1 - v_f)} \quad (3.8)$$

Equation 3.8 is plotted in Figure 3.2 as a function of  $\frac{E_f}{E_m}$  ratio and fiber volume fraction. In polymer matrix composites, the fiber modulus is much greater than the matrix modulus. In most polymer matrix composites,  $\frac{E_f}{E_m} > 10$ . Thus, even for  $v_f = 0.2$ , fibers carry  $>70\%$  of the composite load. Increasing the fiber volume fraction increases the fiber load fraction as well as the composite load. Although cylindrical fibers can be theoretically packed to almost 90% volume fraction, the practical limit is close to  $\sim 80\%$ . Over this limit, the matrix will not be able to wet the fibers.

In general, the fiber failure strain is lower than the matrix failure strain, that is,  $\epsilon_{fu} < \epsilon_{mu}$ . Assuming all fibers have the same tensile strength and the tensile rupture of fibers immediately precipitates a tensile rupture of the composite, the

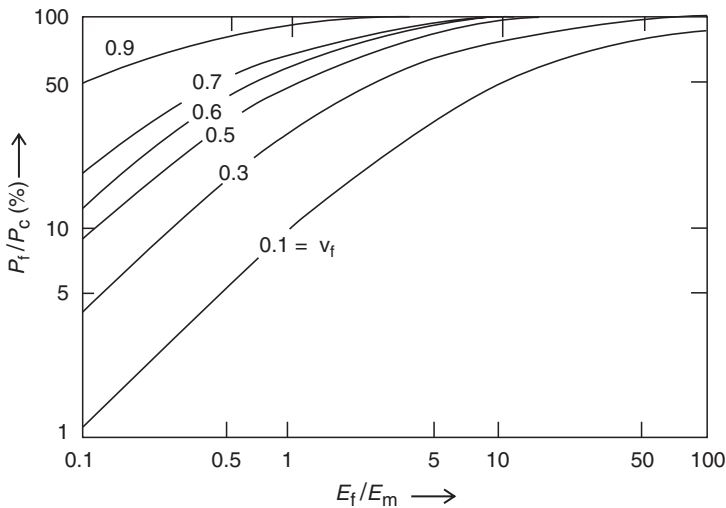


**FIGURE 3.2** Fraction of load shared by fibers in longitudinal tensile loading of a unidirectional continuous fiber lamina.

longitudinal tensile strength  $\sigma_{Ltu}$  of a unidirectional continuous fiber composite can be estimated as

$$\sigma_{Ltu} = \sigma_{fu}v_f + \sigma'_m(1 - v_f), \quad (3.9)$$

where

$\sigma_{fu}$  = fiber tensile strength (assuming a single tensile strength value for all fibers, which is not actually the case)

$\sigma'_m$  = matrix stress at the fiber failure strain, that is, at  $\epsilon_m = \epsilon_{fu}$  (Figure 3.1)

For effective reinforcement of the matrix, that is, for  $\sigma_{Ltu} > \sigma_{mu}$ , the fiber volume fraction in the composite must be greater than a critical value. This *critical fiber volume fraction* is calculated by setting  $\sigma_{Ltu} = \sigma_{mu}$ . Thus, from Equation 3.9,

$$\text{Critical } v_f = \frac{\sigma_{mu} - \sigma'_m}{\sigma_{fu} - \sigma'_m}. \quad (3.10a)$$

Equation 3.9 assumes that the matrix is unable to carry the load transferred to it after the fibers have failed, and therefore, the matrix fails immediately after the fiber failure. However, at low fiber volume fractions, it is possible that the matrix will be able to carry additional load even after the fibers have failed. For this to occur,

$$\sigma_{mu}(1 - v_f) > \sigma_{fu}v_f + \sigma'_m(1 - v_f),$$

from which the *minimum fiber volume fraction* can be calculated as

$$\text{Minimum } v_f = \frac{\sigma_{mu} - \sigma'_m}{\sigma_{mu} + \sigma_{fu} - \sigma'_m}. \quad (3.10b)$$

If the fiber volume fraction is less than the minimum value given by Equation 3.10b, the matrix will continue to carry the load even after the fibers have failed at  $\sigma_f = \sigma_{fu}$ . As the load on the composite is increased, the strain in the matrix will also increase, but some of the load will be transferred to the fibers. The fibers will continue to break into smaller and smaller lengths, and with decreasing fiber length, the average stress in the fibers will continue to decrease. Eventually, the matrix will fail when the stress in the matrix reaches  $\sigma_{mu}$ , causing the composite to fail also. The longitudinal tensile strength of the composite in this case will be  $\sigma_{mu}(1 - v_f)$ .

Figure 3.3 shows the longitudinal strength variation with fiber volume fraction for a unidirectional continuous fiber composite containing an elastic, brittle matrix. Table 3.1 shows critical fiber volume fraction and minimum fiber

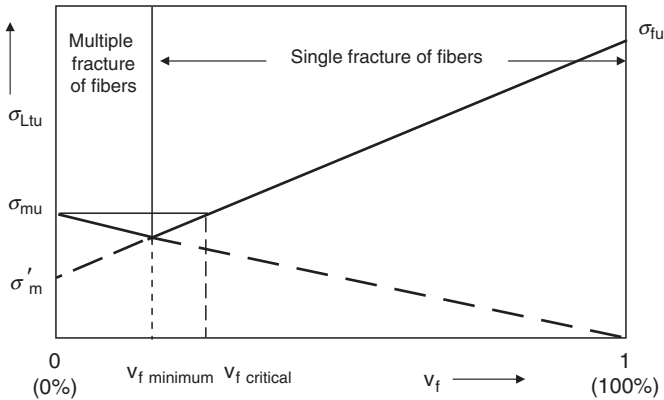


**FIGURE 3.3** Longitudinal tensile strength variation with fiber volume fraction in a unidirectional continuous fiber composite in which the matrix failure strain is greater than the fiber failure strain.

volume fraction for unidirectional continuous fiber-reinforced epoxy. For all practical applications, fiber volume fractions are much greater than these values.

There are other stresses in the fibers as well as the matrix besides the longitudinal stresses. For example, transverse stresses, both tangential and radial, may arise due to the difference in Poisson's ratios,  $\nu_f$  and  $\nu_m$ , between the fibers and matrix. If  $\nu_f < \nu_m$ , the matrix tends to contract more in the transverse directions than the fibers as the composite is loaded in tension in the longitudinal direction. This creates a radial pressure at the interface and, as a result, the matrix near the interface experiences a tensile stress in the tangential

**TABLE 3.1**  
**Critical and Minimum Fiber Volume Fractions in E-glass, Carbon, and Boron Fiber-Reinforced Epoxy Matrix<sup>a</sup> Composite**

Property	E-Glass Fiber	Carbon Fiber	Boron Fiber
$E_f$	$10 \times 10^6$ psi	$30 \times 10^6$ psi	$55 \times 10^6$ psi
$\sigma_{fu}$	250,000 psi	400,000 psi	450,000 psi
$\epsilon_{fu} = \frac{\sigma_{fu}}{E_f}$	0.025	0.0133	0.0082
$\sigma'_m = E_m \epsilon_{fu}$	2,500 psi	1,330 psi	820 psi
Critical $v_f$	3.03%	2.17%	2.04%
Minimum $v_f$	2.9%	2.12%	2%

<sup>a</sup> Matrix properties:  $\sigma_{mu} = 10,000$  psi,  $E_m = 0.1 \times 10^6$  psi, and  $\epsilon_{mu} = 0.1$ .

direction and a compressive stress in the radial direction. Tangential and radial stresses in the fibers are both compressive. However, all these stresses are relatively small compared with the longitudinal stresses.

Another source of internal stresses in the lamina is due to the difference in thermal contraction between the fibers and matrix as the lamina is cooled down from the fabrication temperature to room temperature. In general, the matrix has a higher coefficient of thermal expansion (or contraction), and, therefore, tends to contract more than the fibers, creating a “squeezing” effect on the fibers. A three-dimensional state of residual stresses is created in the fibers as well as in the matrix. These stresses can be calculated using the equations given in Appendix A.2.

### 3.1.1.2 Unidirectional Discontinuous Fibers

Tensile load applied to a discontinuous fiber lamina is transferred to the fibers by a shearing mechanism between fibers and matrix. Since the matrix has a lower modulus, the longitudinal strain in the matrix is higher than that in adjacent fibers. If a perfect bond is assumed between the two constituents, the difference in longitudinal strains creates a shear stress distribution across the fiber–matrix interface. Ignoring the stress transfer at the fiber end cross sections and the interaction between the neighboring fibers, we can calculate the normal stress distribution in a discontinuous fiber by a simple force equilibrium analysis (Figure 3.4).

Consider an infinitesimal length  $dx$  at a distance  $x$  from one of the fiber ends (Figure 3.4). The force equilibrium equation for this length is

$$\left(\frac{\pi}{4} d_f^2\right)(\sigma_f + d\sigma_f) - \left(\frac{\pi}{4} d_f^2\right)\sigma_f - (\pi d_f dx)\tau = 0,$$

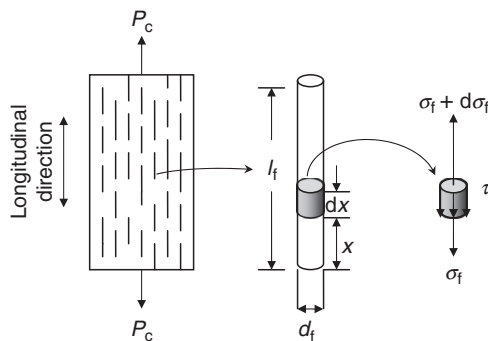


**FIGURE 3.4** Longitudinal tensile loading of a unidirectional discontinuous fiber lamina.

which on simplification gives

$$\frac{d\sigma_f}{dx} = \frac{4\tau}{d_f}, \quad (3.11)$$

where

- $\sigma_f$  = longitudinal stress in the fiber at a distance  $x$  from one of its ends
- $\tau$  = shear stress at the fiber–matrix interface
- $d_f$  = fiber diameter

Assuming no stress transfer at the fiber ends, that is,  $\sigma_f = 0$  at  $x = 0$ , and integrating Equation 3.11, we determine the longitudinal stress distribution in the fiber as

$$\sigma_f = \frac{4}{d_f} \int_0^x \tau \, dx. \quad (3.12)$$

For simple analysis, let us assume that the interfacial shear stress is constant and is equal to  $\tau_i$ . With this assumption, integration of Equation 3.12 gives

$$\sigma_f = \frac{4\tau_i}{d_f} x. \quad (3.13)$$

From Equation 3.13, it can be observed that for a composite lamina containing discontinuous fibers, the fiber stress is not uniform. According to Equation 3.13, it is zero at each end of the fiber (i.e.,  $x = 0$ ) and it increases linearly with  $x$ . The maximum fiber stress occurs at the central portion of the fiber (Figure 3.5). The maximum fiber stress that can be achieved at a given load is

$$(\sigma_f)_{\max} = 2\tau_i \frac{l_t}{d_f}, \quad (3.14)$$

where  $x = l_t/2$  = load transfer length from each fiber end. Thus, the load transfer length,  $l_t$ , is the minimum fiber length in which the maximum fiber stress is achieved.

For a given fiber diameter and fiber–matrix interfacial condition, a critical fiber length  $l_c$  is calculated from Equation 3.14 as

$$l_c = \frac{\sigma_{fu}}{2\tau_i} d_f, \quad (3.15)$$

where

- $\sigma_{fu}$  = ultimate tensile strength of the fiber
- $l_c$  = minimum fiber length required for the maximum fiber stress to be equal to the ultimate tensile strength of the fiber at its midlength (Figure 3.6b)
- $\tau_i$  = shear strength of the fiber–matrix interface or the shear strength of the matrix adjacent to the interface, whichever is less

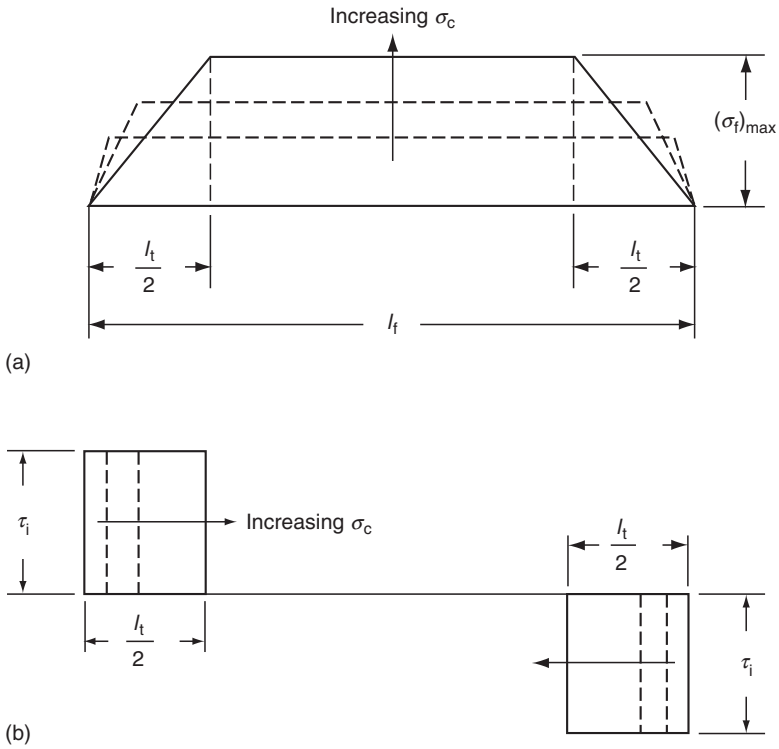


**FIGURE 3.5** Idealized (a) longitudinal stress and (b) shear stress distributions along a discontinuous fiber owing to longitudinal tensile loading.

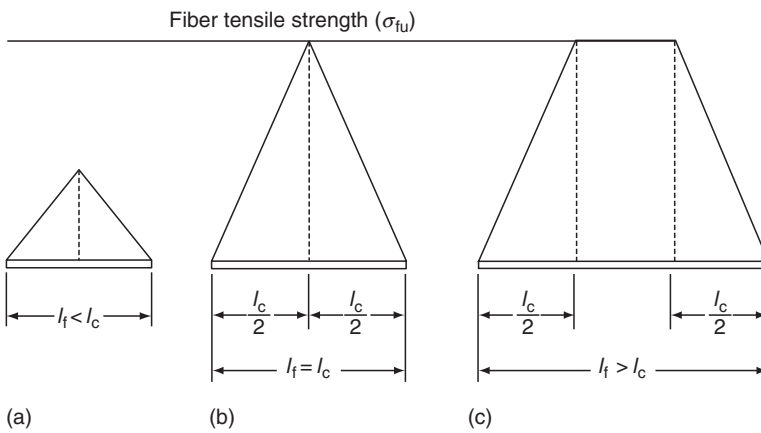


**FIGURE 3.6** Significance of critical fiber length on the longitudinal stresses of a discontinuous fiber.

From [Equations 3.14](#) and [3.15](#), we make the following observations:

1. For  $l_f < l_c$ , the maximum fiber stress may never reach the ultimate fiber strength ([Figure 3.6a](#)). In this case, either the fiber–matrix interfacial bond or the matrix may fail before fibers achieve their potential strength.
2. For  $l_f > l_c$ , the maximum fiber stress may reach the ultimate fiber strength over much of its length ([Figure 3.6c](#)). However, over a distance equal to  $l_c/2$  from each end, the fiber remains less effective.
3. For effective fiber reinforcement, that is, for using the fiber to its potential strength, one must select  $l_f \gg l_c$ .
4. For a given fiber diameter and strength,  $l_c$  can be controlled by increasing or decreasing  $\tau_i$ . For example, a matrix-compatible coupling agent may increase  $\tau_i$ , which in turn decreases  $l_c$ . If  $l_c$  can be reduced relative to  $l_f$  through proper fiber surface treatments, effective reinforcement can be achieved without changing the fiber length.

Although normal stresses near the two fiber ends, that is, at  $x < l_f/2$ , are lower than the maximum fiber stress, their contributions to the total load-carrying capacity of the fiber cannot be completely ignored. Including these end stress distributions, an average fiber stress is calculated as

$$\bar{\sigma}_f = \frac{1}{l_f} \int_0^{l_f} \sigma_f \, dx,$$

which gives

$$\bar{\sigma}_f = (\sigma_f)_{\max} \left(1 - \frac{l_t}{2l_f}\right). \quad (3.16)$$

Note that the load transfer length for  $l_f < l_c$  is  $\frac{l_f}{2}$ , whereas that for  $l_f > l_c$  is  $\frac{l_c}{2}$ .

For  $l_f > l_c$ , the longitudinal tensile strength of a unidirectional discontinuous fiber composite is calculated by substituting  $(\sigma_f)_{\max} = \sigma_{fu}$  and  $l_t = l_c$  ([Figure 3.6c](#)). Thus,

$$\begin{aligned} \sigma_{Ltu} &= \bar{\sigma}_{fu} v_f + \sigma'_m (1 - v_f) \\ &= \sigma_{fu} \left(1 - \frac{l_c}{2l_f}\right) v_f + \sigma'_m (1 - v_f). \end{aligned} \quad (3.17)$$

In [Equation 3.17](#), it is assumed that all fibers fail at the same strength level of  $\sigma_{fu}$ . Comparison of [Equations 3.9](#) and [3.17](#) shows that discontinuous fibers always strengthen a matrix to a lesser degree than continuous fibers. However,

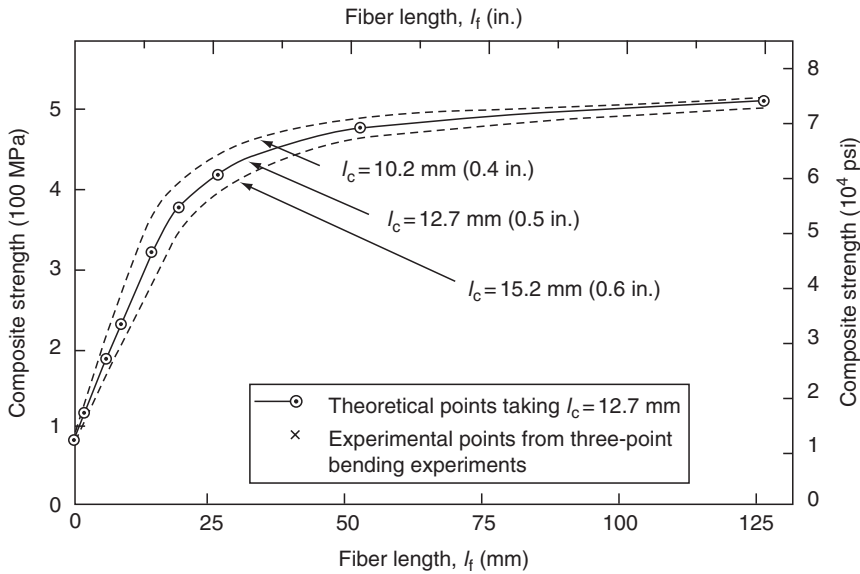


**FIGURE 3.7** Variation in the longitudinal strength of a unidirectional discontinuous fiber composite as a function of fiber length. (After Hancock, P. and Cuthbertson, R.C., *J. Mater. Sci.*, 5, 762, 1970.)

for  $l_f > 5l_c$ , strengthening greater than 90% can be achieved even with discontinuous fibers. An example is shown in Figure 3.7.

For  $l_f < l_c$ , there will be no fiber failure. Instead, the lamina fails primarily because of matrix tensile failure. Since the average tensile stress in the fiber is  $\bar{\sigma}_f = \tau_i \frac{l_f}{d_f}$ , the longitudinal tensile strength of the composite is given by

$$\sigma_{Ltu} = \tau_i \frac{l_f}{d_f} v_f + \sigma_{mu}(1 - v_f), \quad (3.18)$$

where  $\sigma_{mu}$  is the tensile strength of the matrix material.

A simple method of determining the fiber–matrix interfacial shear strength is called a single fiber fragmentation test, which is based on the observation that fibers do not break if their length is less than the critical value. In this test, a single fiber is embedded along the centerline of a matrix tensile specimen (Figure 3.8). When the specimen is tested in axial tension, the tensile stress is transferred to the fiber by shear stress at the fiber–matrix interface. The embedded fiber breaks when the maximum tensile stress in the fiber reaches its tensile strength. With increased loading, the fiber breaks into successively shorter lengths until the fragmented lengths become so short that the maximum

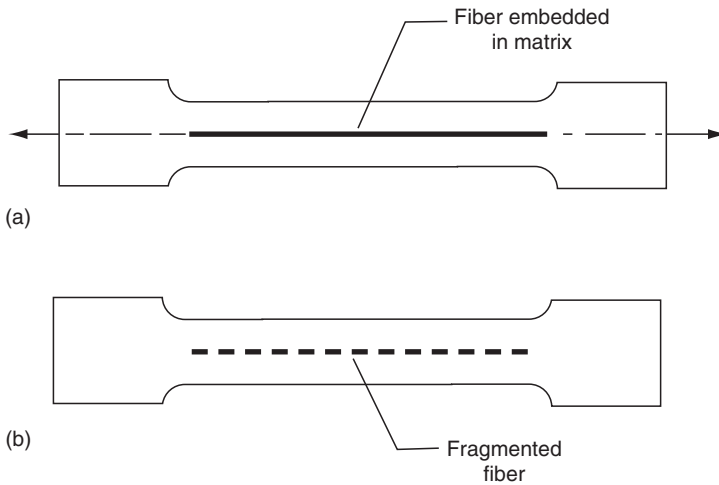


**FIGURE 3.8** Single fiber fragmentation test to determine fiber–matrix interfacial shear strength.

tensile stress can no longer reach the fiber tensile strength. The fragmented fiber lengths at this point are theoretically equal to the critical fiber length,  $l_c$ . However, actual (measured) fragment lengths vary between  $l_c/2$  and  $l_c$ . Assuming a uniform distribution for the fragment lengths and a mean value of  $\bar{l}$  equal to  $0.75l_c$ , Equation 3.15 can be used to calculate the interfacial shear strength  $\tau_{im}$  [3]:

$$\tau_{im} = \frac{3d_f\sigma_{fu}}{8\bar{l}}, \quad (3.19)$$

where  $\bar{l}$  is the mean fragment length.

Equation 3.13 was obtained assuming that the interfacial shear stress  $\tau_i$  is a constant. The analysis that followed Equation 3.13 was used to demonstrate the importance of critical fiber length in discontinuous fiber composites. However, strictly speaking, this analysis is valid only if it can be shown that  $\tau_i$  is a constant. This will be true in the case of a ductile matrix that yields due to high shear stress in the interfacial zone before the fiber–matrix bond fails and then flows plastically with little or no strain hardening (i.e., the matrix behaves as a perfectly plastic material with a constant yield strength as shown in Figure 3.9). When this occurs, the interfacial shear stress is equal to the shear yield strength of the matrix (which is approximately equal to half of its tensile yield strength) and remains constant at this value. If the fiber–matrix bond fails before matrix yielding, a frictional force may be generated at the interface, which transfers the load from the matrix to the fibers through slippage (sliding). In a polymer matrix composite, the source of this frictional force is the radial pressure on the fiber surface created by the shrinkage of the matrix as it cools down from the

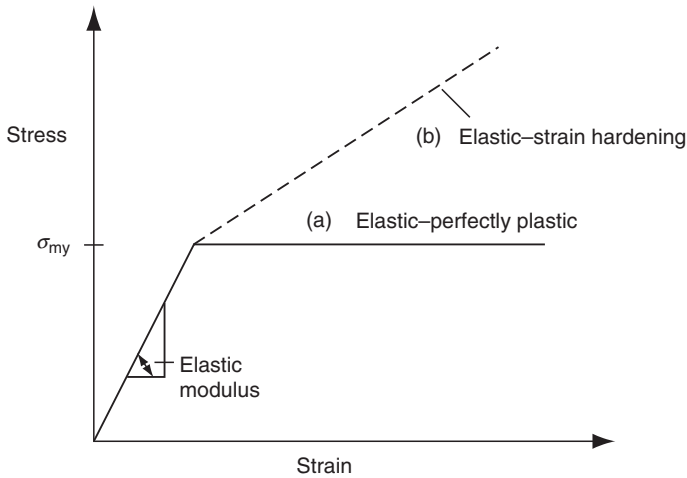


**FIGURE 3.9** Stress–strain diagrams of (a) an elastic–perfectly plastic material and (b) an elastic–strain hardening material.

curing temperature. In this case, the interfacial shear stress is equal to the product of the coefficient of sliding friction and the radial pressure.

When the matrix is in the elastic state and the fiber–matrix bond is still unbroken, the interfacial shear stress is not a constant and varies with  $x$ . Assuming that the matrix has the same strain as the composite, Cox [4] used a simple shear lag analysis to derive the following expression for the fiber stress distribution along the length of a discontinuous fiber:

$$\sigma_f = E_f \varepsilon_1 \left[ 1 - \frac{\cosh \beta \left( \frac{l_f}{2} - x \right)}{\cosh \frac{\beta l_f}{2}} \right] \text{ for } 0 \leq x \leq \frac{l_f}{2}, \quad (3.20)$$

where

$\sigma_f$  = longitudinal fiber stress at a distance  $x$  from its end

$E_f$  = fiber modulus

$\varepsilon_1$  = longitudinal strain in the composite

$$\beta = \sqrt{\frac{2G_m}{E_f r_f^2 \ln(R/r_f)}}$$

where

$G_m$  = matrix shear modulus

$r_f$  = fiber radius

$2R$  = center-to-center distance from a fiber to its nearest neighbor

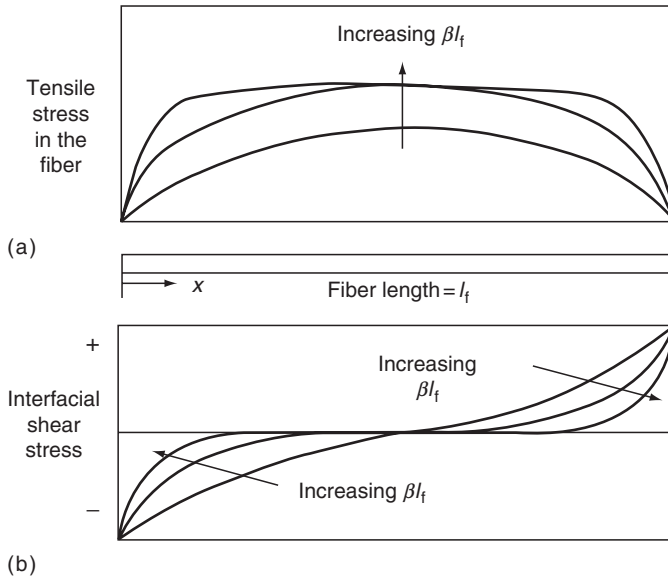


**FIGURE 3.10** (a) Normal stress distribution along the length of a discontinuous fiber according to Equation 3.20 and (b) shear stress distribution at the fiber–matrix interface according to Equation 3.21.

Using Equations 3.11 and 3.20, shear stress at the fiber–matrix interface is obtained as:

$$\tau = \frac{1}{2} E_f \varepsilon_1 \beta r_f \frac{\sinh \beta \left( \frac{l_f}{2} - x \right)}{\cosh \frac{\beta l_f}{2}}. \quad (3.21)$$

Equations 3.20 and 3.21 are plotted in Figure 3.10 for various values of  $\beta l_f$ . It shows that the fiber stress builds up over a shorter load transfer length if  $\beta l_f$  is high. This means that not only a high fiber length to diameter ratio (called the *fiber aspect ratio*) but also a high ratio of  $G_m/E_f$  is desirable for strengthening a discontinuous fiber composite.

Note that the stress distribution in Figure 3.5 or 3.10 does not take into account the interaction between fibers. Whenever a discontinuity due to fiber end occurs, a stress concentration must arise since the tensile stress normally assumed by the fiber without the discontinuity must be taken up by the surrounding fibers. As a result, the longitudinal stress distribution for each fiber may contain a number of peaks.

### EXAMPLE 3.1

A unidirectional fiber composite contains 60 vol% of HMS-4 carbon fibers in an epoxy matrix. Using the fiber properties in Table 2.1 and matrix properties as  $E_m = 3.45$  GPa and  $\sigma_{my} = 138$  MPa, determine the longitudinal tensile strength of the composite for the following cases:

1. The fibers are all continuous.
2. The fibers are 3.17 mm long and  $\tau_i$  is (i) 4.11 MPa or (ii) 41.1 MPa.

#### SOLUTION

Since HMS-4 carbon fibers are linearly elastic, their failure strain is

$$\varepsilon_{fu} = \frac{\sigma_{fu}}{E_f} = \frac{2480 \text{ MPa}}{345 \times 10^3 \text{ MPa}} = 0.0072.$$

Assuming that the matrix behaves in an elastic-perfectly plastic manner, its yield strain can be calculated as

$$\varepsilon_{my} = \frac{\sigma_{my}}{E_m} = \frac{138 \text{ MPa}}{3.45 \times 10^3 \text{ MPa}} = 0.04.$$

Thus, the fibers are expected to break before the matrix yields and the stress in the matrix at the instance of fiber failure is

$$\sigma'_m = E_m \varepsilon_{fu} = (3.45 \times 10^3 \text{ MPa})(0.0072) = 24.84 \text{ MPa}.$$

1. Using Equation 3.9, we get

$$\begin{aligned}\sigma_{Ltu} &= (2480)(0.6) + (24.84)(1 - 0.6) \\ &= 1488 + 9.94 = 1497.94 \text{ MPa}.\end{aligned}$$

2. (i) When  $\tau_i = 4.11$  MPa, the critical fiber length is

$$l_c = \frac{2480 \text{ MPa}}{(2)(4.11 \text{ MPa})}(8 \times 10^{-3} \text{ mm}) = 2.414 \text{ mm}.$$

Since  $l_f > l_c$ , we can use Equation 3.17 to calculate

$$\begin{aligned}\sigma_{Ltu} &= (2480) \left[ 1 - \frac{2.414}{(2)(3.17)} \right] (0.6) + (24.84)(1 - 0.6) \\ &= 921.43 + 9.94 = 931.37 \text{ MPa}.\end{aligned}$$

- (ii) When  $\tau_i = 41.1$  MPa,  $l_c = 0.2414$  mm. Thus,  $l_f > l_c$ .

Equation 3.17 now gives  $\sigma_{Ltu} = 1441.28$  MPa.

This example demonstrates that with the same fiber length, it is possible to achieve a high longitudinal tensile strength for the composite by increasing the interfacial shear stress. Physically, this means that the bonding between the fibers and the matrix must be improved.

### 3.1.1.3 Microfailure Modes in Longitudinal Tension

In deriving Equations 3.9 and 3.17, it was assumed that all fibers have equal strength and the composite lamina fails immediately after fiber failure. In practice, fiber strength is not a unique value; instead it follows a statistical distribution. Therefore, it is expected that a few fibers will break at low stress levels. Although the remaining fibers will carry higher stresses, they may not fail simultaneously.

When a fiber breaks (Figure 3.11), the normal stress at each of its broken ends becomes zero. However, over a distance of  $l_c/2$  from each end, the stress builds back up to the average value by shear stress transfer at the fiber–matrix interface (Figure 3.11c). Additionally, the stress states in a region close to the broken ends contain

1. Stress concentrations at the void created by the broken fiber
2. High shear stress concentrations in the matrix near the fiber ends
3. An increase in the average normal stress in adjacent fibers (Figure 3.11b)

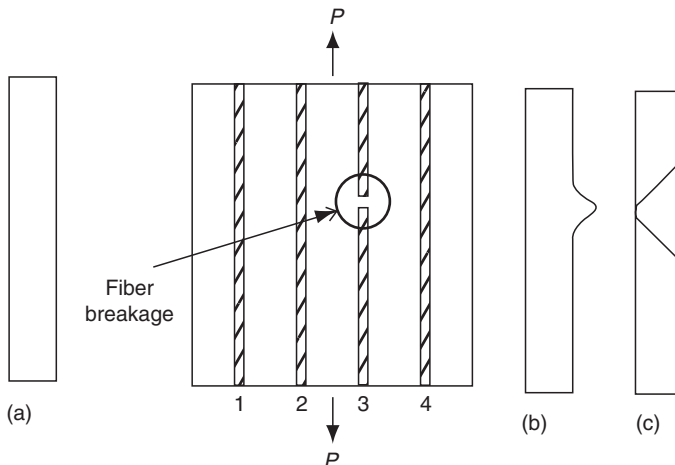


**FIGURE 3.11** Longitudinal stress distributions (a) in unidirectional continuous fibers before the failure of fiber 3, (b) in fibers 2 and 4 after the failure of fiber 3, and (c) in fiber 3 after it fails.

Owing to these local stress magnifications, possibilities for several microfailure modes exist:

1. Partial or total debonding of the broken fiber from the surrounding matrix due to high interfacial shear stresses at its ends. As a result, the fiber effectiveness is reduced either completely or over a substantial length (Figure 3.12a).
2. Initiation of a microcrack in the matrix due to high stress concentration at the ends of the void (Figure 3.12b).

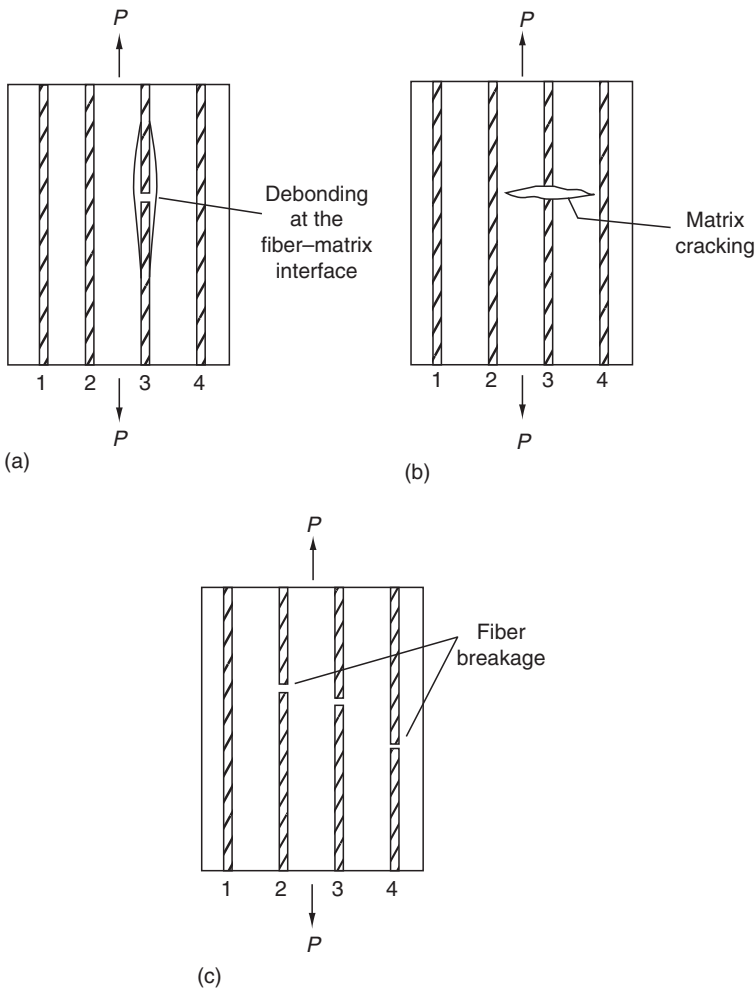


**FIGURE 3.12** Possible microfailure modes following the breakage of fiber 3.

3. Plastic deformation (microyielding) in the matrix, particularly if the matrix is ductile.
4. Failure of other fibers in the vicinity of the first fiber break due to high average normal stresses and the local stress concentrations (Figure 3.12c). Each fiber break creates additional stress concentrations in the matrix as well as in other fibers. Eventually, many of these fiber breaks and the surrounding matrix microcracks may join to form a long microcrack in the lamina.

The presence of longitudinal stress ( $\sigma_{yy}$ ) concentration at the tip of an advancing crack is well known. Cook and Gordon [5] have shown that the stress components  $\sigma_{xx}$  and  $\tau_{xy}$  may also reach high values slightly ahead of the crack tip (Figure 3.13a). Depending on the fiber–matrix interfacial strength, these stress components are capable of debonding the fibers from the surrounding matrix even before they fail in tension (Figure 3.13b). Fiber–matrix debonding ahead of the crack tip has the effect of blunting the crack front and reducing the notch sensitivity of the material. High fiber strength and low interfacial strength promote debonding over fiber tensile failure.

With increasing load, fibers continue to break randomly at various locations in the lamina. Because of the statistical distribution of surface flaws, the

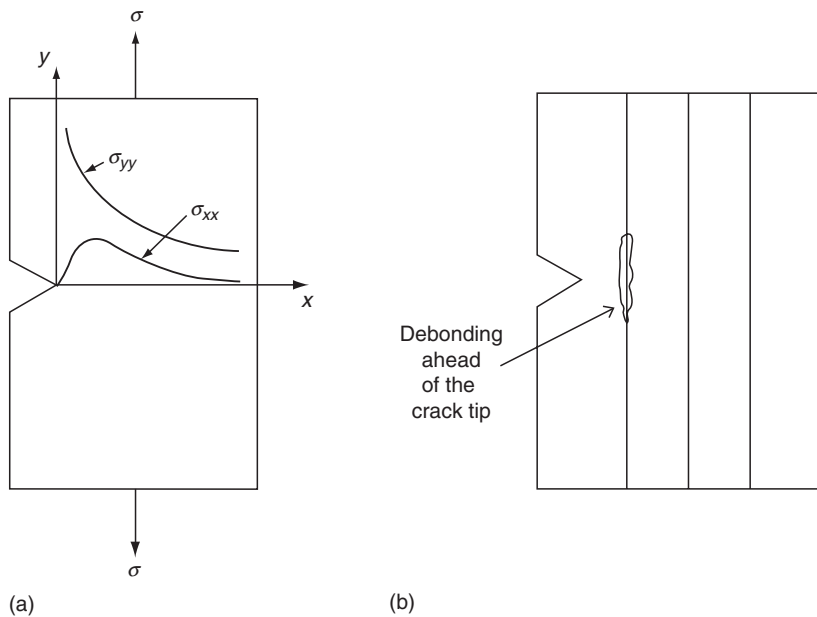


**FIGURE 3.13** Schematic representation of (a) normal stress distributions and (b) fiber–matrix debonding ahead of a crack tip.

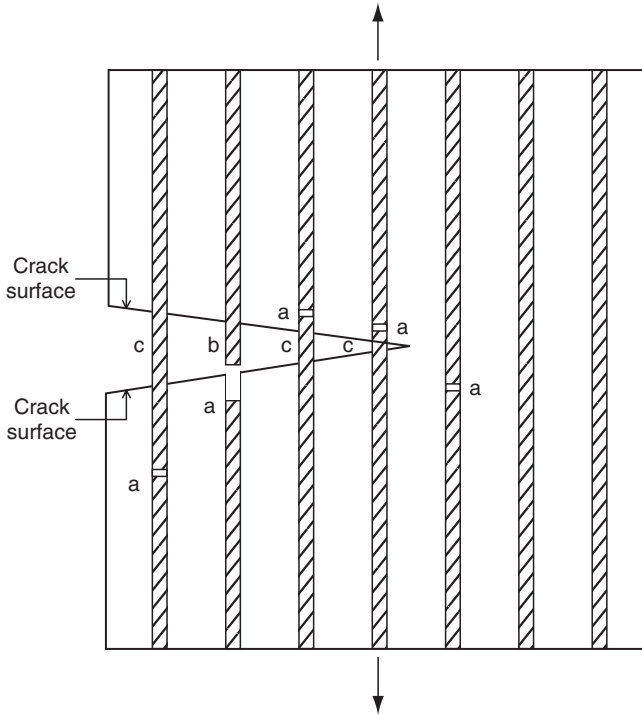


**FIGURE 3.14** Schematic representation of fiber pullout and matrix bridging by broken fibers (a) fiber breakage; (b) fiber pullout; and (c) matrix bridging.

fiber failure does not always occur in the crack plane (Figure 3.14). Therefore, the opening of the matrix crack may cause broken fibers to pull out from the surrounding matrix (Figure 3.15), which is resisted by the friction at the fiber–matrix interface. If the interfacial strength is high or the broken fiber lengths are greater than  $l_c/2$ , the fiber pullout is preceded by either debonding or fiber failure even behind the crack front. Thus, broken fibers act as a bridge between the two faces of the matrix crack. In some instances, multiple parallel cracks are formed in the matrix normal to the fiber direction. If these cracks are bridged by fibers, the volume of matrix between the cracks may deform significantly before rupture.

Fracture toughness of a unidirectional  $0^\circ$  lamina is the sum of the energies consumed by various microfailure processes, namely, fiber fracture, matrix cracking or yielding, debonding, and fiber pullout. Theoretical models to calculate the energy contributions from some of these failure modes are given in Table 3.2. Although the true nature of the fracture process and stress fields are not known, these models can serve to recognize the variables that play



**FIGURE 3.15** Fracture surface of a randomly oriented discontinuous fiber composite showing the evidence of fiber pullout.

major roles in the development of high fracture toughness for a fiber-reinforced composite lamina. It should be noted that energy contributions from the fracturing of brittle fibers and a brittle matrix are negligible (<10%) compared with those listed in [Table 3.2](#).

### 3.1.2 TRANSVERSE TENSILE LOADING

When a transverse tensile load is applied to the lamina, the fibers act as hard inclusions in the matrix instead of the principal load-carrying members. Although the matrix modulus is increased by the presence of fibers, local stresses and strains in the surrounding matrix are higher than the applied stress. [Figure 3.16b](#) shows the variation of radial stress ( $\sigma_{rr}$ ) and tangential stress ( $\sigma_{\theta\theta}$ ) in a lamina containing a single cylindrical fiber. Near the fiber–matrix interface, the radial stress is tensile and is nearly 50% higher than the applied stress. Because of this radial stress component, cracks normal to the loading direction

---

**TABLE 3.2**  
**Important Energy Absorption Mechanisms During Longitudinal Tensile Loading of a Unidirectional Continuous Fiber Lamina**

Stress relaxation energy (energy dissipated owing to reduction in stresses at the ends of a broken fiber [6])	$E_r = \frac{v_f \sigma_{fu}^2 l_c}{6E_f}$
Stored elastic energy in a partially debonded fiber [7]	$E_s = \frac{v_f \sigma_{fu}^2 y}{4E_f} \text{ (where } y = \text{debonded length of the fiber when it breaks)}$
Fiber pullout energy [8]	$E_{po} = \frac{v_f \sigma_{fu} l_c^2}{12l_f} \text{ for } l_f > l_c$ $= \frac{v_f \sigma_{fu} l_f^2}{12l_c} \text{ for } l_f < l_c$
Energy absorption by matrix deformation between parallel matrix cracks [9]	$E_{md} = \frac{(1 - v_f)^2}{v_f} \left( \frac{\sigma_{mu} d_f}{4\tau_i} \right) U_m$ (where $U_m$ = energy required in deforming unit volume of the matrix to rupture)

*Notes:*

1. All energy expressions are on the basis of unit fracture surface area.
  2. Debonding of fibers ahead of a crack tip or behind a crack tip is an important energy absorption mechanism. However, no suitable energy expression is available for this mechanism.
  3. Energy absorption may also occur because of yielding of fibers or matrix if either of these constituents is ductile in nature.
- 

may develop either at the fiber–matrix interface or in the matrix at  $\theta = 90^\circ$  (Figure 3.16c).

In a lamina containing a high volume fraction of fibers, there will be interactions of stress fields from neighboring fibers. Adams and Doner [10] used a finite difference method to calculate the stresses in unidirectional composites under transverse loading. A rectangular packing arrangement of parallel fibers was assumed, and solutions were obtained for various interfiber spacings representing different fiber volume fractions. Radial stresses at the fiber–matrix interface for 55% and 75% fiber volume fractions are shown in Figure 3.17. The maximum principal stress increases with increasing  $E_f/E_m$  ratio and fiber volume fraction, as indicated in Figure 3.18. The transverse modulus of the composite has a similar trend. Although an increased transverse modulus is desirable in many applications, an increase in local stress concentrations at high volume fractions and high fiber modulus may reduce the transverse strength of the composite (Table 3.3).

The simplest model used for deriving the equation for the transverse modulus of a unidirectional continuous fiber-reinforced composite is shown in Figure 3.19

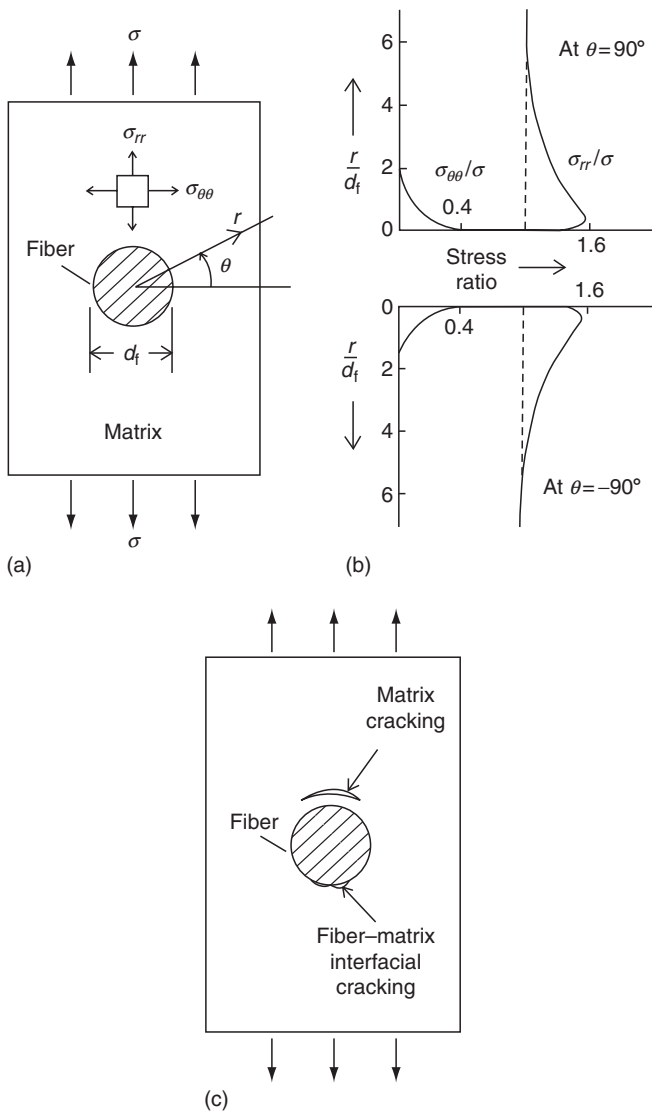


**FIGURE 3.16** (a) Transverse tensile loading on a lamina containing a single cylindrical fiber, (b) stress distribution around a single fiber due to transverse tensile loading, and (c) possible microfailure modes.

in which the fibers and the matrix are replaced by their respective “equivalent” volumes and are depicted as two structural elements (slabs) with strong bonding across their interface. The tensile load is acting normal to the fiber direction. The other assumptions made in this simple slab model are as follows.

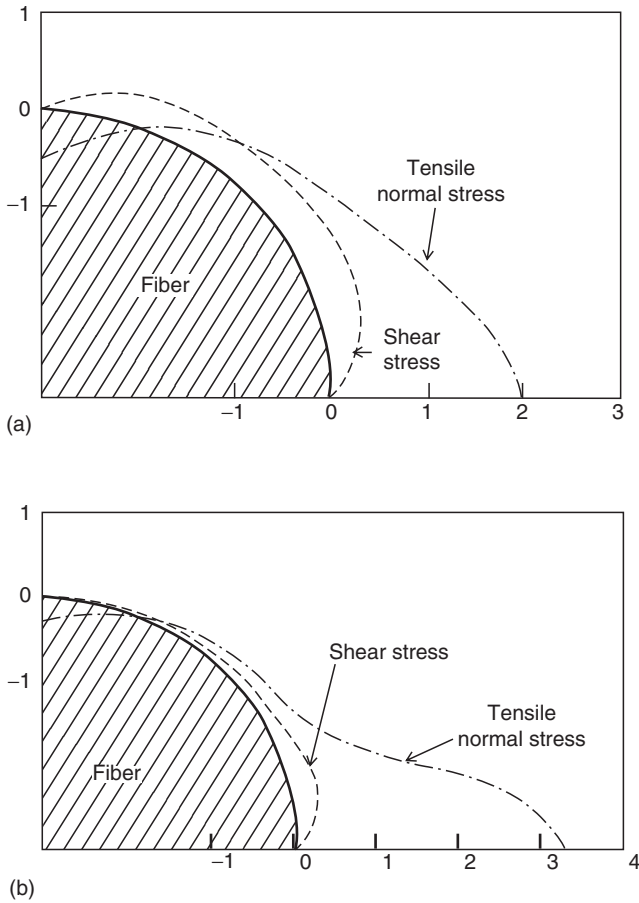


**FIGURE 3.17** Variation of shear stress  $\tau_{r\theta}$  and normal stress  $\sigma_{rr}$  at the surface of a circular fiber in a square array subjected to an average tensile stress  $\sigma$  transverse to the fiber directions: (a)  $v_f = 55\%$  and (b)  $v_f = 75\%$ . (After Adams, D.F. and Doner, D.R., *J. Compos. Mater.*, 1, 152, 1967.)

1. Total deformation in the transverse direction is the sum of the total fiber deformation and the total matrix deformation, that is,  $\Delta W_c = \Delta W_f + \Delta W_m$ .
2. Tensile stress in the fibers and the tensile stress in the matrix are both equal to the tensile stress in the composite, that is,  $\sigma_f = \sigma_m = \sigma_c$ .

Since  $\varepsilon_c = \frac{\Delta W_c}{W_c}$ ,  $\varepsilon_f = \frac{\Delta W_f}{W_f}$ , and  $\varepsilon_m = \frac{\Delta W_m}{W_m}$ , the deformation equation  $\Delta W_c = \Delta W_f + \Delta W_m$  can be written as

$$\varepsilon_c W_c = \varepsilon_f W_f + \varepsilon_m W_m. \quad (3.22)$$

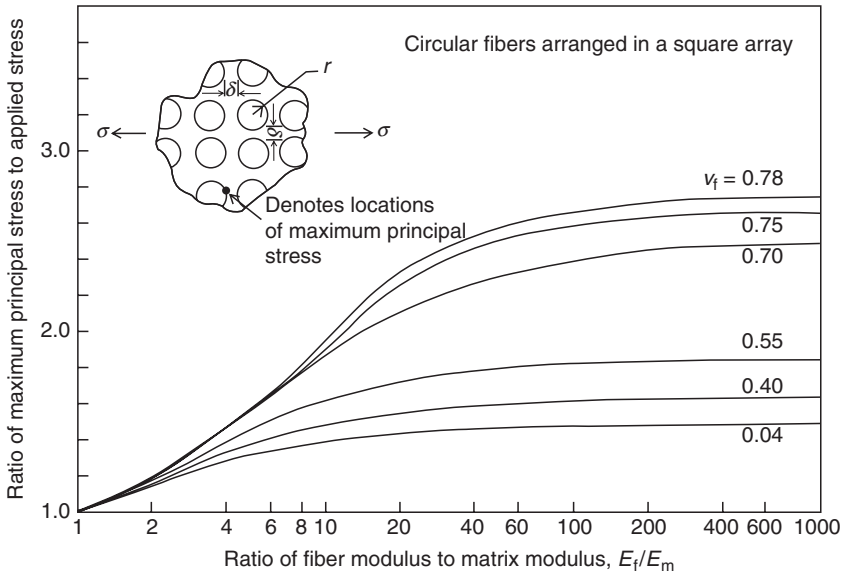


**FIGURE 3.18** Ratio of the maximum principal stress in the matrix to the applied transverse stress on the composite for various fiber volume fractions. (After Adams, D.F. and Doner, D.R., *J. Compos. Mater.*, 1, 152, 1967.)

**TABLE 3.3**  
**Effect of Transverse Loading in a Unidirectional Composite**

Composite Material	$\frac{E_f}{E_m}$	$v_f$ (%)	Transverse Modulus, GPa (Msi)	Transverse Strength, MPa (ksi)
E-glass-epoxy	20	39	8.61 (1.25)	47.2 (6.85)
		67	18.89 (2.74)	30.87 (4.48)
E-glass-epoxy	24	46	8.96 (1.30)	69.1 (10.03)
		57	13.23 (1.92)	77.92 (11.31)
		68	21.91 (3.18)	67.93 (9.86)
		73	25.9 (3.76)	41.27 (5.99)
Boron-epoxy	120	65	23.43 (3.4)	41.96 (6.09)

Source: Adapted from Adams, D.F. and Doner, D.R., *J. Compos. Mater.*, 1, 152, 1967.

Dividing both sides by  $W_c$  and noting that  $\frac{W_f}{W_c} = v_f$  and  $\frac{W_m}{W_c} = v_m$ , we can rewrite Equation 3.22 as

$$\varepsilon_c = \varepsilon_f v_f + \varepsilon_m v_m. \quad (3.23)$$

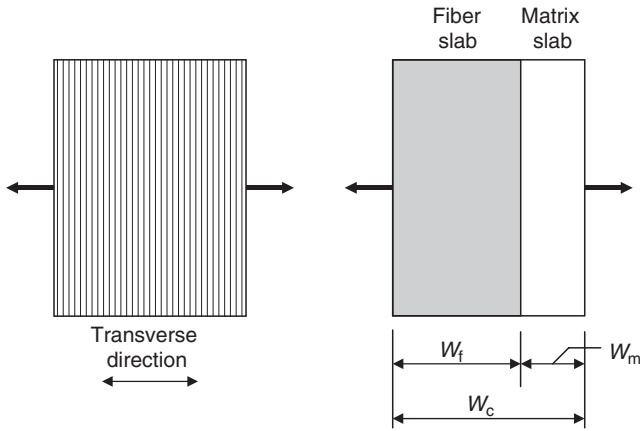


**FIGURE 3.19** Transverse loading of a unidirectional continuous fiber lamina and the equivalent slab model.

Since  $\varepsilon_c = \frac{\sigma_c}{E_T}$ ,  $\varepsilon_f = \frac{\sigma_f}{E_f}$ , and  $\varepsilon_m = \frac{\sigma_m}{E_m}$ , Equation 3.23 can be written as

$$\frac{\sigma_c}{E_T} = \frac{\sigma_f}{E_f} v_f + \frac{\sigma_m}{E_m} v_m. \quad (3.24)$$

In Equation 3.24,  $E_T$  is the transverse modulus of the unidirectional continuous fiber composite.

Finally, since it is assumed that  $\sigma_f = \sigma_m = \sigma_c$ , Equation 3.24 becomes

$$\frac{1}{E_T} = \frac{v_f}{E_f} + \frac{v_m}{E_m}. \quad (3.25)$$

Rearranging Equation 3.25, the expression for the transverse modulus  $E_T$  becomes

$$E_T = \frac{E_f E_m}{E_f v_m + E_m v_f} = \frac{E_f E_m}{E_f - v_f (E_f - E_m)}. \quad (3.26)$$

Equation 3.26 shows that the transverse modulus increases nonlinearly with increasing fiber volume fraction. By comparing Equations 3.7 and 3.26, it can be seen that the transverse modulus is lower than the longitudinal modulus and is influenced more by the matrix modulus than by the fiber modulus.

A simple equation for predicting the transverse tensile strength of a unidirectional continuous fiber lamina [11] is

$$\sigma_{Ttu} = \frac{\sigma_{mu}}{K_\sigma}, \quad (3.27)$$

where

$$K_{\sigma} = \frac{1 - v_f[1 - (E_m/E_f)]}{1 - (4v_f/\pi)^{1/2}[1 - (E_m/E_f)]}$$

Equation 3.27 assumes that the transverse tensile strength of the composite is limited by the ultimate tensile strength of the matrix. Note that  $K_{\sigma}$  represents the maximum stress concentration in the matrix in which fibers are arranged in a square array. The transverse tensile strength values predicted by Equation 3.27 are found to be in reasonable agreement with those predicted by the finite difference method for fiber volume fractions <60% [2]. Equation 3.27 predicts that for a given matrix, the transverse tensile strength decreases with increasing fiber modulus as well as increasing fiber volume fraction.

### 3.1.3 LONGITUDINAL COMPRESSIVE LOADING

An important function of the matrix in a fiber-reinforced composite material is to provide lateral support and stability for fibers under longitudinal compressive loading. In polymer matrix composites in which the matrix modulus is relatively low compared with the fiber modulus, failure in longitudinal compression is often initiated by localized buckling of fibers. Depending on whether the matrix behaves in an elastic manner or shows plastic deformation, two different localized buckling modes are observed: *elastic microbuckling* and *fiber kinking*.

Rosen [12] considered two possible elastic microbuckling modes of fibers in an elastic matrix as demonstrated in Figure 3.20. The extensional mode of

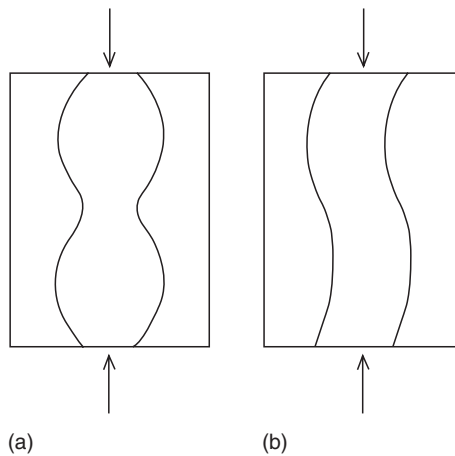


**FIGURE 3.20** Fiber microbuckling modes in a unidirectional continuous fiber composite under longitudinal compressive loading: (a) extensional mode and (b) shear mode.

microbuckling occurs at low fiber volume fractions ( $v_f < 0.2$ ) and creates an extensional strain in the matrix because of out-of-phase buckling of fibers. The shear mode of microbuckling occurs at high fiber volume fractions and creates a shear strain in the matrix because of in-phase buckling of fibers. Using buckling theory for columns in an elastic foundation, Rosen [12] predicted the compressive strengths in extensional mode and shear mode as

$$\text{Extensional mode: } \sigma_{\text{Lcu}} = 2v_f \left( \frac{v_f E_m E_f}{3(1 - v_f)} \right)^{1/2}, \quad (3.28a)$$

$$\text{Shear mode: } \sigma_{\text{Lcu}} = \frac{G_m}{(1 - v_f)}, \quad (3.28b)$$

where

$G_m$  is the matrix shear modulus

$v_f$  is the fiber volume fraction

Since most fiber-reinforced composites contain fiber volume fraction  $>30\%$ , the shear mode is more important than the extensional mode. As Equation 3.28b shows, the shear mode is controlled by the matrix shear modulus as well as fiber volume fraction. The measured longitudinal compressive strengths are generally found to be lower than the theoretical values calculated from Equation 3.28b. Some experimental data suggest that the longitudinal compressive strength follows a rule of mixtures prediction similar to Equation 3.9.

The second important failure mode in longitudinal compressive loading is fiber kinking, which occurs in highly localized areas in which the fibers are initially slightly misaligned from the direction of the compressive loading. Fiber bundles in these areas rotate or tilt by an additional angle from their initial configuration to form kink bands and the surrounding matrix undergoes large shearing deformation (Figure 3.21). Experiments conducted on glass and carbon fiber-reinforced composites show the presence of fiber breakage at the ends of kink bands [13]; however, whether fiber breakage precedes or follows the kink band formation has not been experimentally verified. Assuming an elastic-perfectly plastic shear stress–shear strain relationship for the matrix, Budiansky and Fleck [14] have determined the stress at which kinking is initiated as

$$\sigma_{\text{ck}} = \frac{\tau_{\text{my}}}{\varphi + \gamma_{\text{my}}}, \quad (3.29)$$

where

$\tau_{\text{my}}$  = shear yield strength of the matrix

$\gamma_{\text{my}}$  = shear yield strain of the matrix

$\varphi$  = initial angle of fiber misalignment

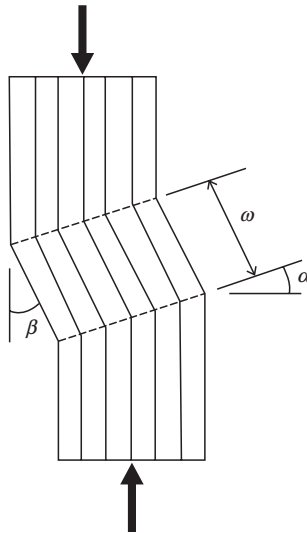


**FIGURE 3.21** Kink band geometry.  $\alpha$  = Kink band angle,  $\beta$  = Fiber tilt angle, and  $\omega$  = Kink band width.

Besides fiber microbuckling and fiber kinking, a number of other failure modes have also been observed in longitudinal compressive loading of unidirectional continuous fiber-reinforced composites. They include shear failure of the composite, compressive failure or yielding of the reinforcement, longitudinal splitting in the matrix due to Poisson's ratio effect, matrix yielding, interfacial debonding, and fiber splitting or fibrillation (in Kevlar 49 composites). Factors that appear to improve the longitudinal compressive strength of unidirectional composites are increasing values of the matrix shear modulus, fiber tensile modulus, fiber diameter, matrix ultimate strain, and fiber–matrix interfacial strength. Fiber misalignment or bowing, on the other hand, tends to reduce the longitudinal compressive strength.

### 3.1.4 TRANSVERSE COMPRESSIVE LOADING

In transverse compressive loading, the compressive load is applied normal to the fiber direction, and the most common failure mode observed is the matrix shear failure along planes that are parallel to the fiber direction, but inclined to the loading direction (Figure 3.22). The failure is initiated by fiber–matrix debonding. The transverse compressive modulus and strength are considerably lower than the longitudinal compressive modulus and strength. The transverse compressive modulus is higher than the matrix modulus and is close to the transverse tensile modulus. The transverse compressive strength is found to be nearly independent of fiber volume fraction [15].

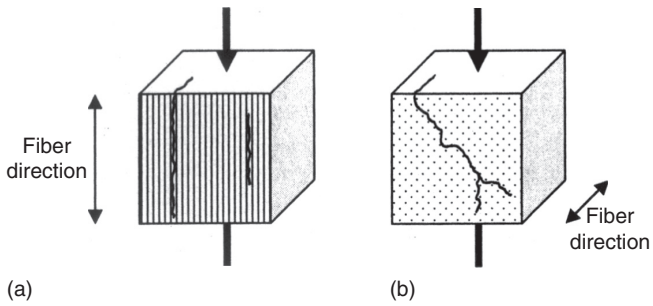


**FIGURE 3.22** Shear failure (a) in longitudinal compression (compressive load parallel to the fiber direction) and (b) in transverse compression (compressive load normal to the fiber direction).

## 3.2 CHARACTERISTICS OF A FIBER-REINFORCED LAMINA

### 3.2.1 FUNDAMENTALS

#### 3.2.1.1 Coordinate Axes

Consider a thin lamina in which fibers are positioned parallel to each other in a matrix, as shown in Figure 3.23. To describe its elastic properties, we first define two right-handed coordinate systems, namely, the 1-2- $z$  system and the

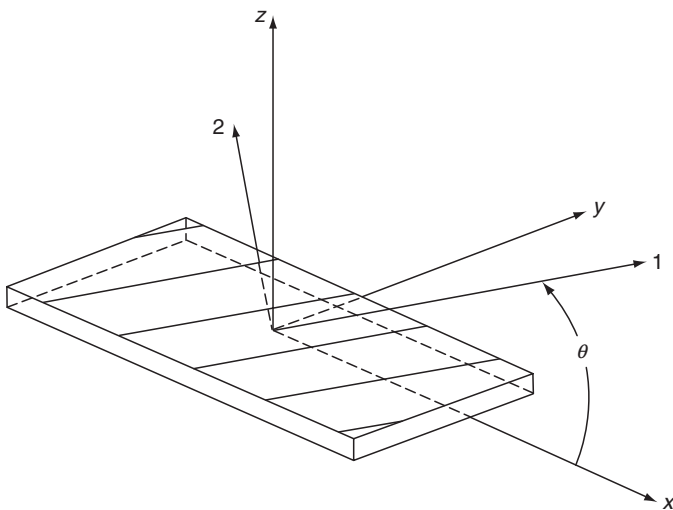


**FIGURE 3.23** Definition of principal material axes and loading axes for a lamina.

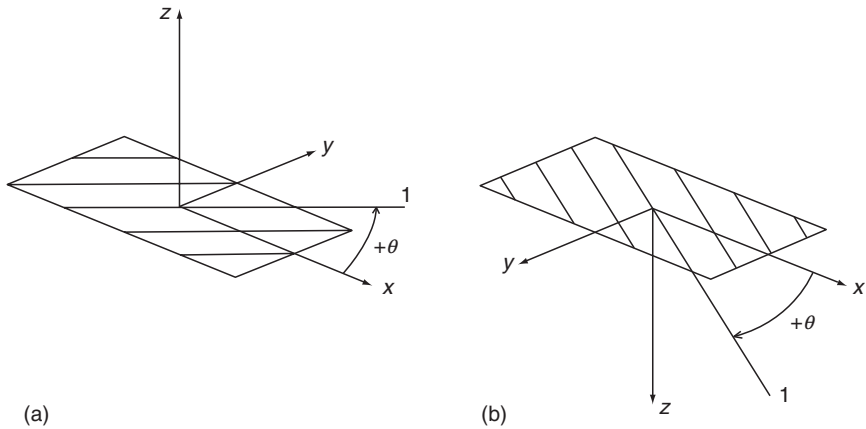


**FIGURE 3.24** Right-handed coordinate systems. Note the difference in fiber orientation in (a) and (b).

$x$ - $y$ - $z$  system. Both 1-2 and  $x$ - $y$  axes are in the plane of the lamina, and the  $z$  axis is normal to this plane. In the 1-2- $z$  system, axis 1 is along the fiber length and represents the longitudinal direction of the lamina, and axis 2 is normal to the fiber length and represents the transverse direction of the lamina. Together they constitute the *principal material directions* in the plane of the lamina. In the  $xyz$  system,  $x$  and  $y$  axes represent the *loading directions*.

The angle between the positive  $x$  axis and the 1-axis is called the *fiber orientation angle* and is represented by  $\theta$ . The sign of this angle depends on the right-handed coordinate system selected. If the  $z$  axis is vertically upward to the lamina plane,  $\theta$  is positive when measured counterclockwise from the positive  $x$  axis (Figure 3.24a). On the other hand, if the  $z$  axis is vertically downward,  $\theta$  is positive when measured clockwise from the positive  $x$  axis (Figure 3.24b). In a  $0^\circ$  lamina, the principal material axis 1 coincides with the loading axis  $x$ , but in a  $90^\circ$  lamina, the principal material axis 1 is at a  $90^\circ$  angle with the loading axis  $x$ .

### 3.2.1.2 Notations

Fiber and matrix properties are denoted by subscripts  $f$  and  $m$ , respectively. Lamina properties, such as tensile modulus, Poisson's ratio, and shear modulus, are denoted by two subscripts. The first subscript represents the loading direction, and the second subscript represents the direction in which the particular property is measured. For example,  $\nu_{12}$  represents the ratio of strain in direction 2 to the applied strain in direction 1, and  $\nu_{21}$  represents the ratio of strain in direction 1 to the applied strain in direction 2.

Stresses and strains are also denoted with double subscripts (Figure 3.25). The first of these subscripts represents the direction of the outward normal to the plane in which the stress component acts. The second subscript represents

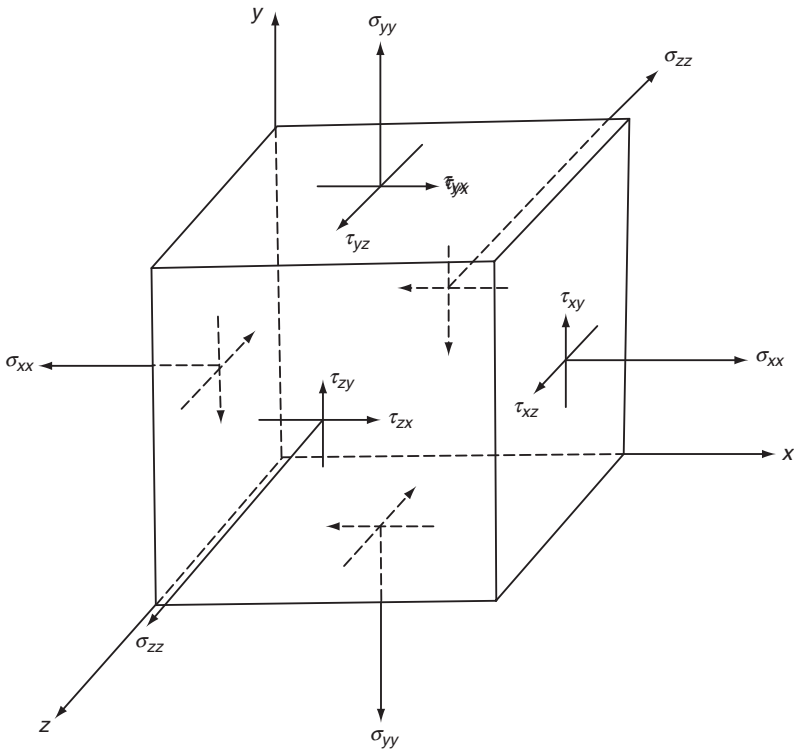


**FIGURE 3.25** Normal stress and shear stress components.

the direction of the stress component. Thus, for example, the subscript  $x$  in the shear stress component  $\tau_{xy}$  represents the outward normal to the  $yz$  plane and the subscript  $y$  represents its direction. The stress components  $\sigma_{xx}$ ,  $\sigma_{yy}$ , and  $\tau_{xy}$  are called *in-plane (intralaminar) stresses*, whereas  $\sigma_{zz}$ ,  $\tau_{xz}$ , and  $\tau_{yz}$  are called *interlaminar stresses*.

In order to visualize the direction (sense) of various stress components, we adopt the following sign conventions:

1. If the outward normal to a stress plane is directed in a positive coordinate direction, we call it a positive plane. A negative plane has its outward normal pointing in the negative coordinate direction.
2. A stress component is positive in sign if it acts in a positive direction on a positive plane or in a negative direction on a negative plane. On the other hand, the stress component is negative in sign if it acts in a negative direction on a positive plane or in a positive direction on a negative plane. Thus, all stress components in Figure 3.25 are positive in sign.

### 3.2.1.3 Stress and Strain Transformations in a Thin Lamina under Plane Stress

In stress analysis of a thin lamina with fiber orientation angle  $\theta$ , it is often desirable to transform stresses in the  $xy$  directions to stresses in the 12 directions. The stress transformation equations are

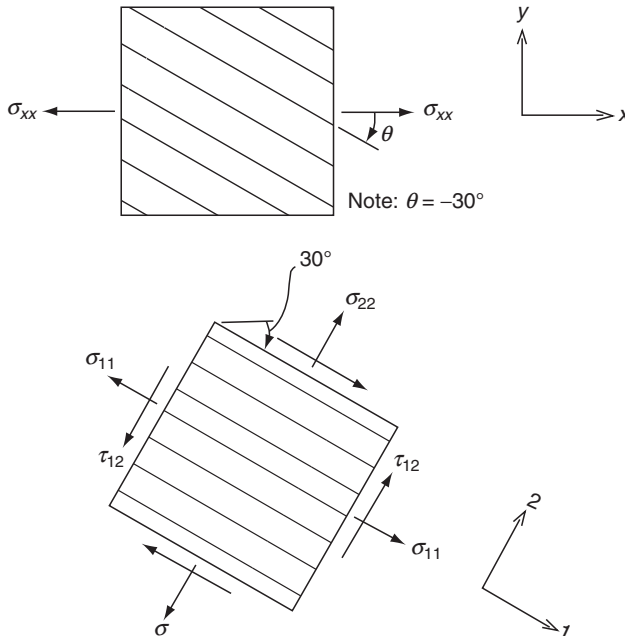
$$\begin{aligned}\sigma_{11} &= \sigma_{xx} \cos^2 \theta + \sigma_{yy} \sin^2 \theta + 2\tau_{xy} \cos \theta \sin \theta, \\ \sigma_{22} &= \sigma_{xx} \sin^2 \theta + \sigma_{yy} \cos^2 \theta - 2\tau_{xy} \cos \theta \sin \theta, \\ \tau_{12} &= (-\sigma_{xx} + \sigma_{yy}) \sin \theta \cos \theta + \tau_{xy}(\cos^2 \theta - \sin^2 \theta).\end{aligned}\quad (3.30)$$

where  $\sigma_{xx}$ ,  $\sigma_{yy}$ , and  $\tau_{xy}$  are applied stresses in the  $xy$  directions and  $\sigma_{11}$ ,  $\sigma_{22}$ , and  $\tau_{12}$  are transformed stresses in the 12 directions. Similar equations can also be written for strain transformation by replacing each  $\sigma$  with  $\varepsilon$  and each  $\tau$  with  $\gamma/2$  in Equation 3.30. Thus, the strain transformation equations are

$$\begin{aligned}\varepsilon_{11} &= \varepsilon_{xx} \cos^2 \theta + \varepsilon_{yy} \sin^2 \theta + \gamma_{xy} \cos \theta \sin \theta, \\ \varepsilon_{22} &= \varepsilon_{xx} \sin^2 \theta + \varepsilon_{yy} \cos^2 \theta - \gamma_{xy} \cos \theta \sin \theta, \\ \gamma_{12} &= 2(-\varepsilon_{xx} + \varepsilon_{yy}) \sin \theta \cos \theta + \gamma_{xy}(\cos^2 \theta - \sin^2 \theta).\end{aligned}\quad (3.31)$$

#### EXAMPLE 3.2

A normal stress  $\sigma_{xx}$  of 10 MPa is applied on a unidirectional angle-ply lamina containing fibers at  $30^\circ$  to the  $x$  axis, as shown at the top of the figure. Determine the stresses in the principal material directions.



## SOLUTION

Since  $\sigma_{yy} = \tau_{xy} = 0$ , the transformation equations become

$$\begin{aligned}\sigma_{11} &= \sigma_{xx} \cos^2 \theta, \\ \sigma_{22} &= \sigma_{xx} \sin^2 \theta, \\ \tau_{12} &= -\sigma_{xx} \sin \theta \cos \theta.\end{aligned}$$

In this example,  $\sigma_{xx} = +10$  MPa and  $\theta = -30^\circ$ . Therefore,

$$\begin{aligned}\sigma_{11} &= 7.5 \text{ MPa}, \\ \sigma_{22} &= 2.5 \text{ MPa}, \\ \tau_{12} &= 4.33 \text{ MPa}.\end{aligned}$$

The stresses in the principal material directions are shown in the figure.

### 3.2.1.4 Isotropic, Anisotropic, and Orthotropic Materials

In an isotropic material, properties are the same in all directions. Thus, the material contains an infinite number of planes of material property symmetry passing through a point. In an anisotropic material, properties are different in all directions so that the material contains no planes of material property symmetry. Fiber-reinforced composites, in general, contain three orthogonal planes of material property symmetry, namely, the 1–2, 2–3, and 1–3 plane shown in Figure 3.26, and are classified as *orthotropic materials*. The intersections of

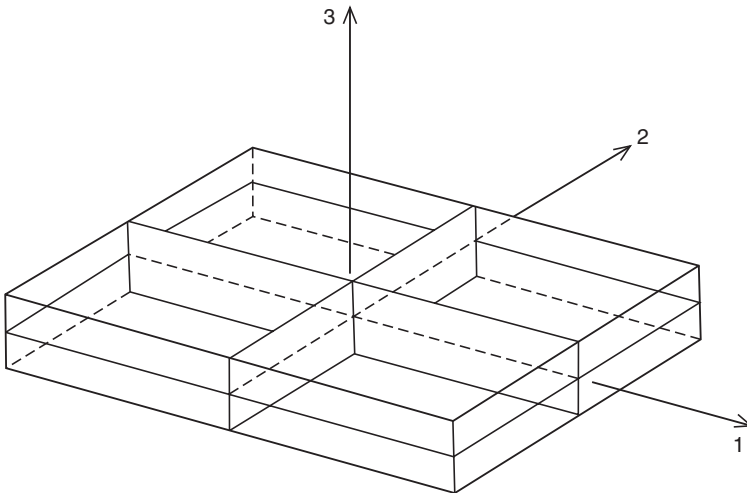


**FIGURE 3.26** Three planes of symmetry in an orthotropic material.

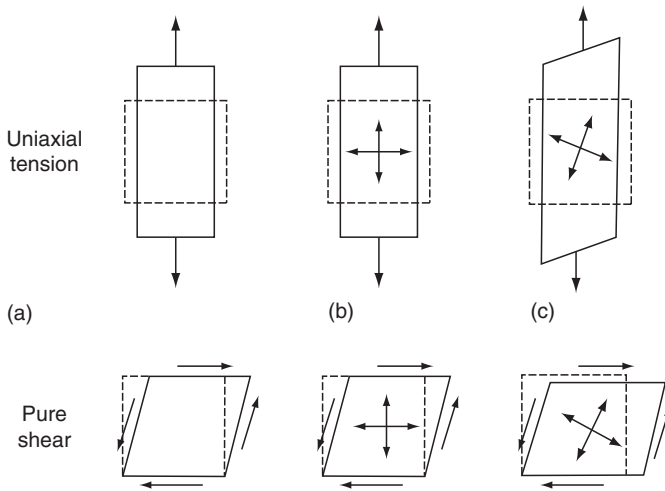


**FIGURE 3.27** Differences in the deformations of isotropic, specially orthotropic and anisotropic materials subjected to uniaxial tension ((a) Isotropic, (b) Special orthotropic, and (c) General orthotropic and anisotropic) and pure shear stresses.

these three planes of symmetry, namely, axes 1, 2, and 3, are called the principal material directions.

Differences in the mechanical behavior of isotropic, orthotropic, and anisotropic materials are demonstrated schematically in Figure 3.27. Tensile normal stresses applied in any direction on an isotropic material cause elongation in the direction of the applied stresses and contractions in the two transverse directions. Similar behavior is observed in orthotropic materials only if the normal stresses are applied in one of the principal material directions. However, normal stresses applied in any other direction create both extensional and shear deformations. In an anisotropic material, a combination of extensional and shear deformation is produced by a normal stress acting in any direction. This phenomenon of creating both extensional and shear deformations by the application of either normal or shear stresses is termed *extension-shear coupling* and is not observed in isotropic materials.

The difference in material property symmetry in isotropic, orthotropic, and anisotropic materials is also reflected in the mechanics and design of these types of materials. Two examples are given as follows.

1. The elastic stress–strain characteristics of an isotropic material are described by three elastic constants, namely, Young’s modulus  $E$ , Poisson’s ratio  $\nu$ , and shear modulus  $G$ . Only two of these three elastic

constants are independent since they can be related by the following equation:

$$G = \frac{E}{2(1 + \nu)}. \quad (3.32)$$

The number of independent elastic constants required to characterize anisotropic and orthotropic materials are 21 and 9, respectively [16]. For an orthotropic material, the nine independent elastic constants are  $E_{11}$ ,  $E_{22}$ ,  $E_{33}$ ,  $G_{12}$ ,  $G_{13}$ ,  $G_{23}$ ,  $\nu_{12}$ ,  $\nu_{13}$ , and  $\nu_{23}$ .

Unidirectionally oriented fiber composites are a special class of orthotropic materials. Referring to Figure 3.28, which shows a

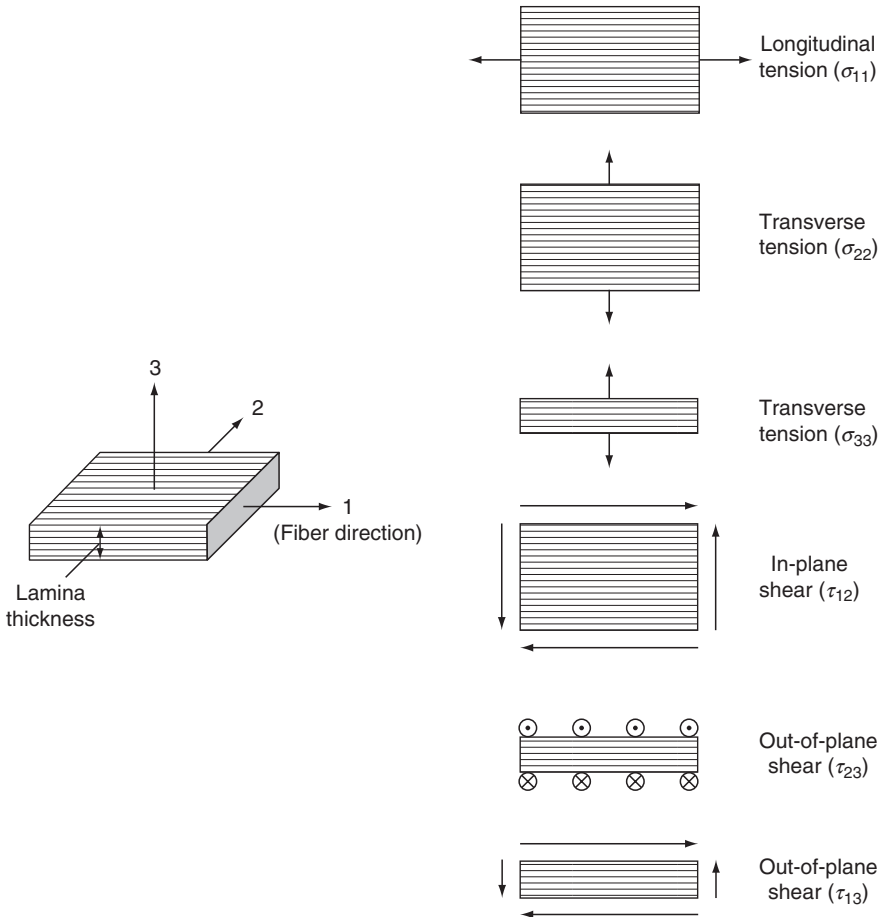


**FIGURE 3.28** Tensile and shear loading on a unidirectional continuous fiber composite.

composite in which the fibers are in the 12 plane, it can be visualized that the elastic properties are equal in the 2–3 direction so that  $E_{22} = E_{33}$ ,  $\nu_{12} = \nu_{13}$ , and  $G_{12} = G_{13}$ . Furthermore,  $G_{23}$  can be expressed in terms of  $E_{22}$  and  $\nu_{23}$  by an expression similar to Equation 3.32.

$$G_{23} = \frac{E_{22}}{2(1 + \nu_{23})}. \quad (3.33)$$

Thus, the number of independent elastic constants for a unidirectionally oriented fiber composite reduces to 5, namely,  $E_{11}$ ,  $E_{22}$ ,  $\nu_{12}$ ,  $G_{12}$ , and  $\nu_{23}$ . Such composites are often called *transversely isotropic*.

Note that  $\nu_{21} \neq \nu_{12}$  and  $\nu_{31} \neq \nu_{13}$ , but  $\nu_{31} = \nu_{21}$ . However,  $\nu_{21}$  is related to  $\nu_{12}$  by the following equation, and therefore is not an independent elastic constant.

$$\nu_{21} = \left( \frac{E_{22}}{E_{11}} \right) \nu_{12}. \quad (3.34)$$

Christensen [17] has shown that in the case of unidirectional fiber-reinforced composites with fibers oriented in the 1-direction,  $\nu_{23}$  can be related to  $\nu_{12}$  and  $\nu_{21}$  using the following equation:

$$\nu_{23} = \nu_{32} = \nu_{12} \frac{(1 - \nu_{21})}{(1 - \nu_{12})}. \quad (3.35)$$

Equation 3.35 fits the experimental data within the range of experimental accuracy. Thus, for a unidirectional fiber-reinforced composite, the number of independent elastic constants is reduced from 5 to 4.

2. For an isotropic material, the sign convention for shear stresses and shear strains is of little practical significance, since its mechanical behavior is independent of the direction of shear stress. For an orthotropic or anisotropic material, the direction of shear stress is critically important in determining its strength and modulus [18]. For example, consider a unidirectional fiber-reinforced lamina (Figure 3.29) subjected to states of pure shear of opposite sense. For positive shear (Figure 3.29a), the maximum (tensile) principal stress is parallel to the fiber direction that causes fiber fracture. For negative shear (Figure 3.29b), the maximum (tensile) principal stress is normal to the fiber direction, which causes either a matrix failure or a fiber–matrix interface failure. Obviously, a positive shear condition will favor a higher load-carrying capacity than the negative shear condition. For an isotropic material, shear strength is equal in all directions. Therefore, the direction of shear stress will not influence the failure of the material.

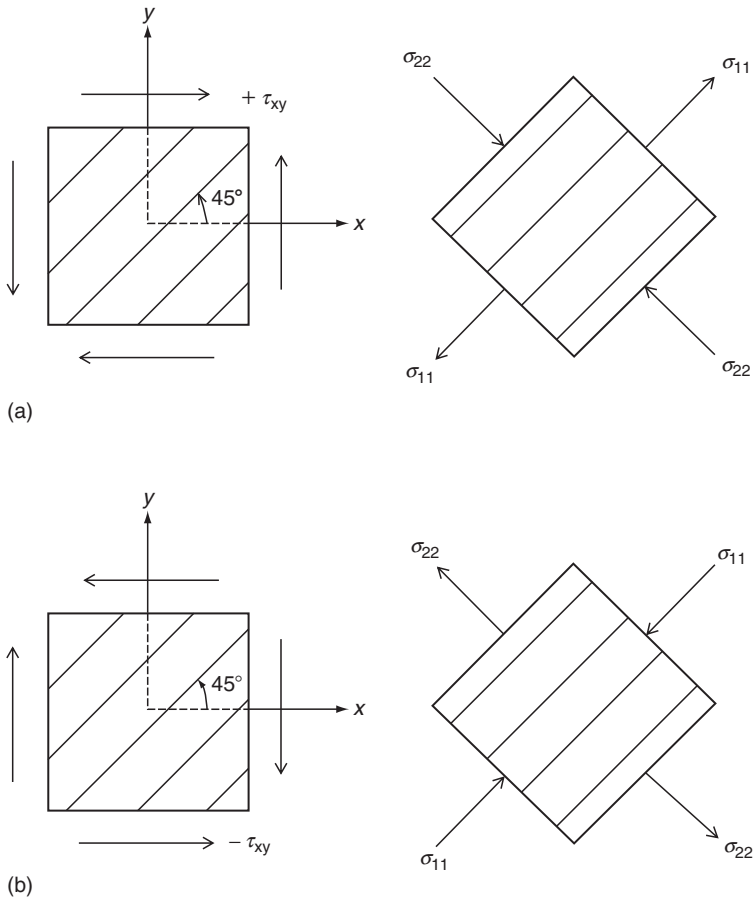


**FIGURE 3.29** Normal stress components parallel and perpendicular to the fibers due to (a) positive shear stress and (b) negative shear stress on a 45° lamina.

### 3.2.2 ELASTIC PROPERTIES OF A LAMINA

#### 3.2.2.1 Unidirectional Continuous Fiber 0° Lamina

Elastic properties of a unidirectional continuous fiber 0° lamina (Figure 3.30) are calculated from the following equations.

1. Referring to Figure 3.30a in which the tensile stress is applied in the 1-direction,  
Longitudinal modulus:

$$E_{11} = E_f v_f + E_m v_m \quad (3.36)$$

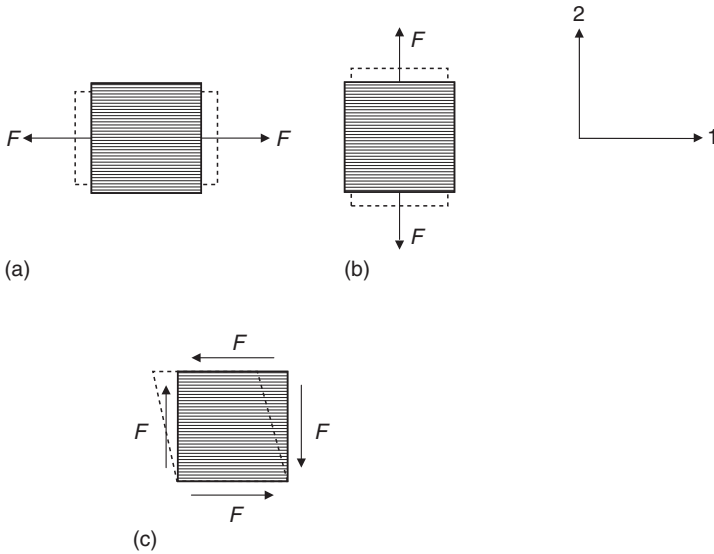


**FIGURE 3.30** Applications of (a) longitudinal tensile stress, (b) transverse tensile stress, and (c) in-plane shear stress on a unidirectional continuous fiber 0° lamina.

and

Major Poisson's ratio:

$$\nu_{12} = \nu_f \nu_f + \nu_m \nu_m, \tag{3.37}$$

where  $\nu_{12} = - \frac{\text{Strain in the 2-direction}}{\text{Strain in the 1-direction (i.e., the stress direction)}}$ .

- Referring to Figure 3.30b in which the tensile stress is applied in the 2-direction

Transverse modulus:

$$E_{22} = \frac{E_f E_m}{E_f \nu_m + E_m \nu_f} \tag{3.38}$$

and

Minor Poisson's ratio:

$$\nu_{21} = \frac{E_{22}}{E_{11}} \nu_{12}, \tag{3.39}$$

where  $\nu_{21} = - \frac{\text{Strain in the 1-direction}}{\text{Strain in the 2-direction (i.e., the stress direction)}}$ .

3. Referring to [Figure 3.30c](#) in which the shear stress is applied in 12 plane

In-plane shear modulus:

$$G_{12} = G_{21} = \frac{G_f G_m}{G_f v_m + G_m v_f}. \quad (3.40)$$

The following points should be noted from [Equations 3.36](#) through [3.40](#):

1. The longitudinal modulus ( $E_{11}$ ) is always greater than the transverse modulus ( $E_{22}$ ) (Figure 3.31).
2. The fibers contribute more to the development of the longitudinal modulus, and the matrix contributes more to the development of the transverse modulus.
3. The major Poisson's ratio ( $\nu_{12}$ ) is always greater than the minor Poisson's ratio ( $\nu_{21}$ ). Since these Poisson's ratios are related to [Equation 3.39](#), only one of them can be considered independent.
4. As for  $E_{22}$ , the matrix contributes more to the development of  $G_{12}$  than the fibers.
5. Four independent elastic constants, namely,  $E_{11}$ ,  $E_{22}$ ,  $\nu_{12}$ , and  $G_{12}$ , are required to describe the in-plane elastic behavior of a lamina. The ratio  $E_{11}/E_{22}$  is often considered a *measure of orthotropy*.

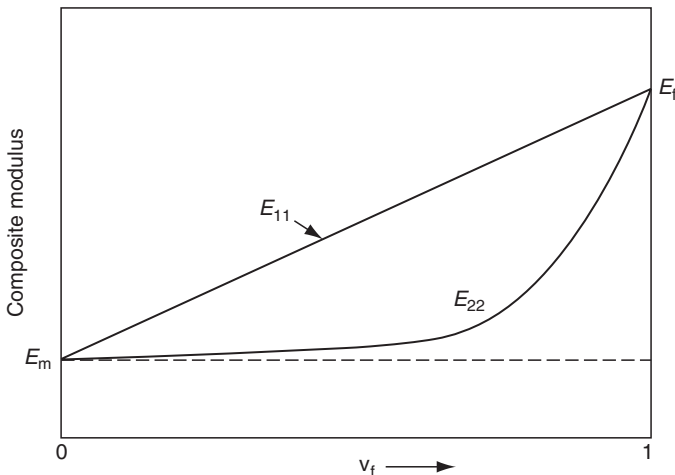


**FIGURE 3.31** Variations of longitudinal and transverse modulus of a unidirectional continuous fiber  $0^\circ$  lamina with fiber volume fraction.

Equations 3.36 through 3.40 are derived using the simple mechanics of materials approach along with the following assumptions:

1. Both fibers and matrix are linearly elastic isotropic materials.
2. Fibers are uniformly distributed in the matrix.
3. Fibers are perfectly aligned in the 1-direction.
4. There is perfect bonding between fibers and matrix.
5. The composite lamina is free of voids.

Since, in practice, none of these assumptions is completely valid, these equations provide only approximate values for the elastic properties of a continuous fiber 0° lamina. It has been found that the values of  $E_{11}$  and  $\nu_{12}$  predicted by Equations 3.36 and 3.37 agree well with the experimental data, but values of  $E_{22}$  and  $G_{12}$  predicted by Equations 3.38 and 3.40 are lower than the experimental data [19]. Both  $E_{22}$  and  $G_{12}$  are sensitive to void content, fiber anisotropy, and the matrix Poisson's ratio. Since equations based on the theory of elasticity or the variational approach, for example, are difficult to solve, Equations 3.36 through 3.40 or empirically modified versions of these equations (see Appendix A.3) are used frequently for the laminate design.

In Equations 3.36 through 3.40, it is assumed that both fibers and matrix are isotropic materials. While the matrix in most fiber-reinforced composites exhibits isotropic behavior, many reinforcing fibers are not isotropic and their elastic modulus in the longitudinal direction,  $E_{fL}$ , is much greater than their elastic modulus in the transverse direction,  $E_{fT}$ . Accordingly, Equations 3.36 and 3.38 should be modified in the following manner.

$$E_{11} = E_{fL}v_f + E_m v_m, \tag{3.41}$$

$$E_{22} = \frac{E_{fT}E_m}{E_{fT}v_m + E_m v_f}. \tag{3.42}$$

The Poisson's ratio of the fiber in Equation 3.37 should be represented by  $\nu_{fLT}$ , and its shear modulus in Equation 3.40 should be represented by  $G_{fLT}$ . Since for most of the fibers,  $E_{fT}$ ,  $\nu_{fLT}$ , and  $G_{fLT}$  are difficult to measure and are not available, Equations 3.36 and 3.40 are commonly used albeit the errors that they can introduce.

### EXAMPLE 3.3

To demonstrate the difference between  $\nu_{12}$  and  $\nu_{21}$ , consider the following example in which a square composite plate containing unidirectional continuous T-300 carbon fiber-reinforced epoxy is subjected to a uniaxial tensile load of 1000 N. The plate thickness is 1 mm. The length ( $L_o$ ) and width ( $W_o$ ) of the plate are 100 mm each.

Consider two loading cases, where

1. Load is applied parallel to the fiber direction
2. Load is applied normal to the fiber direction

Calculate the changes in length and width of the plate in each case. The basic elastic properties of the composite are given in Appendix A.5.

### SOLUTION

From Appendix A.5,  $E_{11} = 138 \text{ GPa}$ ,  $E_{22} = 10 \text{ GPa}$ , and  $\nu_{12} = 0.21$ . Using Equation 3.39, we calculate  $\nu_{21}$ .

$$\nu_{21} = \frac{E_{22}}{E_{11}} \nu_{12} = \left( \frac{10 \text{ GPa}}{138 \text{ GPa}} \right) (0.21) = 0.0152.$$

1. Tensile load is applied parallel to the fiber direction, that is, in the 1-direction. Therefore,  $\sigma_{11} = \frac{1000 \text{ N}}{(100 \text{ mm})(1 \text{ mm})} = 10 \text{ MPa}$  and  $\sigma_{22} = 0$ . Now, we calculate the normal strains  $\varepsilon_{11}$  and  $\varepsilon_{22}$ .

$$\varepsilon_{11} = \frac{\sigma_{11}}{E_{11}} = \frac{10 \text{ MPa}}{138 \text{ GPa}} = 0.725 \times 10^{-4},$$

$$\varepsilon_{22} = -\nu_{12} \varepsilon_{11} = -(0.21) (0.725 \times 10^{-4}) = -0.152 \times 10^{-4}.$$

Since  $\varepsilon_{11} = \frac{\Delta L}{L_0}$  and  $\varepsilon_{22} = \frac{\Delta W}{W_0}$ ,

$$\Delta L = L_0 \varepsilon_{11} = (100 \text{ mm}) (0.725 \times 10^{-4}) = 0.00725 \text{ mm},$$

$$\Delta W = W_0 \varepsilon_{22} = (100 \text{ mm}) (-0.152 \times 10^{-4}) = -0.00152 \text{ mm}.$$

2. Tensile load is applied normal to the fiber direction, that is, in the 2-direction. Therefore,  $\sigma_{22} = \frac{1000 \text{ N}}{(100 \text{ mm})(1 \text{ mm})} = 10 \text{ MPa}$  and  $\sigma_{11} = 0$ . The normal strains in this case are

$$\varepsilon_{22} = \frac{\sigma_{22}}{E_{22}} = \frac{10 \text{ MPa}}{10 \text{ GPa}} = 10 \times 10^{-4},$$

$$\varepsilon_{11} = -\nu_{21} \varepsilon_{22} = -(0.0152) (10 \times 10^{-4}) = -0.152 \times 10^{-4}.$$

Since  $\varepsilon_{11} = \frac{\Delta L}{L_0}$  and  $\varepsilon_{22} = \frac{\Delta W}{W_0}$ ,

$$\Delta L = L_0 \varepsilon_{11} = (100 \text{ mm}) (-0.152 \times 10^{-4}) = -0.00152 \text{ mm},$$

$$\Delta W = W_0 \varepsilon_{22} = (100 \text{ mm}) (10 \times 10^{-4}) = 0.1 \text{ mm}.$$

### 3.2.2.2 Unidirectional Continuous Fiber Angle-Ply Lamina

The following equations are used to calculate the elastic properties of an angle-ply lamina in which continuous fibers are aligned at an angle  $\theta$  with the positive  $x$  direction (Figure 3.32):

$$\frac{1}{E_{xx}} = \frac{\cos^4 \theta}{E_{11}} + \frac{\sin^4 \theta}{E_{22}} + \frac{1}{4} \left( \frac{1}{G_{12}} - \frac{2\nu_{12}}{E_{11}} \right) \sin^2 2\theta, \quad (3.43)$$

$$\frac{1}{E_{yy}} = \frac{\sin^4 \theta}{E_{11}} + \frac{\cos^4 \theta}{E_{22}} + \frac{1}{4} \left( \frac{1}{G_{12}} - \frac{2\nu_{12}}{E_{11}} \right) \sin^2 2\theta, \quad (3.44)$$

$$\frac{1}{G_{xy}} = \frac{1}{E_{11}} + \frac{2\nu_{12}}{E_{11}} + \frac{1}{E_{22}} - \left( \frac{1}{E_{11}} + \frac{2\nu_{12}}{E_{11}} + \frac{1}{E_{22}} - \frac{1}{G_{12}} \right) \cos^2 2\theta, \quad (3.45)$$

$$\nu_{xy} = E_{xx} \left[ \frac{\nu_{12}}{E_{11}} - \frac{1}{4} \left( \frac{1}{E_{11}} + \frac{2\nu_{12}}{E_{11}} + \frac{1}{E_{22}} - \frac{1}{G_{12}} \right) \sin^2 2\theta \right], \quad (3.46)$$

$$\nu_{yx} = \frac{E_{yy}}{E_{xx}} \nu_{xy}, \quad (3.47)$$

where  $E_{11}$ ,  $E_{22}$ ,  $\nu_{12}$ , and  $G_{12}$  are calculated using [Equations 3.36](#) through [3.40](#).

[Figure 3.33](#) shows the variation of  $E_{xx}$  as a function of fiber orientation angle  $\theta$  for an angle-ply lamina. Note that at  $\theta = 0^\circ$ ,  $E_{xx}$  is equal to  $E_{11}$ , and at  $\theta = 90^\circ$ ,  $E_{xx}$  is equal to  $E_{22}$ . Depending on the shear modulus  $G_{12}$ ,  $E_{xx}$  can be

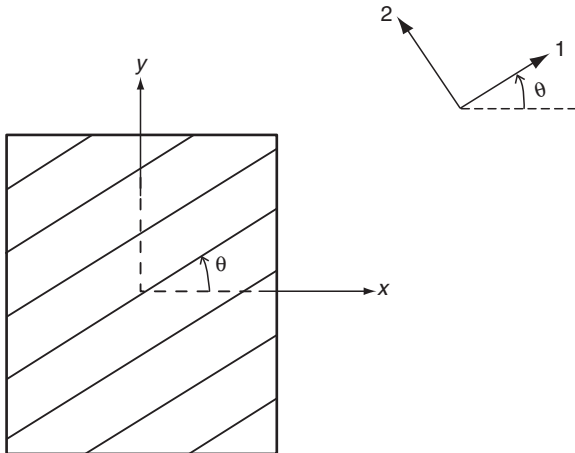


**FIGURE 3.32** Unidirectional continuous fiber angle-ply lamina.

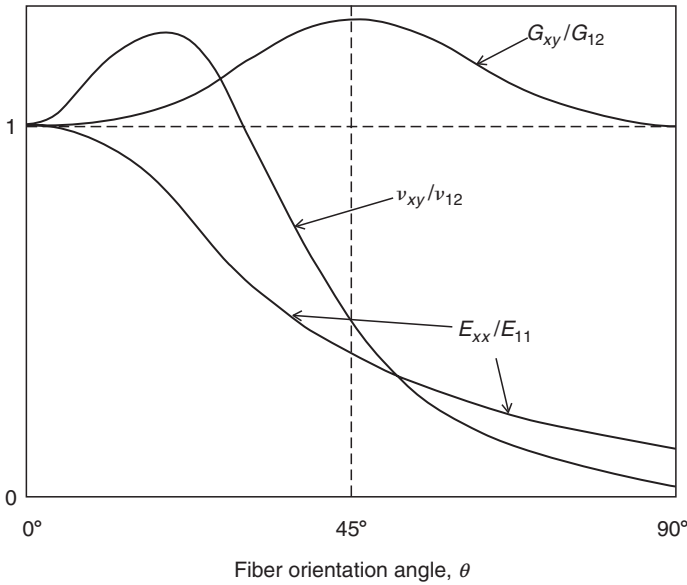


**FIGURE 3.33** Variation of elastic constants of continuous E-glass fiber lamina with fiber-orientation angle.

either greater than  $E_{11}$  or less than  $E_{22}$  at some intermediate values of  $\theta$ . The range of  $G_{12}$  for which  $E_{xx}$  is within  $E_{11}$  and  $E_{22}$  [20] is given by

$$\frac{E_{11}}{2(1 + \nu_{12})} > G_{12} > \frac{E_{11}}{2\left(\frac{E_{11}}{E_{22}} + \nu_{12}\right)}. \quad (3.48)$$

For glass fiber–epoxy, high-strength carbon fiber–epoxy, and Kevlar 49 fiber–epoxy composites,  $G_{12}$  is within the range given by Equation 3.48, and therefore, for these composite laminas,  $E_{22} < E_{xx} < E_{11}$ . However, for very high-modulus carbon fiber–epoxy and boron fiber–epoxy composites,  $G_{12}$  is less than the lower limit in Equation 3.48, and therefore for a range of angles between  $0^\circ$  and  $90^\circ$ ,  $E_{xx}$  for these laminas can be lower than  $E_{22}$ .

### 3.2.2.3 Unidirectional Discontinuous Fiber $0^\circ$ Lamina

Elastic properties of a unidirectional discontinuous fiber  $0^\circ$  lamina are calculated using the following equations (Figure 3.34).

Longitudinal modulus:

$$E_{11} = \frac{1 + 2(l_f/d_f)\eta_L\nu_f}{1 - \eta_L\nu_f} E_m, \quad (3.49)$$

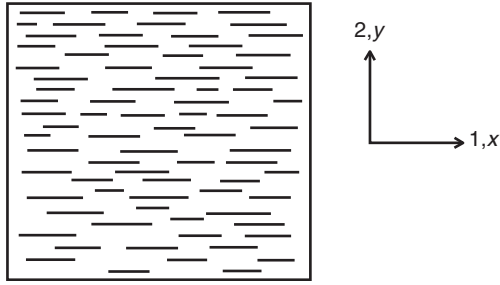


**FIGURE 3.34** Unidirectional discontinuous fiber 0° lamina.

Transverse modulus:

$$E_{22} = \frac{1 + 2\eta_T\nu_f}{1 - \eta_T\nu_f} E_m, \quad (3.50)$$

Shear modulus:

$$G_{12} = G_{21} = \frac{1 + \eta_G\nu_f}{1 - \eta_G\nu_f} G_m, \quad (3.51)$$

Major Poisson's ratio:

$$\nu_{12} = \nu_f\nu_f + \nu_m\nu_m, \quad (3.52)$$

Minor Poisson's ratio:

$$\nu_{21} = \frac{E_{22}}{E_{11}} \nu_{12}, \quad (3.53)$$

where

$$\begin{aligned} \eta_L &= \frac{(E_f/E_m) - 1}{(E_f/E_m) + 2(l_f/d_f)} \\ \eta_T &= \frac{(E_f/E_m) - 1}{(E_f/E_m) + 2} \\ \eta_G &= \frac{(G_f/G_m) - 1}{(G_f/G_m) + 1} \end{aligned} \quad (3.54)$$

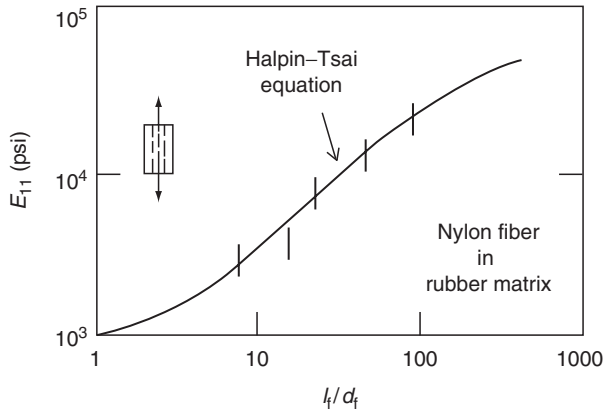


**FIGURE 3.35** Variation of longitudinal modulus of a unidirectional discontinuous fiber lamina with fiber length–diameter ratio. (After Halpin, J.C., *J. Compos. Mater.*, 3, 732, 1969.)

Equations 3.49 through 3.53 are derived from the Halpin–Tsai equations (Appendix A.4) with the following assumptions:

1. Fiber cross section is circular.
2. Fibers are arranged in a square array.
3. Fibers are uniformly distributed throughout the matrix.
4. Perfect bonding exists between the fibers and the matrix.
5. Matrix is free of voids.

Fiber aspect ratio, defined as the ratio of average fiber length  $l_f$  to fiber diameter  $d_f$ , has a significant effect on the longitudinal modulus  $E_{11}$  (Figure 3.35). On the other hand, the transverse modulus  $E_{22}$  is not affected by the fiber aspect ratio. Furthermore, the longitudinal modulus  $E_{11}$  for a discontinuous fiber  $0^\circ$  lamina is always less than that for a continuous fiber  $0^\circ$  lamina.

### 3.2.2.4 Randomly Oriented Discontinuous Fiber Lamina

A thin lamina containing randomly oriented discontinuous fibers (Figure 3.36) exhibits planar isotropic behavior. The properties are ideally the same in all directions in the plane of the lamina. For such a lamina, the tensile modulus and shear modulus are calculated from

$$E_{\text{random}} = \frac{3}{8} E_{11} + \frac{5}{8} E_{22}, \quad (3.55)$$

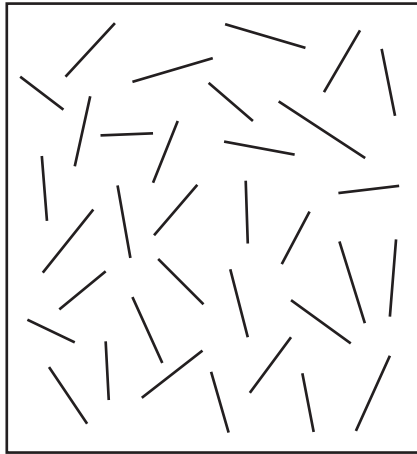


**FIGURE 3.36** Randomly oriented discontinuous fiber lamina.

$$G_{\text{random}} = \frac{1}{8}E_{11} + \frac{1}{4}E_{22}, \quad (3.56)$$

where  $E_{11}$  and  $E_{22}$  are the longitudinal and transverse tensile moduli given by Equations 3.49 and 3.50, respectively, for a unidirectional discontinuous fiber  $0^\circ$  lamina of the same fiber aspect ratio and same fiber volume fraction as the randomly oriented discontinuous fiber composite. The Poisson's ratio in the plane of the lamina is

$$\nu_{\text{random}} = \frac{E_{\text{random}}}{2G_{\text{random}}} - 1. \quad (3.57)$$

### EXAMPLE 3.4

Consider a sheet molding compound composite, designated SMC-R65, containing E-glass fibers in a thermoset polyester matrix. The following data are known.

For E-glass fiber,

$$\begin{aligned} E_f &= 68.9 \text{ GPa} \\ \rho_f &= 2.54 \text{ g/cm}^3 \\ l_f &= 25 \text{ mm} \\ d_f &= 2.5 \text{ mm}. \end{aligned}$$

For polyester,

$$\begin{aligned} E_m &= 3.45 \text{ GPa} \\ \rho_m &= 1.1 \text{ g/cm}^3. \end{aligned}$$

Calculate the tensile modulus, shear modulus, and Poisson's ratio for the material.

## SOLUTION

Step 1: Calculate the fiber volume fraction  $v_f$ .

Fiber weight fraction in SMC-R65 is  $w_f = 0.65$ . Therefore, from Equation 2.7,

$$v_f = \frac{0.65/2.54}{(0.65/2.54) + (1 - 0.65)/1.1} = 0.446 \text{ or } 44.6\%.$$

Step 2: Calculate  $E_{11}$  for a unidirectional lamina containing 44.6 vol% discontinuous fibers of length  $l_f = 25$  mm.

$$\frac{E_f}{E_m} = \frac{68.9}{3.45} = 19.97,$$
$$\frac{l_f}{d_f} = \frac{25}{2.5} = 10.$$

Therefore, from Equation 3.54,

$$\eta_L = \frac{19.97 - 1}{19.97 + (2)(10)} = 0.475.$$

Using Equation 3.49, we calculate

$$E_{11} = \frac{1 + (2)(10)(0.475)(0.446)}{1 - (0.475)(0.446)}$$
$$= 22.93 \text{ GPa.}$$

Step 3: Calculate  $E_{22}$  for a unidirectional lamina containing 44.6 vol% discontinuous fibers of length  $l_f = 25$  mm. From Equation 3.54,

$$\eta_T = \frac{19.97 - 1}{19.97 + 2} = 0.863.$$

Using Equation 3.50, we calculate

$$E_{22} = \frac{1 + (2)(0.863)(0.446)}{1 - (0.863)(0.446)}$$
$$= 9.93 \text{ GPa.}$$

Step 4: Calculate  $E$  and  $G$  for SMC-R65 using values of  $E_{11}$  and  $E_{22}$  in Equations 3.55 and 3.56, and then calculate  $\nu$  using Equation 3.57.

$$E = E_{\text{random}} = \frac{3}{8}E_{11} + \frac{5}{8}E_{22} = 14.81 \text{ GPa,}$$
$$G = G_{\text{random}} = \frac{1}{8}E_{11} + \frac{1}{4}E_{22} = 5.35 \text{ GPa,}$$
$$\nu = \nu_{\text{random}} = \frac{E}{2G} - 1 = 0.385.$$

### 3.2.3 COEFFICIENTS OF LINEAR THERMAL EXPANSION [21]

For a unidirectional continuous fiber lamina, coefficients of linear thermal expansion in the  $0^\circ$  and  $90^\circ$  directions can be calculated from the following equations:

$$\alpha_{11} = \frac{\alpha_{fl}E_f\nu_f + \alpha_m E_m\nu_m}{E_f\nu_f + E_m\nu_m} \quad (3.58)$$

and

$$\alpha_{22} = (1 + \nu_f) \frac{(\alpha_{fl} + \alpha_{fr})}{2} \nu_f + (1 + \nu_m)\alpha_m\nu_m - \alpha_{11}\nu_{12}, \quad (3.59)$$

where

$$\nu_{12} = \nu_f\nu_f + \nu_m\nu_m$$

$\alpha_{fl}$  = coefficient of linear thermal expansion for the fiber in the longitudinal direction

$\alpha_{fr}$  = coefficient of linear thermal expansion for the fiber in the radial direction

$\alpha_m$  = coefficient of linear thermal expansion for the matrix

Equations 3.58 and 3.59 are plotted in Figure 3.37 as a function of fiber volume fraction for a typical glass fiber-reinforced polymer matrix composite for which  $\alpha_m \gg \alpha_f$ . It should be noted that the coefficient of linear thermal expansion in such composites is greater in the transverse ( $90^\circ$ ) direction than in the longitudinal ( $0^\circ$ ) direction.

If the fibers are at an angle  $\theta$  with the  $x$  direction, the coefficients of thermal expansion in the  $x$  and  $y$  directions can be calculated using  $\alpha_{11}$  and  $\alpha_{22}$ :

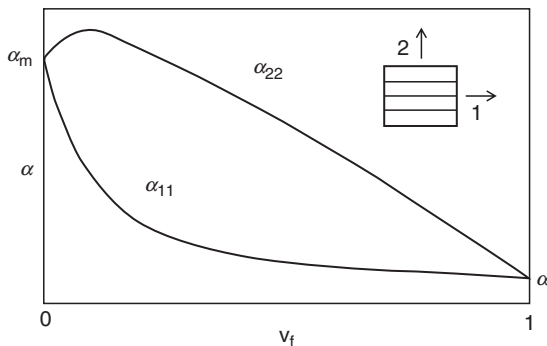


**FIGURE 3.37** Variation of longitudinal and transverse coefficients of thermal expansion with fiber volume fraction in a  $0^\circ$  unidirectional continuous E-glass fiber-reinforced epoxy lamina.

$$\begin{aligned}
\alpha_{xx} &= \alpha_{11} \cos^2 \theta + \alpha_{22} \sin^2 \theta, \\
\alpha_{yy} &= \alpha_{11} \sin^2 \theta + \alpha_{22} \cos^2 \theta, \\
\alpha_{xy} &= (2 \sin \theta \cos \theta) (\alpha_{11} - \alpha_{22}),
\end{aligned}
\tag{3.60}$$

where  $\alpha_{xx}$  and  $\alpha_{yy}$  are coefficients of linear expansion and  $\alpha_{xy}$  is the coefficient of shear expansion. It is important to observe that, unless  $\theta = 0^\circ$  or  $90^\circ$ , a change in temperature produces a shear strain owing to the presence of  $\alpha_{xy}$ . The other two coefficients,  $\alpha_{xx}$  and  $\alpha_{yy}$ , produce extensional strains in the  $x$  and  $y$  directions, respectively.

### 3.2.4 STRESS–STRAIN RELATIONSHIPS FOR A THIN LAMINA

#### 3.2.4.1 Isotropic Lamina

For a thin isotropic lamina in plane stress (i.e.,  $\sigma_{zz} = \tau_{xz} = \tau_{yz} = 0$ ) (Figure 3.38), the strain–stress relations in the elastic range are

$$\begin{aligned}
\varepsilon_{xx} &= \frac{1}{E} (\sigma_{xx} - \nu \sigma_{yy}), \\
\varepsilon_{yy} &= \frac{1}{E} (-\nu \sigma_{xx} + \sigma_{yy}), \\
\gamma_{xy} &= \frac{1}{G} \tau_{xy},
\end{aligned}
\tag{3.61}$$

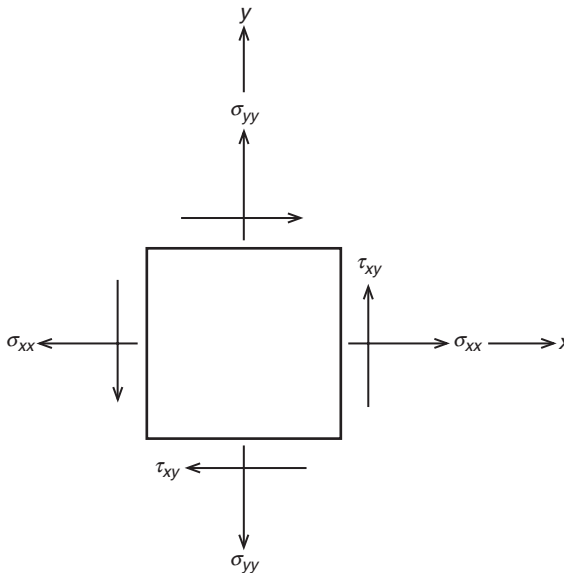


**FIGURE 3.38** Stresses in an isotropic lamina under a plane stress condition.

where  $E$ ,  $G$ , and  $\nu$  represent the Young's modulus, shear modulus, and Poisson's ratio, respectively.

An important point to note in Equation 3.61 is that there is no coupling between the shear stress  $\tau_{xy}$  and normal stresses  $\sigma_{xx}$  and  $\sigma_{yy}$ . In other words, shear stress  $\tau_{xy}$  does not influence the normal strains  $\epsilon_{xx}$  and  $\epsilon_{yy}$  just as the normal stresses  $\sigma_{xx}$  and  $\sigma_{yy}$  do not influence the shear strain  $\gamma_{xy}$ .

### 3.2.4.2 Orthotropic Lamina

For a thin orthotropic lamina in plane stress ( $\sigma_{zz} = \tau_{xz} = \tau_{yz} = 0$ ) (Figure 3.39), the strain–stress relations in the elastic range are

$$\epsilon_{xx} = \frac{\sigma_{xx}}{E_{xx}} - \nu_{yx} \frac{\sigma_{yy}}{E_{yy}} - m_x \tau_{xy}, \tag{3.62}$$

$$\epsilon_{yy} = -\nu_{xy} \frac{\sigma_{xx}}{E_{xx}} + \frac{\sigma_{yy}}{E_{yy}} - m_y \tau_{xy}, \tag{3.63}$$

$$\gamma_{xy} = -m_x \sigma_{xx} - m_y \sigma_{yy} + \frac{\tau_{xy}}{G_{xy}}, \tag{3.64}$$

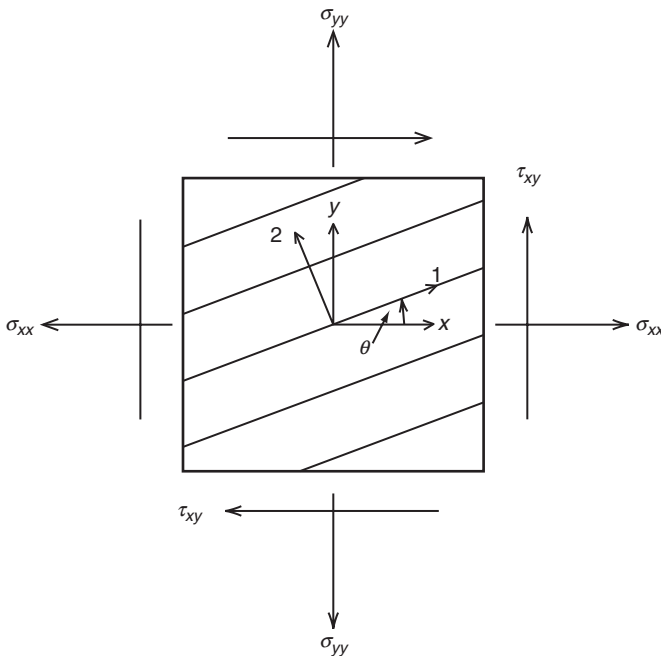


FIGURE 3.39 Stresses in a general orthotropic lamina under a plane stress condition.

where  $E_{xx}$ ,  $E_{yy}$ ,  $G_{xy}$ ,  $\nu_{xy}$ , and  $\nu_{yx}$  are elastic constants for the lamina obtained from Equations 3.43 through 3.47 and  $m_x$  and  $m_y$  are given by the following equations:

$$m_x = (\sin 2\theta) \left[ \frac{\nu_{12}}{E_{11}} + \frac{1}{E_{22}} - \frac{1}{2G_{12}} - (\cos^2 \theta) \left( \frac{1}{E_{11}} + \frac{2\nu_{12}}{E_{11}} + \frac{1}{E_{22}} - \frac{1}{G_{12}} \right) \right], \quad (3.65)$$

$$m_y = (\sin 2\theta) \left[ \frac{\nu_{12}}{E_{11}} + \frac{1}{E_{22}} - \frac{1}{2G_{12}} - (\sin^2 \theta) \left( \frac{1}{E_{11}} + \frac{2\nu_{12}}{E_{11}} + \frac{1}{E_{22}} - \frac{1}{G_{12}} \right) \right]. \quad (3.66)$$

The new elastic constants  $m_x$  and  $m_y$  represent the influence of shear stresses on extensional strains in Equations 3.62 and 3.63 and the influence of normal stresses on shear strain in Equation 3.64. These constants are called *coefficients of mutual influence*.

The following important observations can be made from Equations 3.62 through 3.66:

1. Unlike isotropic lamina, extensional and shear deformations are coupled in a general orthotropic lamina; that is, normal stresses cause both normal strains and shear strains, and shear stress causes both shear strain and normal strains. The effects of such extension-shear coupling phenomena are demonstrated in Figure 3.27c.
2. For  $\theta = 0^\circ$  and  $90^\circ$ , both  $m_x$  and  $m_y$  are zero, and therefore, for these fiber orientations, there is no extension-shear coupling. Such a lamina, in which the principal material axes (1 and 2 axes) coincide with the loading axes ( $x$  and  $y$  axes), is called *specialty orthotropic*. For a specialty orthotropic lamina (Figure 3.40), the strain–stress relations are

$$\varepsilon_{xx} = \varepsilon_{11} = \frac{\sigma_{xx}}{E_{11}} - \nu_{21} \frac{\sigma_{yy}}{E_{22}}, \quad (3.67)$$

$$\varepsilon_{yy} = \varepsilon_{22} = -\nu_{12} \frac{\sigma_{xx}}{E_{11}} + \frac{\sigma_{yy}}{E_{22}}, \quad (3.68)$$

$$\gamma_{xy} = \gamma_{yx} = \gamma_{12} = \gamma_{21} = \frac{\tau_{xy}}{G_{12}}. \quad (3.69)$$

3. Both  $m_x$  and  $m_y$  are functions of the fiber orientation angle  $\theta$  and exhibit maximum values at an intermediate angle between  $\theta = 0^\circ$  and  $90^\circ$  (Figure 3.41).

A critical point to note is that, unlike isotropic materials, the directions of principal stresses and principal strains do not coincide in a general orthotropic lamina. The only exception is found for specialty orthotropic lamina in which principal stresses are in the same direction as the material principal axes.

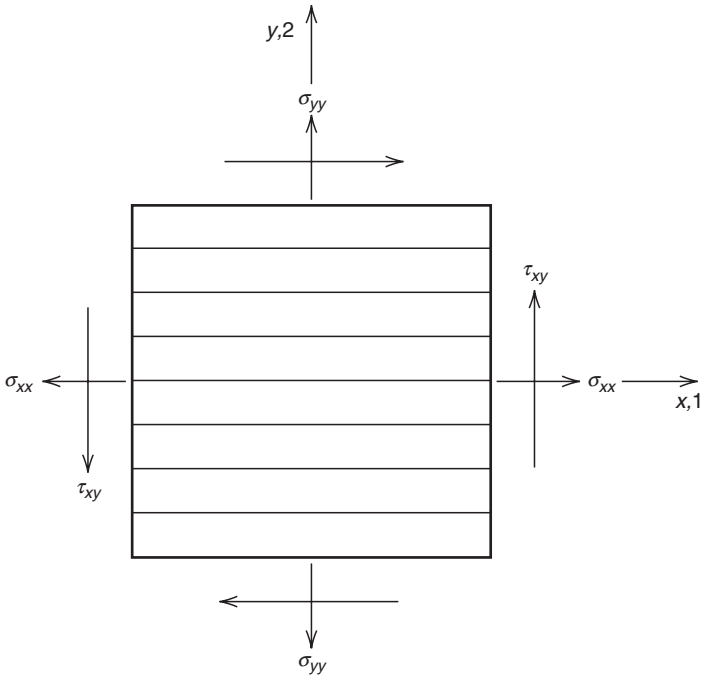


**FIGURE 3.40** Stresses in a specially orthotropic lamina under a plane stress condition.

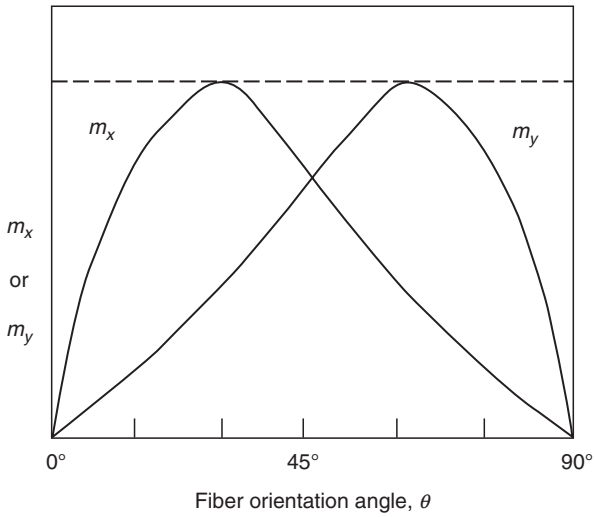


**FIGURE 3.41** Variation of coefficients of mutual influence with fiber orientation angle in an E-glass fiber–epoxy lamina.

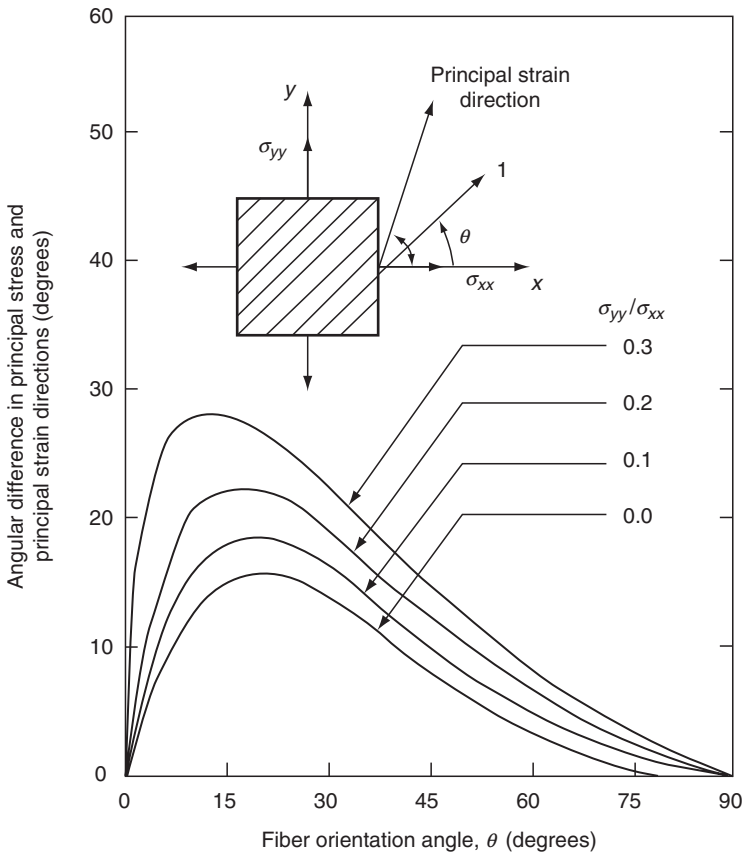


**FIGURE 3.42** Difference in principal stress and principal strain directions as a function of fiber orientation angle in an E-glass-epoxy composite ( $E_{11}/E_{22} = 2.98$ ). Note that, for the biaxial normal stress condition shown in this figure,  $\sigma_{xx}$  and  $\sigma_{yy}$  represent the principal stresses  $\sigma_1$  and  $\sigma_2$ , respectively. (After Greszczuk, L.B., *Orientation Effects in the Mechanical Behavior of Anisotropic Structural Materials*, ASTM STP, 405, 1, 1966.)

Greszczuk [22] has shown that the difference between the principal stress and principal strain directions is a function of the material orthotropy (i.e., the ratio  $E_{11}/E_{22}$ ) as well as the ratio of the two principal stresses (i.e., the ratio  $\sigma_2/\sigma_1$ , Figure 3.42).

### EXAMPLE 3.5

A thin plate is subjected to a biaxial stress field of  $\sigma_{xx} = 1$  GPa and  $\sigma_{yy} = 0.5$  GPa. Calculate the strains in the  $xy$  directions if the plate is made of (a) steel, (b) a  $0^\circ$  unidirectional boron-epoxy composite, and (c) a  $45^\circ$  unidirectional boron-epoxy composite.

Use the elastic properties of the boron-epoxy composite given in Appendix A.5.

## SOLUTION

1. Using  $E = 207$  GPa and  $\nu = 0.33$  for steel in [Equation 3.61](#), we obtain

$$\begin{aligned}\varepsilon_{xx} &= \frac{1}{207} [1 - (0.33)(0.5)] = 4.034 \times 10^{-3}, \\ \varepsilon_{yy} &= \frac{1}{207} [-(0.33)(1) + 0.5] = 0.821 \times 10^{-3}, \\ \gamma_{xy} &= 0.\end{aligned}$$

2. For the  $0^\circ$  unidirectional boron–epoxy (from [Appendix A.5](#)):

$$\begin{aligned}E_{11} &= 207 \text{ GPa (same as steel's modulus)} \\ E_{22} &= 19 \text{ GPa} \\ \nu_{12} &= 0.21 \\ G_{12} &= 6.4 \text{ GPa.}\end{aligned}$$

We first calculate  $\nu_{21}$ :

$$\nu_{21} = (0.21) \frac{19}{207} = 0.0193.$$

Since  $0^\circ$  unidirectional boron–epoxy is a specially orthotropic lamina, we use [Equations 3.67](#) through [3.69](#) to obtain

$$\begin{aligned}\varepsilon_{xx} &= \frac{1}{207} - (0.0193) \frac{0.5}{19} = 4.323 \times 10^{-3}, \\ \varepsilon_{yy} &= -(0.21) \frac{1}{207} + \frac{0.5}{19} = 25.302 \times 10^{-3}, \\ \gamma_{xy} &= 0.\end{aligned}$$

3. We first need to calculate the elastic constants of the  $45^\circ$  boron–epoxy laminate using [Equations 3.43](#) through [3.47](#):

$$\begin{aligned}E_{xx} = E_{yy} &= 18.896 \text{ GPa,} \\ \nu_{xy} = \nu_{yx} &= 0.476.\end{aligned}$$

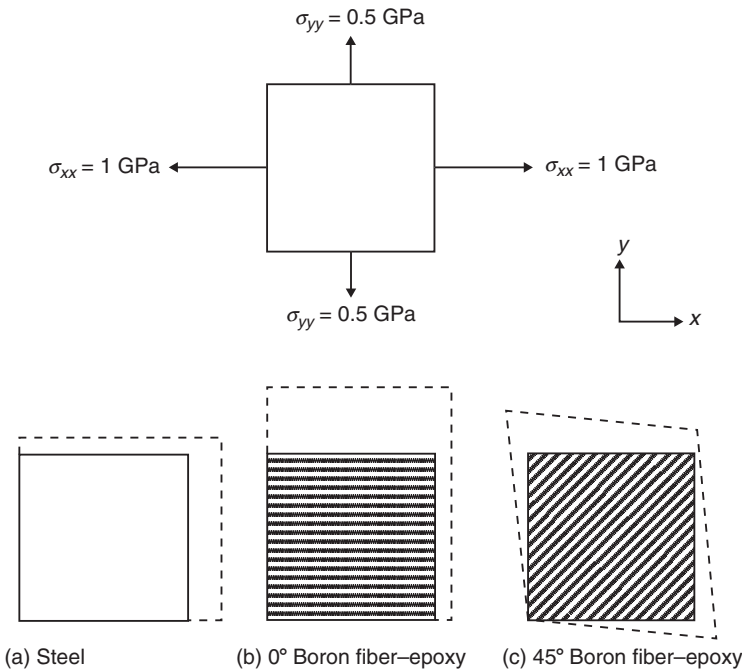
Next, we calculate the coefficients of mutual influence using [Equations 3.65](#) and [3.66](#):

$$m_x = m_y = 0.0239 \text{ GPa}^{-1}.$$

Now, we use [Equations 3.62](#) through [3.64](#) to calculate:

$$\begin{aligned}\varepsilon_{xx} &= \frac{1}{18.896} - (0.476) \frac{0.5}{18.896} = 40.326 \times 10^{-3}, \\ \varepsilon_{yy} &= -(0.476) \frac{1}{18.896} + \frac{0.5}{18.896} = 1.270 \times 10^{-3}, \\ \gamma_{xy} &= -(0.0239) (1 + 0.5) = -35.85 \times 10^{-3}.\end{aligned}$$

Note that although the shear stress is zero, there is a shear strain due to extension-shear coupling. This causes a distortion of the plate in addition to the extensions due to  $\varepsilon_{xx}$  and  $\varepsilon_{yy}$  as shown in the figure. In addition, note that a negative shear strain means that the initial  $90^\circ$  angle between the adjacent edges of the stress element is increased.



### 3.2.5 COMPLIANCE AND STIFFNESS MATRICES

#### 3.2.5.1 Isotropic Lamina

For an isotropic lamina, [Equation 3.61](#) can be written in the matrix form as

$$\begin{bmatrix} \varepsilon_{xx} \\ \varepsilon_{yy} \\ \gamma_{xy} \end{bmatrix} = \begin{bmatrix} \frac{1}{E} & -\frac{\nu}{E} & 0 \\ -\frac{\nu}{E} & \frac{1}{E} & 0 \\ 0 & 0 & \frac{1}{G} \end{bmatrix} \begin{bmatrix} \sigma_{xx} \\ \sigma_{yy} \\ \tau_{xy} \end{bmatrix} = [S] \begin{bmatrix} \sigma_{xx} \\ \sigma_{yy} \\ \tau_{xy} \end{bmatrix}, \quad (3.70)$$

where  $[S]$  represents the *compliance matrix* relating strains to known stresses. The inverse of the compliance matrix is called the *stiffness matrix*, which is used in relating stresses to known strains. Thus, the stiffness matrix  $[Q]$  for an isotropic lamina is

$$[Q] = [S]^{-1} = \begin{bmatrix} \frac{E}{1-\nu^2} & \frac{\nu E}{1-\nu^2} & 0 \\ \frac{\nu E}{1-\nu^2} & \frac{E}{1-\nu^2} & 0 \\ 0 & 0 & G \end{bmatrix}. \quad (3.71)$$

### 3.2.5.2 Specially Orthotropic Lamina ( $\theta = 0^\circ$ or $90^\circ$ )

Arranging Equations 3.67 through 3.69 in matrix form, we can write the strain–stress relation for a specially orthotropic lamina as

$$\begin{bmatrix} \epsilon_{xx} \\ \epsilon_{yy} \\ \gamma_{xy} \end{bmatrix} = \begin{bmatrix} S_{11} & S_{12} & 0 \\ S_{21}(=S_{12}) & S_{22} & 0 \\ 0 & 0 & S_{66} \end{bmatrix} \begin{bmatrix} \sigma_{xx} \\ \sigma_{yy} \\ \tau_{xy} \end{bmatrix} = [S] \begin{bmatrix} \sigma_{xx} \\ \sigma_{yy} \\ \tau_{xy} \end{bmatrix}, \quad (3.72)$$

where

$$\begin{aligned} S_{11} &= \frac{1}{E_{11}} \\ S_{12} = S_{21} &= -\frac{\nu_{12}}{E_{11}} = -\frac{\nu_{21}}{E_{22}} \\ S_{22} &= \frac{1}{E_{22}} \\ S_{66} &= \frac{1}{G_{12}} \end{aligned} \quad (3.73)$$

The  $[S]$  matrix is the compliance matrix for the specially orthotropic lamina. Inverting Equation 3.72, we can write the stress–strain relations for a specially orthotropic lamina as

$$\begin{bmatrix} \sigma_{xx} \\ \sigma_{yy} \\ \tau_{xy} \end{bmatrix} = \begin{bmatrix} Q_{11} & Q_{12} & 0 \\ Q_{21}(=Q_{12}) & Q_{22} & 0 \\ 0 & 0 & Q_{66} \end{bmatrix} \begin{bmatrix} \epsilon_{xx} \\ \epsilon_{yy} \\ \gamma_{xy} \end{bmatrix} = [Q] \begin{bmatrix} \epsilon_{xx} \\ \epsilon_{yy} \\ \gamma_{xy} \end{bmatrix}, \quad (3.74)$$

where  $[Q]$  represents the stiffness matrix for the specially orthotropic lamina. Various elements in the  $[Q]$  matrix are

$$\begin{aligned}
Q_{11} &= \frac{E_{11}}{1 - \nu_{12}\nu_{21}}, \\
Q_{22} &= \frac{E_{22}}{1 - \nu_{12}\nu_{21}}, \\
Q_{12} = Q_{21} &= \frac{\nu_{12}E_{22}}{1 - \nu_{12}\nu_{21}} = \frac{\nu_{21}E_{11}}{1 - \nu_{12}\nu_{21}}, \\
Q_{66} &= G_{12}.
\end{aligned} \tag{3.75}$$

### 3.2.5.3 General Orthotropic Lamina ( $\theta \neq 0^\circ$ or $90^\circ$ )

The strain–stress relations for a general orthotropic lamina, [Equations 3.62](#) through [3.64](#), can be expressed in matrix notation as

$$\begin{bmatrix} \varepsilon_{xx} \\ \varepsilon_{yy} \\ \gamma_{xy} \end{bmatrix} = \begin{bmatrix} \bar{S}_{11} & \bar{S}_{12} & \bar{S}_{16} \\ \bar{S}_{12} & \bar{S}_{22} & \bar{S}_{26} \\ \bar{S}_{16} & \bar{S}_{26} & \bar{S}_{66} \end{bmatrix} \begin{bmatrix} \sigma_{xx} \\ \sigma_{yy} \\ \tau_{xy} \end{bmatrix} = [\bar{S}] \begin{bmatrix} \sigma_{xx} \\ \sigma_{yy} \\ \tau_{xy} \end{bmatrix}, \tag{3.76}$$

where  $[\bar{S}]$  represents the compliance matrix for the lamina. Various elements in the  $[\bar{S}]$  matrix are expressed in terms of the elements in the  $[S]$  matrix for a specially orthotropic lamina. These expressions are

$$\begin{aligned}
\bar{S}_{11} &= \frac{1}{E_{xx}} = S_{11} \cos^4 \theta + (2S_{12} + S_{66}) \sin^2 \theta \cos^2 \theta + S_{22} \sin^4 \theta, \\
\bar{S}_{12} &= -\frac{\nu_{xy}}{E_{xx}} = S_{12}(\sin^4 \theta + \cos^4 \theta) + (S_{11} + S_{22} - S_{66}) \sin^2 \theta \cos^2 \theta, \\
\bar{S}_{22} &= \frac{1}{E_{yy}} = S_{11} \sin^4 \theta + (2S_{12} + S_{66}) \sin^2 \theta \cos^2 \theta + S_{22} \cos^4 \theta, \\
\bar{S}_{16} &= -m_x = (2S_{11} - 2S_{12} - S_{66}) \sin \theta \cos^3 \theta - (2S_{22} - 2S_{12} - S_{66}) \sin^3 \theta \cos \theta, \\
\bar{S}_{26} &= -m_y = (2S_{11} - 2S_{12} - S_{66}) \sin^3 \theta \cos \theta - (2S_{22} - 2S_{12} - S_{66}) \sin \theta \cos^3 \theta, \\
\bar{S}_{66} &= \frac{1}{G_{xy}} = 2(2S_{11} + 2S_{22} - 4S_{12} - S_{66}) \sin^2 \theta \cos^2 \theta + S_{66}(\sin^4 \theta + \cos^4 \theta).
\end{aligned} \tag{3.77}$$

On substitution for  $S_{11}$ ,  $S_{12}$ , and so on, into Equation 3.77, we obtain the same equations as [Equations 3.43](#) through [3.46](#) for  $E_{xx}$ ,  $E_{yy}$ ,  $G_{xy}$ , and  $\nu_{xy}$ , and [Equations 3.65](#) and [3.66](#) for  $m_x$  and  $m_y$ .

Inverting Equation 3.76, the stress–strain relations for a general orthotropic lamina can be written as

$$\begin{bmatrix} \sigma_{xx} \\ \sigma_{yy} \\ \tau_{xy} \end{bmatrix} = \begin{bmatrix} \bar{Q}_{11} & \bar{Q}_{12} & \bar{Q}_{16} \\ \bar{Q}_{12} & \bar{Q}_{22} & \bar{Q}_{26} \\ \bar{Q}_{16} & \bar{Q}_{26} & \bar{Q}_{66} \end{bmatrix} \begin{bmatrix} \varepsilon_{xx} \\ \varepsilon_{yy} \\ \gamma_{xy} \end{bmatrix} = [\bar{Q}] \begin{bmatrix} \sigma_{xx} \\ \sigma_{yy} \\ \gamma_{xy} \end{bmatrix}, \tag{3.78}$$

where  $[\bar{Q}]$  represents the stiffness matrix for the lamina. Various elements in the  $[\bar{Q}]$  matrix are expressed in terms of the elements in the  $[Q]$  matrix as

$$\begin{aligned}
 \bar{Q}_{11} &= Q_{11} \cos^4 \theta + 2(Q_{12} + 2Q_{66}) \sin^2 \theta \cos^2 \theta + Q_{22} \sin^4 \theta, \\
 \bar{Q}_{12} &= Q_{12}(\sin^4 \theta + \cos^4 \theta) + (Q_{11} + Q_{22} - 4Q_{66}) \sin^2 \theta \cos^2 \theta, \\
 \bar{Q}_{22} &= Q_{11} \sin^4 \theta + 2(Q_{12} + 2Q_{66}) \sin^2 \theta \cos^2 \theta + Q_{22} \cos^4 \theta, \\
 \bar{Q}_{16} &= (Q_{11} - Q_{12} - 2Q_{66}) \sin \theta \cos^3 \theta + (Q_{12} - Q_{22} + 2Q_{66}) \sin^3 \theta \cos \theta, \\
 \bar{Q}_{26} &= (Q_{11} - Q_{12} - 2Q_{66}) \sin^3 \theta \cos \theta + (Q_{12} - Q_{22} + 2Q_{66}) \sin \theta \cos^3 \theta, \\
 \bar{Q}_{66} &= (Q_{11} + Q_{22} - 2Q_{12} - 2Q_{66}) \sin^2 \theta \cos^2 \theta + Q_{66}(\sin^4 \theta + \cos^4 \theta). \quad (3.79)
 \end{aligned}$$

In using [Equations 3.77](#) and 3.79, the following points should be noted:

1. Elements  $\bar{S}_{16}$  and  $\bar{S}_{26}$  in the  $[\bar{S}]$  matrix or  $\bar{Q}_{16}$  and  $\bar{Q}_{26}$  in the  $[\bar{Q}]$  matrix represent extension-shear coupling.
2. From [Equation 3.77](#) or 3.79, it appears that there are six elastic constants that govern the stress-strain behavior of a lamina. However, a closer examination of these equations would indicate that  $\bar{S}_{16}$  and  $\bar{S}_{26}$  (or  $\bar{Q}_{16}$  and  $\bar{Q}_{26}$ ) are linear combinations of the four basic elastic constants, namely,  $\bar{S}_{11}$ ,  $\bar{S}_{12}$ ,  $\bar{S}_{22}$ , and  $\bar{S}_{66}$ , and therefore are not independent.
3. Elements in both the  $[\bar{S}]$  and  $[\bar{Q}]$  matrices are expressed in terms of the properties in the principal material directions, namely,  $E_{11}$ ,  $E_{22}$ ,  $G_{12}$ , and  $\nu_{12}$ , which can be either experimentally determined or predicted from the constituent properties using [Equations 3.36](#) through [3.40](#).
4. Elements in the  $[\bar{Q}]$  and  $[\bar{S}]$  matrices can be expressed in terms of five invariant properties of the lamina, as shown below.

Using trigonometric identities, Tsai and Pagano [23] have shown that the elements in the  $[\bar{Q}]$  matrix can be written as

$$\begin{aligned}
 \bar{Q}_{11} &= U_1 + U_2 \cos 2\theta + U_3 \cos 4\theta, \\
 \bar{Q}_{12} &= \bar{Q}_{21} = U_4 - U_3 \cos 4\theta, \\
 \bar{Q}_{22} &= U_1 - U_2 \cos 2\theta + U_3 \cos 4\theta, \\
 \bar{Q}_{16} &= \frac{1}{2} U_2 \sin 2\theta + U_3 \sin 4\theta, \\
 \bar{Q}_{26} &= \frac{1}{2} U_2 \sin 2\theta - U_3 \sin 4\theta, \\
 \bar{Q}_{66} &= U_5 - U_3 \cos 4\theta, \quad (3.80)
 \end{aligned}$$

where  $U_1$  through  $U_5$  represent angle-invariant stiffness properties of a lamina and are given as

$$\begin{aligned}
U_1 &= \frac{1}{8}(3Q_{11} + 3Q_{22} + 2Q_{12} + 4Q_{66}), \\
U_2 &= \frac{1}{2}(Q_{11} - Q_{22}), \\
U_3 &= \frac{1}{8}(Q_{11} + Q_{22} - 2Q_{12} - 4Q_{66}), \\
U_4 &= \frac{1}{8}(Q_{11} + Q_{22} + 6Q_{12} - 4Q_{66}), \\
U_5 &= \frac{1}{2}(U_1 - U_4).
\end{aligned} \tag{3.81}$$

It is easy to observe from Equation 3.80 that for fiber orientation angles  $\theta$  and  $-\theta$ ,

$$\begin{aligned}
\bar{Q}_{11}(-\theta) &= \bar{Q}_{11}(\theta), \\
\bar{Q}_{12}(-\theta) &= \bar{Q}_{12}(\theta), \\
\bar{Q}_{22}(-\theta) &= \bar{Q}_{22}(\theta), \\
\bar{Q}_{66}(-\theta) &= \bar{Q}_{66}(\theta), \\
\bar{Q}_{16}(-\theta) &= -\bar{Q}_{16}(\theta), \\
\bar{Q}_{26}(-\theta) &= -\bar{Q}_{26}(\theta).
\end{aligned}$$

Similar expressions for the elements in the  $[\bar{S}]$  matrix are

$$\begin{aligned}
\bar{S}_{11} &= V_1 + V_2 \cos 2\theta + V_3 \cos 4\theta, \\
\bar{S}_{12} = \bar{S}_{21} &= V_4 - V_3 \cos 4\theta, \\
\bar{S}_{22} &= V_1 - V_2 \cos 2\theta + V_3 \cos 4\theta, \\
\bar{S}_{16} &= V_2 \sin 2\theta + 2V_3 \sin 4\theta, \\
\bar{S}_{26} &= V_2 \sin 2\theta - 2V_3 \sin 4\theta, \\
\bar{S}_{66} &= V_5 - 4V_3 \cos 4\theta,
\end{aligned} \tag{3.82}$$

where

$$\begin{aligned}
V_1 &= \frac{1}{8}(3S_{11} + 3S_{22} + 2S_{12} + S_{66}), \\
V_2 &= \frac{1}{2}(S_{11} - S_{22}), \\
V_3 &= \frac{1}{8}(S_{11} + S_{22} - 2S_{12} - S_{66}), \\
V_4 &= \frac{1}{8}(S_{11} + S_{22} + 6S_{12} - S_{66}), \\
V_5 &= 2(V_1 - V_4).
\end{aligned} \tag{3.83}$$

These invariant forms are very useful in computing the elements in  $[\bar{Q}]$  and  $[\bar{S}]$  matrices for a lamina.

### EXAMPLE 3.6

Determine the elements in the stiffness matrix for an angle-ply lamina containing 60 vol% of T-300 carbon fibers in an epoxy matrix. Consider fiber orientation angles of both  $+45^\circ$  and  $-45^\circ$  for the fiber,  $E_f = 220$  GPa and  $\nu_f = 0.2$ , and for the matrix,  $E_m = 3.6$  GPa and  $\nu_m = 0.35$ .

#### SOLUTION

Step 1: Calculate  $E_{11}$ ,  $E_{22}$ ,  $\nu_{12}$ ,  $\nu_{21}$ , and  $G_{12}$  using Equations 3.36 through 3.40.

$$E_{11} = (220)(0.6) + (3.6)(1 - 0.6) = 133.44 \text{ GPa,}$$

$$E_{22} = \frac{(220)(3.6)}{(220)(1 - 0.6) + (3.6)(0.6)} = 8.78 \text{ GPa,}$$

$$\nu_{12} = (0.2)(0.6) + (0.35)(1 - 0.6) = 0.26,$$

$$\nu_{21} = \frac{8.78}{133.44}(0.26) = 0.017.$$

To calculate  $G_{12}$ , we need to know the values of  $G_f$  and  $G_m$ . Assuming isotropic relationships, we estimate

$$G_f = \frac{E_f}{2(1 + \nu_f)} = \frac{220}{2(1 + 0.2)} = 91.7 \text{ GPa,}$$

$$G_m = \frac{E_m}{2(1 + \nu_m)} = \frac{3.6}{2(1 + 0.35)} = 1.33 \text{ GPa.}$$

Therefore,

$$G_{12} = \frac{(91.7)(1.33)}{(91.7)(1 - 0.6) + (1.33)(0.6)} = 3.254 \text{ GPa.}$$

Note that the T-300 carbon fiber is not isotropic, and therefore, the calculation of  $G_f$  based on the isotropic assumption will certainly introduce error. Since the actual value of  $G_f$  is not always available, the isotropic assumption is often made to calculate  $G_f$ .

Step 2: Calculate  $Q_{11}$ ,  $Q_{22}$ ,  $Q_{12}$ ,  $Q_{21}$ , and  $Q_{66}$  using Equation 3.75.

$$Q_{11} = \frac{133.44}{1 - (0.26)(0.017)} = 134.03 \text{ GPa,}$$

$$Q_{22} = \frac{8.78}{1 - (0.26)(0.017)} = 8.82 \text{ GPa,}$$

$$Q_{12} = Q_{21} = \frac{(0.26)(8.78)}{1 - (0.26)(0.017)} = 2.29 \text{ GPa,}$$

$$Q_{66} = 3.254 \text{ GPa.}$$

Step 3: Calculate  $U_1$ ,  $U_2$ ,  $U_3$ ,  $U_4$ , and  $U_5$  using Equation 3.81.

$$U_1 = \frac{1}{8}[(3)(134.03) + (3)(8.82) + (2)(2.29) + (4)(3.254)] = 55.77 \text{ GPa},$$

$$U_2 = \frac{1}{2}(134.03 - 8.82) = 62.6 \text{ GPa},$$

$$U_3 = \frac{1}{8}[134.03 + 8.82 - (2)(2.29) - (4)(3.254)] = 15.66 \text{ GPa},$$

$$U_4 = \frac{1}{8}[134.03 + 8.82 + (6)(2.29) - (4)(3.259)] = 17.95 \text{ GPa},$$

$$U_5 = \frac{1}{2}(55.77 - 17.95) = 18.91 \text{ GPa}.$$

Step 4: Calculate  $\bar{Q}_{11}$ ,  $\bar{Q}_{22}$ ,  $\bar{Q}_{12}$ ,  $\bar{Q}_{16}$ ,  $\bar{Q}_{26}$ , and  $\bar{Q}_{66}$  using Equation 3.80. For a  $\theta = +45^\circ$  lamina,

$$\bar{Q}_{11} = 55.77 + (62.6) \cos 90^\circ + (15.66) \cos 180^\circ = 40.11 \text{ GPa},$$

$$\bar{Q}_{22} = 55.77 - (62.6) \cos 90^\circ + (15.66) \cos 180^\circ = 40.11 \text{ GPa},$$

$$\bar{Q}_{12} = 17.95 - (15.66) \cos 180^\circ = 33.61 \text{ GPa},$$

$$\bar{Q}_{66} = 18.91 - (15.66) \cos 180^\circ = 34.57 \text{ GPa},$$

$$\bar{Q}_{16} = \frac{1}{2}(62.6) \sin 90^\circ + (15.66) \sin 180^\circ = 31.3 \text{ GPa},$$

$$\bar{Q}_{26} = \frac{1}{2}(62.6) \sin 90^\circ - (15.66) \sin 180^\circ = 31.3 \text{ GPa}.$$

Similarly, for a  $\theta = -45^\circ$  lamina,

$$\bar{Q}_{11} = 40.11 \text{ GPa},$$

$$\bar{Q}_{22} = 40.11 \text{ GPa},$$

$$\bar{Q}_{12} = 33.61 \text{ GPa},$$

$$\bar{Q}_{66} = 34.57 \text{ GPa},$$

$$\bar{Q}_{16} = -31.3 \text{ GPa},$$

$$\bar{Q}_{26} = -31.3 \text{ GPa}.$$

In the matrix form,

$$[\bar{Q}]_{45^\circ} = \begin{bmatrix} 40.11 & 33.61 & 31.3 \\ 33.61 & 40.11 & 31.3 \\ 31.3 & 31.3 & 34.57 \end{bmatrix} \text{ GPa},$$

$$[\bar{Q}]_{-45^\circ} = \begin{bmatrix} 40.11 & 33.61 & -31.3 \\ 33.61 & 40.11 & -31.3 \\ -31.3 & -31.3 & 34.57 \end{bmatrix} \text{ GPa}.$$

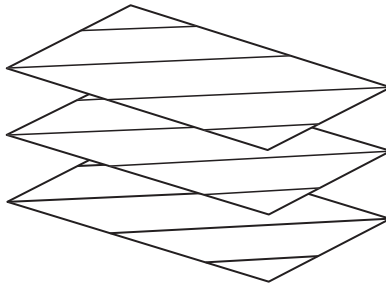


FIGURE 3.43 Unidirectional laminate.

### 3.3 LAMINATED STRUCTURE

#### 3.3.1 FROM LAMINA TO LAMINATE

A laminate is constructed by stacking a number of laminas in the thickness ( $z$ ) direction. Examples of a few special types of laminates and the standard lamination code are given as follows:

*Unidirectional laminate:* In a unidirectional laminate (Figure 3.43), fiber orientation angles are the same in all laminas. In unidirectional  $0^\circ$  laminates, for example,  $\theta = 0^\circ$  in all laminas.

*Angle-ply laminate:* In an angle-ply laminate (Figure 3.44), fiber orientation angles in alternate layers are  $/\theta/ -\theta/ \theta/ -\theta/$  when  $\theta \neq 0^\circ$  or  $90^\circ$ .

*Cross-ply laminate:* In a cross-ply laminate (Figure 3.45), fiber orientation angles in alternate layers are  $/0^\circ/ 90^\circ/ 0^\circ/ 90^\circ/$ .

*Symmetric laminate:* In a symmetric laminate, the ply orientation is symmetrical about the centerline of the laminate; that is, for each ply above the midplane, there is an identical ply (in material, thickness, and fiber orientation angle) at an equal distance below the midplane. Thus, for a symmetric laminate,

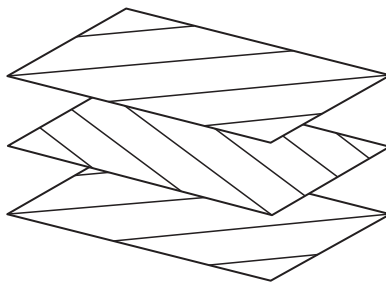
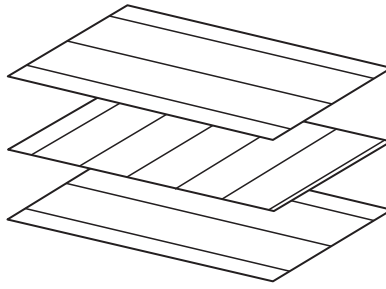


FIGURE 3.44 Angle-ply laminate.



**FIGURE 3.45** Cross-ply laminate.

$$\theta(z) = \theta(-z),$$

where  $z$  is the distance from the midplane of the laminate. Some examples of symmetric laminates and their codes are listed.

1.            1   2   3   4   5   6  
               [0/+45/90/90 +45/0]  
 Code:            [0/45/90]<sub>S</sub>

Subscript S in the code indicates symmetry about the midplane.

2.            1   2   3   4   5  
               [0/+45/90/ $\overline{+45}$ /0]  
 Code:            [0/45/ $\overline{90}$ ]<sub>S</sub>

The bar over 90 indicates that the plane of symmetry passes midway through the thickness of the 90° lamina.

3.            1   2   3   4   5   6   7  
               [0/+45/ $\overline{-45}$ /90/ $\overline{-45}$ / $\overline{+45}$ /0]  
 Code:            [0/ $\pm 45$ / $\overline{90}$ ]<sub>S</sub>

Adjacent +45° and -45° laminas are grouped as  $\pm 45^\circ$ .

4.            1   2   3   4   5   6   7   8   9   10   11   12   13   14  
               [0/90/0/0/0/0/0/45/45/0/0/0/0/90/0]  
 Code:            [0/90/0<sub>4</sub>/45]<sub>S</sub>

Four adjacent 0° plies are grouped together as 0<sub>4</sub>.

5.            1   2   3   4   5   6   7   8   9   10  
               [0/45/ $\overline{-45}$ / $\overline{+45}$ / $\overline{-45}$ / $\overline{-45}$ / $\overline{+45}$ / $\overline{-45}$ / $\overline{+45}$ /0]  
 Code:            [0/( $\pm 45$ )<sub>2</sub>]<sub>S</sub>

Two adjacent  $\pm 45^\circ$  plies are grouped as  $(\pm 45)_2$ .

6.  $[0/45/-45/45/-45/45/-45/0/0/0/0/0/-45/45/-45/45/-45/45/0]$   
Code:  $[0/(\pm 45)_3/0_2/\bar{0}]_S$

7.  $[\theta/-\theta/\theta/-\theta/-\theta/\theta/-\theta/\theta]$   
Code:  $[\theta/-\theta]_{2S}$  or  $[\pm\theta]_{2S}$

Two adjacent  $\pm\theta$  plies on each side of the plane of symmetry are denoted by the subscript 2S.

8. Symmetric angle-ply laminate  
 $[\theta/ -\theta/ \theta/-\theta/\theta/-\theta/\theta]$   
Code:  $[\pm\theta/\theta/-\bar{\theta}]_S$

Note that symmetric angle-ply laminates contain an odd number of plies.

9. Symmetric cross-ply laminate  
 $[0/90/0/90/0/90/0/90/0]$   
Code:  $[(0/90)_2/\bar{0}]_S$

Note that symmetric cross-ply laminates contain an odd number of plies.

10. Hybrid (interply) laminate.  
 $[0_B/0_B/45_C/-45_C/90_G/90_G/-45_C/45_C/0_B/0_B]$   
Code:  $[0_{2B}/(\pm 45)_C/90_G]_S$

where B, C, and G represent boron, carbon, and glass fiber, respectively.

*Antisymmetric laminate:* In antisymmetric laminates, the ply orientation is antisymmetric about the centerline of the laminate; that is, for each ply of fiber orientation angle  $\theta$  above the midplane, there is a ply of fiber orientation angle  $-\theta$  with identical material and thickness at an equal distance below the midplane. Thus, for an antisymmetric laminate,

$$\theta(z) = -\theta(-z).$$

For example,  $\theta/ -\theta/ \theta / -\theta$  is an antisymmetric laminate. In contrast,  $\theta/-\theta/-\theta/\theta$  is symmetric.

*Unsymmetric laminate:* In unsymmetric laminates, there is no symmetry or antisymmetry. Examples are  $0/0/0/90/90/90$  and  $0/\theta/-\theta/90$ .

*Quasi-isotropic laminate:* These laminates are made of three or more laminas of identical thickness and material with equal angles between each adjacent lamina. Thus, if the total number of laminas is  $n$ , the orientation angles of the laminas are at increments of  $\pi/n$ . The resulting laminate

exhibits an in-plane isotropic elastic behavior in the  $xy$  plane. However, its strength properties may still vary with the direction of loading. Examples of simple quasi-isotropic laminates are  $[+60/0/-60]$  and  $[+45/0/-45/90]$ . Other combinations of these stacking sequences, such as  $[0/+60/-60]$  and  $[0/+45/-45/90]$ , also exhibit in-plane isotropic elastic behavior. A very common and widely used quasi-isotropic symmetrical stacking sequence is  $[0/\pm 45/90]_S$ .

### 3.3.2 LAMINATION THEORY

Lamination theory is useful in calculating stresses and strains in each lamina of a thin laminated structure. Beginning with the stiffness matrix of each lamina, the step-by-step procedure in lamination theory includes

1. Calculation of stiffness matrices for the laminate
2. Calculation of midplane strains and curvatures for the laminate due to a given set of applied forces and moments
3. Calculation of in-plane strains  $\epsilon_{xx}$ ,  $\epsilon_{yy}$ , and  $\gamma_{xy}$  for each lamina
4. Calculation of in-plane stresses  $\sigma_{xx}$ ,  $\sigma_{yy}$ , and  $\tau_{xy}$  in each lamina

The derivation of lamination theory is given in Ref. [16]. The principal equations and a number of examples are presented in the following sections.

#### 3.3.2.1 Assumptions

Basic assumptions in the lamination theory are

1. Laminate is thin and wide (width  $\gg$  thickness).
2. A perfect interlaminar bond exists between various laminas.
3. Strain distribution in the thickness direction is linear.
4. All laminas are macroscopically homogeneous and behave in a linearly elastic manner.

The geometric midplane of the laminate contains the  $xy$  axes, and the  $z$  axis defines the thickness direction. The total thickness of the laminate is  $h$ , and the thickness of various laminas are represented by  $t_1$ ,  $t_2$ ,  $t_3$ , and so on. The total number of laminas is  $N$ . A sketch for the laminate is shown in [Figure 3.46](#).

#### 3.3.2.2 Laminate Strains

Following assumption 3, laminate strains are linearly related to the distance from the midplane as

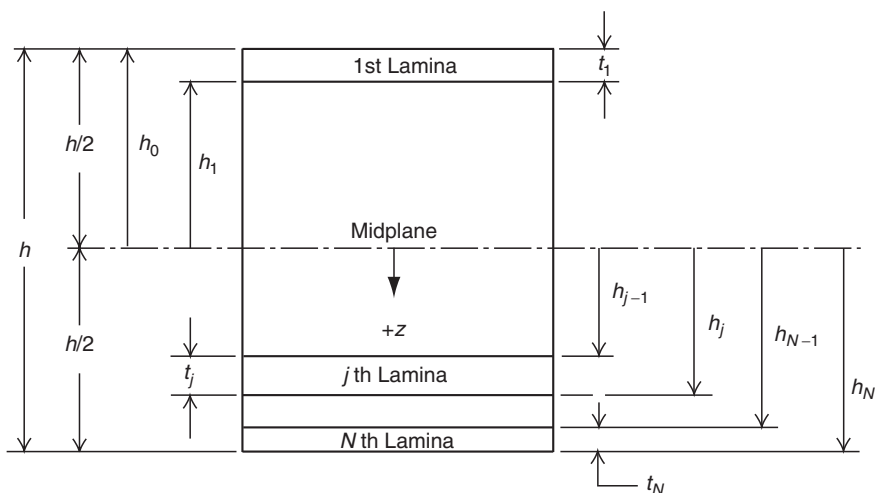


FIGURE 3.46 Laminate geometry.

$$\begin{aligned}
 \varepsilon_{xx} &= \varepsilon_{xx}^{\circ} + zk_{xx}, \\
 \varepsilon_{yy} &= \varepsilon_{yy}^{\circ} + zk_{yy}, \\
 \gamma_{xy} &= \gamma_{xy}^{\circ} + zk_{xy},
 \end{aligned}
 \tag{3.84}$$

where

- $\varepsilon_{xx}^{\circ}, \varepsilon_{yy}^{\circ}$  = midplane normal strains in the laminate
- $\gamma_{xy}^{\circ}$  = midplane shear strain in the laminate
- $k_{xx}, k_{yy}$  = bending curvatures of the laminate
- $k_{xy}$  = twisting curvature of the laminate
- $z$  = distance from the midplane in the thickness direction

### 3.3.2.3 Laminate Forces and Moments

Applied force and moment resultant (Figure 3.47) on a laminate are related to the midplane strains and curvatures by the following equations:

$$\begin{aligned}
 N_{xx} &= A_{11}\varepsilon_{xx}^{\circ} + A_{12}\varepsilon_{yy}^{\circ} + A_{16}\gamma_{xy}^{\circ} + B_{11}k_{xx} + B_{12}k_{yy} + B_{16}k_{xy}, \\
 N_{yy} &= A_{12}\varepsilon_{xx}^{\circ} + A_{22}\varepsilon_{yy}^{\circ} + A_{26}\gamma_{xy}^{\circ} + B_{12}k_{xx} + B_{22}k_{yy} + B_{26}k_{xy}, \\
 N_{xy} &= A_{16}\varepsilon_{xx}^{\circ} + A_{26}\varepsilon_{yy}^{\circ} + A_{66}\gamma_{xy}^{\circ} + B_{16}k_{xx} + B_{26}k_{yy} + B_{66}k_{xy}, \\
 M_{xx} &= B_{11}\varepsilon_{xx}^{\circ} + B_{12}\varepsilon_{yy}^{\circ} + B_{16}\gamma_{xy}^{\circ} + D_{11}k_{xx} + D_{12}k_{yy} + D_{16}k_{xy}, \\
 M_{yy} &= B_{12}\varepsilon_{xx}^{\circ} + B_{22}\varepsilon_{yy}^{\circ} + B_{26}\gamma_{xy}^{\circ} + D_{12}k_{xx} + D_{22}k_{yy} + D_{26}k_{xy}, \\
 M_{xy} &= B_{16}\varepsilon_{xx}^{\circ} + B_{26}\varepsilon_{yy}^{\circ} + B_{66}\gamma_{xy}^{\circ} + D_{16}k_{xx} + D_{26}k_{yy} + D_{66}k_{xy}.
 \end{aligned}$$

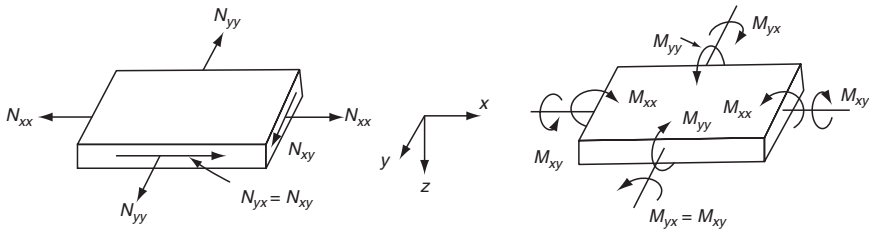


**FIGURE 3.47** In-plane, bending, and twisting loads applied on a laminate.

In matrix notation,

$$\begin{bmatrix} N_{xx} \\ N_{yy} \\ N_{xy} \end{bmatrix} = [A] \begin{bmatrix} \epsilon_{xx}^{\circ} \\ \epsilon_{yy}^{\circ} \\ \gamma_{xy}^{\circ} \end{bmatrix} + [B] \begin{bmatrix} k_{xx} \\ k_{yy} \\ k_{xy} \end{bmatrix} \quad (3.85)$$

and

$$\begin{bmatrix} M_{xx} \\ M_{yy} \\ M_{xy} \end{bmatrix} = [B] \begin{bmatrix} \epsilon_{xx}^{\circ} \\ \epsilon_{yy}^{\circ} \\ \gamma_{xy}^{\circ} \end{bmatrix} + [D] \begin{bmatrix} k_{xx} \\ k_{yy} \\ k_{xy} \end{bmatrix}, \quad (3.86)$$

where

- $N_{xx}$  = normal force resultant in the  $x$  direction (per unit width)
- $N_{yy}$  = normal force resultant in the  $y$  direction (per unit width)
- $N_{xy}$  = shear force resultant (per unit width)
- $M_{xx}$  = bending moment resultant in the  $yz$  plane (per unit width)
- $M_{yy}$  = bending moment resultant in the  $xz$  plane (per unit width)
- $M_{xy}$  = twisting moment (torsion) resultant (per unit width)

$[A]$  = extensional stiffness matrix for the laminate (unit: N/m or lb/in.)

$$[A] = \begin{bmatrix} A_{11} & A_{12} & A_{16} \\ A_{12} & A_{22} & A_{26} \\ A_{16} & A_{26} & A_{66} \end{bmatrix}, \quad (3.87)$$

$[B]$  = coupling stiffness matrix for the laminate (unit: N or lb)

$$[B] = \begin{bmatrix} B_{11} & B_{12} & B_{16} \\ B_{12} & B_{22} & B_{26} \\ B_{16} & B_{26} & B_{66} \end{bmatrix}, \quad (3.88)$$

$[D]$  = bending stiffness matrix for the laminate (unit: N m or lb in.)

$$[D] = \begin{bmatrix} D_{11} & D_{12} & D_{16} \\ D_{12} & D_{22} & D_{26} \\ D_{16} & D_{26} & D_{66} \end{bmatrix}. \quad (3.89)$$

Referring to [Equation 3.85](#), it can be observed that

1.  $A_{16}$  and  $A_{26}$  couple in-plane normal forces to midplane shear strain and in-plane shear force to midplane normal strains.
2.  $B_{11}$ ,  $B_{12}$ , and  $B_{22}$  couple in-plane normal forces to bending curvatures and bending moments to midplane normal strains.
3.  $B_{16}$  and  $B_{26}$  couple in-plane normal forces to twisting curvature and twisting moment to midplane normal strains.
4.  $B_{66}$  couples in-plane shear force to twisting curvature and twisting moment to midplane shear strain.
5.  $D_{16}$  and  $D_{26}$  couple bending moments to twisting curvature and twisting moment to bending curvatures.

The couplings between normal forces and shear strains, bending moments and twisting curvatures, and so on, occur only in laminated structures and not in a monolithic structure. If the laminate is properly constructed, some of these couplings can be eliminated. For example, if the laminate is constructed such that both  $A_{16}$  and  $A_{26} = 0$ , there will be no coupling between in-plane normal forces and midplane shear strains, that is, in-plane normal forces will not cause shear deformation of the laminate. Similarly, if the laminate is constructed such that both  $D_{16}$  and  $D_{26} = 0$ , there will be coupling between bending moments and twisting curvature, that is, bending moments will not cause twisting of the laminate. These special constructions are described in the following section.

### 3.3.2.4 Elements in Stiffness Matrices

The elements in  $[A]$ ,  $[B]$ , and  $[D]$  matrices are calculated from

$$A_{mn} = \sum_{j=1}^N (\bar{Q}_{mn})_j (h_j - h_{j-1}), \quad (3.90)$$

$$B_{mn} = \frac{1}{2} \sum_{j=1}^N (\bar{Q}_{mn})_j (h_j^2 - h_{j-1}^2), \quad (3.91)$$

$$D_{mn} = \frac{1}{3} \sum_{j=1}^N (\bar{Q}_{mn})_j (h_j^3 - h_{j-1}^3), \quad (3.92)$$

where

- $N$  = total number of laminas in the laminate
- $(\bar{Q}_{mn})_j$  = elements in the  $[\bar{Q}]$  matrix of the  $j$ th lamina
- $h_{j-1}$  = distance from the midplane to the top of the  $j$ th lamina
- $h_j$  = distance from the midplane to the bottom of the  $j$ th lamina

For the coordinate system shown in Figure 3.46,  $h_j$  is positive below the midplane and negative above the midplane.

The elements of the stiffness matrices  $[A]$ ,  $[B]$ , and  $[D]$  are functions of the elastic properties of each lamina and its location with respect to the midplane of the laminate. The following observations are important regarding these stiffness matrices:

1. If  $[B]$  is a nonzero matrix, a normal force, such as  $N_{xx}$ , will create extension and shear deformations as well as bending-twisting curvatures. Similarly, a bending moment, such as  $M_{xx}$ , will create bending and twisting curvatures as well as extension-shear deformations. Such “extension-bending coupling,” represented by the  $[B]$  matrix, is unique in laminated structures regardless of whether the layers are isotropic or orthotropic. The coupling occurs because of the stacking of layers.
2. For a *symmetric* laminate,  $[B] = [0]$  and there is no extension-bending coupling. To construct a symmetric laminate, every lamina of  $+\theta$  orientation above the midplane must be matched with an identical (in thickness and material) lamina of  $+\theta$  orientation at the same distance below the midplane (Figure 3.48). Note that a symmetric angle-ply or cross-ply laminate contains an odd number of plies.

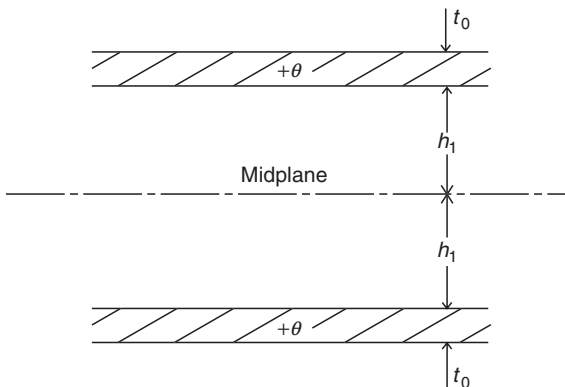


**FIGURE 3.48** Symmetric laminate configuration for which  $[B] = [0]$ , and therefore no extension-bending coupling.

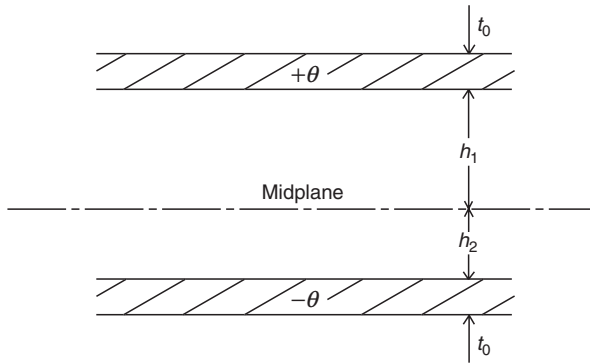


**FIGURE 3.49** Balanced laminate configuration for which  $A_{16} = A_{26} = 0$ , and therefore no extension-shear coupling.

3. If for every lamina of  $+\theta$  orientation, there is an identical (equal in thickness and material) lamina of  $-\theta$  orientation (Figure 3.49), the normal stress–shear strain coupling (represented by  $A_{16}$  and  $A_{26}$  in the  $[A]$  matrix) for the laminate is zero. The locations of these two laminas are arbitrary. Such a laminate is called *balanced*; for example,  $[0/+30/-30/+30/-30/0]$  is a balanced laminate for which  $A_{16} = A_{26} = 0$ . Note that, with proper positioning of layers, it is possible to prepare a balanced symmetric laminate. For example,  $[0/+30/-30/-30/+30/0]$  is a balanced symmetric laminate, for which  $A_{16} = A_{26} = 0$  as well as  $[B] = [0]$ .
4. If for every lamina of  $+\theta$  orientation above the midplane, there is an identical lamina (in thickness and material) of  $-\theta$  orientation at the same distance below the midplane (Figure 3.50), the bending

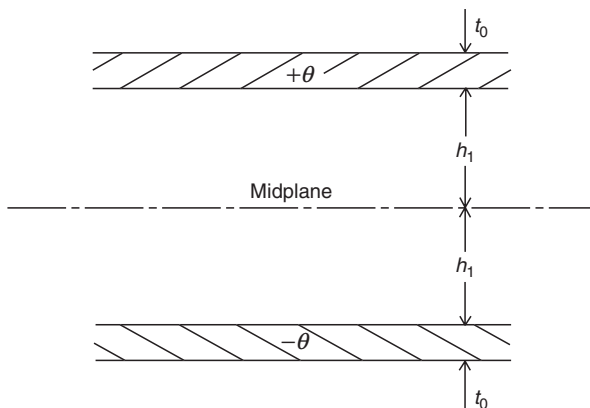
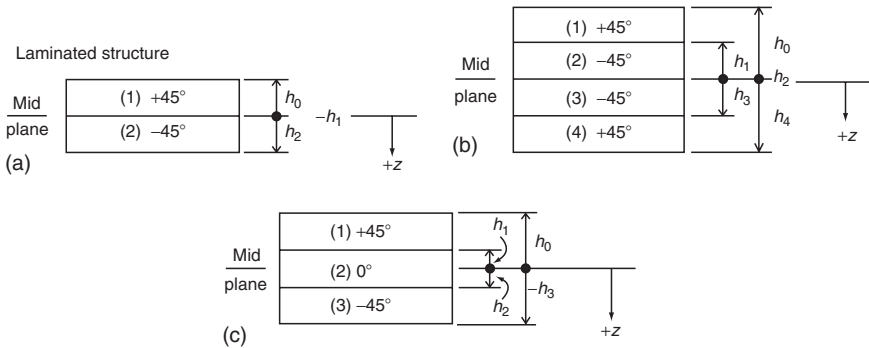


**FIGURE 3.50** Laminate configuration for which  $D_{16} = D_{26} = 0$ , and therefore no bending-twisting coupling.

moment-twisting curvature coupling (represented by  $D_{16}$  and  $D_{26}$  in the  $[D]$  matrix) for the laminate is zero. For example, for a  $[0/+30/-30/+30/-30/0]$  laminate,  $D_{16} = D_{26} = 0$ . Note that the  $D_{16}$  and  $D_{26}$  terms cannot be zero for a symmetric laminate, unless  $\theta = 0^\circ$  and  $90^\circ$ .

### EXAMPLE 3.7

Determine  $[A]$ ,  $[B]$ , and  $[D]$  matrices for (a) a  $[+45/-45]$  angle-ply laminate, (b) a  $[+45/-45]_S$  symmetric laminate, and (c) a  $[+45/0/-45]$  unsymmetric laminate. Each lamina is 6 mm thick and contains 60 vol% of T-300 carbon fiber in an epoxy matrix. Use the same material properties as in Example 3.6.



### SOLUTION

From Example 3.6,  $[\bar{Q}]$  matrices for the  $0^\circ$ ,  $+45^\circ$ , and  $-45^\circ$  layers are written as

$$[\bar{Q}]_{0^\circ} = [Q]_{0^\circ} = \begin{bmatrix} 134.03 & 2.29 & 0 \\ 2.29 & 8.82 & 0 \\ 0 & 0 & 3.254 \end{bmatrix} \text{ GPa,}$$

$$[\bar{Q}]_{+45^\circ} = \begin{bmatrix} 40.11 & 33.61 & 31.3 \\ 33.61 & 40.11 & 31.3 \\ 31.3 & 31.3 & 34.57 \end{bmatrix} \text{ GPa,}$$

$$[\bar{Q}]_{-45^\circ} = \begin{bmatrix} 40.11 & 33.61 & -31.3 \\ 33.61 & 40.11 & -31.3 \\ -31.3 & -31.3 & 34.57 \end{bmatrix} \text{ GPa.}$$

- (a) [+45/-45] Angle-ply laminate: From the figure (top left), we note  $h_0 = -0.006$  m,  $h_1 = 0$ , and  $h_2 = 0.006$  m. In this laminate,  $(\bar{Q}_{mn})_1 = (\bar{Q}_{mn})_{+45^\circ}$  and  $(\bar{Q}_{mn})_2 = (\bar{Q}_{mn})_{-45^\circ}$ . Therefore,

$$\begin{aligned}
 A_{mn} &= (\bar{Q}_{mn})_1(h_1 - h_0) + (\bar{Q}_{mn})_2(h_2 - h_1) \\
 &= 6 \times 10^{-3}(\bar{Q}_{mn})_{+45^\circ} + 6 \times 10^{-3}(\bar{Q}_{mn})_{-45^\circ}, \\
 B_{mn} &= \frac{1}{2} [(\bar{Q}_{mn})_1(h_1^2 - h_0^2) + (\bar{Q}_{mn})_2(h_2^2 - h_1^2)] \\
 &= -18 \times 10^{-6}(\bar{Q}_{mn})_{+45^\circ} + 18 \times 10^{-6}(\bar{Q}_{mn})_{-45^\circ}, \\
 D_{mn} &= \frac{1}{3} [(\bar{Q}_{mn})_1(h_1^3 - h_0^3) + (\bar{Q}_{mn})_2(h_2^3 - h_1^3)] \\
 &= 72 \times 10^{-9}(\bar{Q}_{mn})_{+45^\circ} + 72 \times 10^{-9}(\bar{Q}_{mn})_{-45^\circ}.
 \end{aligned}$$

Substituting for various  $(\bar{Q}_{mn})$  values, we calculate

$$[A] = \begin{bmatrix} 481.32 & 403.32 & 0 \\ 403.32 & 481.32 & 0 \\ 0 & 0 & 414.84 \end{bmatrix} \times 10^6 \text{ N/m},$$

$$[B] = \begin{bmatrix} 0 & 0 & -1126.8 \\ 0 & 0 & -1126.8 \\ -1126.8 & -1126.8 & 0 \end{bmatrix} \times 10^3 \text{ N},$$

$$[D] = \begin{bmatrix} 5775.84 & 4839.84 & 0 \\ 4839.84 & 5775.84 & 0 \\ 0 & 0 & 4978.08 \end{bmatrix} \text{ N m}.$$

Note that for a [+45/-45] angle-ply laminate,  $A_{16} = A_{26} = 0$  (since it is balanced) as well as  $D_{16} = D_{26} = 0$ .

- (b) [(45/-45)]<sub>S</sub> Symmetric laminate: From the figure (top right), we note that  $h_3 = -h_1 = 0.006$  m,  $h_4 = h_0 = 0.012$  m, and  $h_2 = 0$ . In this laminate,

$$(\bar{Q}_{mn})_4 = (\bar{Q}_{mn})_1 = (\bar{Q}_{mn})_{+45^\circ}$$

and

$$(\bar{Q}_{mn})_3 = (\bar{Q}_{mn})_2 = (\bar{Q}_{mn})_{-45^\circ}.$$

Therefore,

$$\begin{aligned} A_{mn} &= (\bar{Q}_{mn})_1(h_1 - h_0) + (\bar{Q}_{mn})_2(h_2 - h_1) + (\bar{Q}_{mn})_3(h_3 - h_2) + (\bar{Q}_{mn})_4(h_4 - h_3) \\ &= (\bar{Q}_{mn})_{+45^\circ}(h_1 - h_0 + h_4 - h_3) + (\bar{Q}_{mn})_{-45^\circ}(h_2 - h_1 + h_3 - h_2) \\ &= 12 \times 10^{-3}(\bar{Q}_{mn})_{+45^\circ} + 12 \times 10^{-3}(\bar{Q}_{mn})_{-45^\circ}, \end{aligned}$$

$$\begin{aligned} B_{mn} &= \frac{1}{2} [(\bar{Q}_{mn})_1(h_1^2 - h_0^2) + (\bar{Q}_{mn})_2(h_2^2 - h_1^2) + (\bar{Q}_{mn})_3(h_3^2 - h_2^2) + (\bar{Q}_{mn})_4(h_4^2 - h_3^2)] \\ &= \frac{1}{2} [(\bar{Q}_{mn})_{+45^\circ}(h_1^2 - h_0^2 + h_4^2 - h_3^2) + (\bar{Q}_{mn})_{-45^\circ}(h_2^2 - h_1^2 + h_3^2 - h_2^2)] \\ &= 0 \quad \text{since } h_1^2 = h_3^2 \text{ and } h_0^2 = h_4^2, \end{aligned}$$

$$\begin{aligned} D_{mn} &= \frac{1}{3} [(\bar{Q}_{mn})_1(h_1^3 - h_0^3) + (\bar{Q}_{mn})_2(h_2^3 - h_1^3) + (\bar{Q}_{mn})_3(h_3^3 - h_2^3) + (\bar{Q}_{mn})_4(h_4^3 - h_3^3)] \\ &= \frac{1}{3} [(\bar{Q}_{mn})_{+45^\circ}(h_1^3 - h_0^3 + h_4^3 - h_3^3) + (\bar{Q}_{mn})_{-45^\circ}(h_2^3 - h_1^3 + h_3^3 - h_2^3)] \\ &= 1008 \times 10^{-9}(\bar{Q}_{mn})_{+45^\circ} + 144 \times 10^{-9}(\bar{Q}_{mn})_{-45^\circ}. \end{aligned}$$

Substituting for various  $(\bar{Q}_{mn})$  values, we calculate

$$[A] = \begin{bmatrix} 962.64 & 806.64 & 0 \\ 806.64 & 962.64 & 0 \\ 0 & 0 & 829.68 \end{bmatrix} \times 10^6 \text{ N/m},$$

$$[B] = [0],$$

$$[D] = \begin{bmatrix} 46.21 & 38.72 & 27.04 \\ 38.72 & 46.21 & 27.04 \\ 27.04 & 27.04 & 39.82 \end{bmatrix} \times 10^3 \text{ N m}.$$

Note that  $[\pm 45]_S$  is a balanced symmetric laminate in which  $A_{16} = A_{26} = 0$  and  $[B] = [0]$ .

(c)  $[+45/0/-45]$  Unsymmetric laminate: From the figure (bottom), we note

$$\begin{aligned} h_2 &= -h_1 = 3 \times 10^{-3} \text{ m}, \\ h_3 &= -h_0 = 9 \times 10^{-3} \text{ m}. \end{aligned}$$

In this laminate,

$$(\bar{Q}_{mn})_1 = (\bar{Q}_{mn})_{+45^\circ},$$

$$(\bar{Q}_{mn})_2 = (\bar{Q}_{mn})_{0^\circ},$$

$$(\bar{Q}_{mn})_3 = (\bar{Q}_{mn})_{-45^\circ}.$$

Therefore,

$$\begin{aligned} A_{mn} &= (\bar{Q}_{mn})_1(h_1 - h_0) + (\bar{Q}_{mn})_2(h_2 - h_1) + (\bar{Q}_{mn})_3(h_3 - h_2) \\ &= 6 \times 10^{-3}(\bar{Q}_{mn})_{+45^\circ} + 6 \times 10^{-3}(\bar{Q}_{mn})_{0^\circ} + 6 \times 10^{-3}(\bar{Q}_{mn})_{-45^\circ}, \end{aligned}$$

$$\begin{aligned} B_{mn} &= \frac{1}{2} [(\bar{Q}_{mn})_1(h_1^2 - h_0^2) + (\bar{Q}_{mn})_2(h_2^2 - h_1^2) + (\bar{Q}_{mn})_3(h_3^2 - h_2^2)] \\ &= -36 \times 10^{-6}(\bar{Q}_{mn})_{+45^\circ} + 36 \times 10^{-6}(\bar{Q}_{mn})_{-45^\circ}, \end{aligned}$$

$$\begin{aligned} D_{mn} &= \frac{1}{3} [(\bar{Q}_{mn})_1(h_1^3 - h_0^3) + (\bar{Q}_{mn})_2(h_2^3 - h_1^3) + (\bar{Q}_{mn})_3(h_3^3 - h_2^3)] \\ &= 234 \times 10^{-9}(\bar{Q}_{mn})_{+45^\circ} + 18 \times 10^{-9}(\bar{Q}_{mn})_{0^\circ} + 234 \times 10^{-9}(\bar{Q}_{mn})_{-45^\circ}. \end{aligned}$$

Substituting for  $[\bar{Q}_{mn}]$  values, we calculate

$$[A] = \begin{bmatrix} 1285.50 & 417.06 & 0 \\ 417.06 & 534.24 & 0 \\ 0 & 0 & 434.36 \end{bmatrix} \times 10^6 \text{ N/m},$$

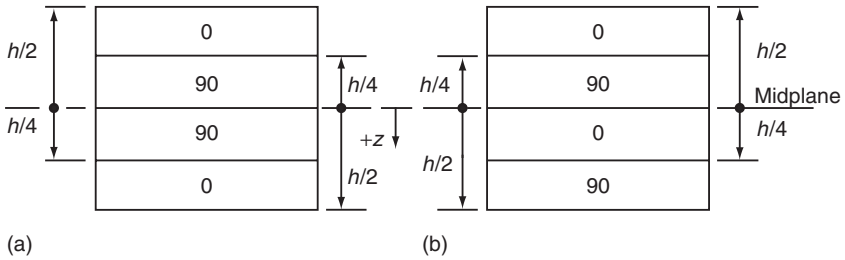
$$[B] = \begin{bmatrix} 0 & 0 & -2253.6 \\ 0 & 0 & -2253.6 \\ -2253.6 & -2253.6 & 0 \end{bmatrix} \times 10^3 \text{ N},$$

$$[D] = \begin{bmatrix} 21,183.84 & 15,770.70 & 0 \\ 15,770.70 & 18,930.24 & 0 \\ 0 & 0 & 16,237.33 \end{bmatrix} \text{ N m}.$$

Comparing cases (a) and (c), we note that the addition of a  $0^\circ$  lamina increases the value of  $A_{11}$  by a significant amount, but  $A_{12}$ ,  $A_{22}$ , and  $A_{66}$  are only marginally improved. Elements in the  $[D]$  matrix are improved owing to the presence of the  $0^\circ$  lamina as well as the additional thickness in the  $[+45/0/-45]$  laminate.

### EXAMPLE 3.8

Compare the stiffness matrices of  $[0/90/90/0]$  and  $[0/90/0/90]$  laminates. Assume each ply has a thickness of  $h/4$ .



### SOLUTION

First, we note that for  $0^\circ$  and  $90^\circ$  plies,

$$\begin{aligned}
 (Q_{11})_0 &= (Q_{22})_{90}, \\
 (Q_{22})_0 &= (Q_{11})_{90}, \\
 (Q_{12})_0 &= (Q_{12})_{90}, \\
 (Q_{66})_0 &= (Q_{66})_{90}, \\
 (Q_{16})_0 &= (Q_{16})_{90} = 0, \\
 (Q_{26})_0 &= (Q_{26})_{90} = 0.
 \end{aligned}$$

For the  $[0/90/90/0]$  laminate on the left,

$$\begin{aligned}
 A_{ij} &= (Q_{ij})_0 \left[ -\frac{h}{4} - \left( -\frac{h}{2} \right) \right] + (Q_{ij})_{90} \left[ 0 - \left( -\frac{h}{4} \right) \right] \\
 &\quad + (Q_{ij})_{90} \left( \frac{h}{4} - 0 \right) + (Q_{ij})_0 \left( \frac{h}{2} - \frac{h}{4} \right) \\
 &= \frac{h}{2} [(Q_{ij})_0 + (Q_{ij})_{90}], \\
 B_{ij} &= 0 \quad (\text{since this is a symmetric laminate}), \\
 D_{ij} &= \frac{1}{3} \left\{ (Q_{ij})_0 \left[ \left( -\frac{h}{4} \right)^3 - \left( -\frac{h}{2} \right)^3 \right] + (Q_{ij})_{90} \left[ 0 - \left( -\frac{h}{4} \right)^3 \right] \right. \\
 &\quad \left. + (Q_{ij})_{90} \left[ \left( \frac{h}{4} \right)^3 - 0 \right] + (Q_{ij})_0 \left[ \left( \frac{h}{2} \right)^3 - \left( \frac{h}{4} \right)^3 \right] \right\} \\
 &= \frac{h^3}{96} [7(Q_{ij})_0 + (Q_{ij})_{90}].
 \end{aligned}$$

For the  $[0/90/0/90]$  laminate on the right,

$$\begin{aligned}
A_{ij} &= (Q_{ij})_0 \left[ \left( -\frac{h}{4} \right) - \left( -\frac{h}{2} \right) \right] + (Q_{ij})_{90} \left[ 0 - \left( -\frac{h}{4} \right) \right] \\
&\quad + (Q_{ij})_0 \left( \frac{h}{4} - 0 \right) + (Q_{ij})_{90} \left( \frac{h}{2} - \frac{h}{4} \right) \\
&= \frac{h}{2} [(Q_{ij})_0 + (Q_{ij})_{90}], \\
B_{ij} &= \frac{1}{2} \left\{ (Q_{ij})_0 \left[ \left( -\frac{h}{4} \right)^2 - \left( -\frac{h}{2} \right)^2 \right] + (Q_{ij})_{90} \left[ 0 - \left( -\frac{h}{4} \right)^2 \right] \right. \\
&\quad \left. + (Q_{ij})_0 \left[ \left( \frac{h}{4} \right)^2 - 0 \right] + (Q_{ij})_{90} \left[ \left( \frac{h}{2} \right)^2 - \left( \frac{h}{4} \right)^2 \right] \right\} \\
&= \frac{h^2}{16} [-(Q_{ij})_0 + (Q_{ij})_{90}], \\
D_{ij} &= \frac{1}{3} \left\{ (Q_{ij})_0 \left[ \left( -\frac{h}{4} \right)^3 - \left( -\frac{h}{2} \right)^3 \right] + (Q_{ij})_{90} \left[ 0 - \left( -\frac{h}{4} \right)^3 \right] \right. \\
&\quad \left. + (Q_{ij})_0 \left[ \left( \frac{h}{4} \right)^3 - 0 \right] + (Q_{ij})_{90} \left[ \left( \frac{h}{2} \right)^3 - \left( \frac{h}{4} \right)^3 \right] \right\} \\
&= \frac{h^3}{24} [(Q_{ij})_0 + (Q_{ij})_{90}].
\end{aligned}$$

This example demonstrates the influence of stacking sequence on the stiffness matrices and the difference it can make to the elastic response of laminates containing similar plies, but arranged in different orders. In this case, although  $[A]$  matrices for the  $[0/90/90/0]$  and  $[0/90/0/90]$  are identical, their  $[B]$  and  $[D]$  matrices are different.

### 3.3.2.5 Midplane Strains and Curvatures

If the normal force and moment resultants acting on a laminate are known, its midplane strains and curvatures can be calculated by inverting [Equations 3.85](#) and [3.86](#). Thus,

$$\begin{bmatrix} \varepsilon_{xx}^{\circ} \\ \varepsilon_{yy}^{\circ} \\ \gamma_{xy}^{\circ} \end{bmatrix} = [A_1] \begin{bmatrix} N_{xx} \\ N_{yy} \\ N_{xy} \end{bmatrix} + [B_1] \begin{bmatrix} M_{xx} \\ M_{yy} \\ M_{xy} \end{bmatrix} \quad (3.93)$$

and

$$\begin{bmatrix} k_{xx} \\ k_{yy} \\ k_{xy} \end{bmatrix} = [C_1] \begin{bmatrix} N_{xx} \\ N_{yy} \\ N_{xy} \end{bmatrix} + [D_1] \begin{bmatrix} M_{xx} \\ M_{yy} \\ M_{xy} \end{bmatrix}, \quad (3.94)$$

where

$$\begin{aligned}
 [A_1] &= [A^{-1}] + [A^{-1}][B][(D^*)^{-1}][B][A^{-1}] \\
 [B_1] &= -[A^{-1}][B][(D^*)^{-1}] \\
 [C_1] &= -[(D^*)^{-1}][B][A^{-1}] = [B_1]^T \\
 [D^*] &= [D] - [B][A^{-1}][B] \\
 [D_1] &= [(D^*)^{-1}]
 \end{aligned} \tag{3.95}$$

Note that for a symmetric laminate,  $[B] = [0]$ , and therefore,  $[A_1] = [A^{-1}]$ ,  $[B_1] = [C_1] = [0]$ , and  $[D_1] = [D^{-1}]$ . In this case, equations for midplane strains and curvatures become

$$\begin{bmatrix} \epsilon_{xx}^o \\ \epsilon_{yy}^o \\ \gamma_{xy}^o \end{bmatrix} = [A^{-1}] \begin{bmatrix} N_{xx} \\ N_{yy} \\ N_{xy} \end{bmatrix} \tag{3.96}$$

and

$$\begin{bmatrix} k_{xx} \\ k_{yy} \\ k_{xy} \end{bmatrix} = [D^{-1}] \begin{bmatrix} M_{xx} \\ M_{yy} \\ M_{xy} \end{bmatrix}. \tag{3.97}$$

Equation 3.96 shows that for a symmetric laminate, in-plane forces cause only in-plane strains and no curvatures. Similarly, Equation 3.97 shows that bending and twisting moments cause only curvatures and no in-plane strains.

### EXAMPLE 3.9

Elastic properties of a balanced symmetric laminate: For a balanced symmetric laminate, the extensional stiffness matrix is

$$[A] = \begin{bmatrix} A_{11} & A_{12} & 0 \\ A_{12} & A_{22} & 0 \\ 0 & 0 & A_{66} \end{bmatrix}$$

and the coupling stiffness matrix  $[B] = [0]$ .

The inverse of the  $[A]$  matrix is

$$[A^{-1}] = \frac{1}{A_{11}A_{22} - A_{12}^2} \begin{bmatrix} A_{22} & -A_{12} & 0 \\ -A_{12} & A_{11} & 0 \\ 0 & 0 & \frac{(A_{11}A_{22} - A_{12}^2)}{A_{66}} \end{bmatrix}.$$

Therefore, Equation 3.96 gives

$$\begin{bmatrix} \varepsilon_{xx}^{\circ} \\ \varepsilon_{yy}^{\circ} \\ \gamma_{xy}^{\circ} \end{bmatrix} = \frac{1}{A_{11}A_{22} - A_{12}^2} \begin{bmatrix} A_{22} & -A_{12} & 0 \\ -A_{12} & A_{11} & 0 \\ 0 & 0 & \frac{(A_{11}A_{22} - A_{12}^2)}{A_{66}} \end{bmatrix} \begin{bmatrix} N_{xx} \\ N_{yy} \\ N_{xy} \end{bmatrix}. \quad (3.98)$$

Let us assume that the laminate is subjected to a uniaxial tensile stress  $\sigma_{xx}$  in the  $x$  direction, and both  $\sigma_{yy}$  and  $\tau_{xy}$  are zero. If the laminate thickness is  $h$ , the tensile force per unit width in the  $x$  direction  $N_{xx} = h\sigma_{xx}$ ,  $N_{yy} = 0$ , and  $N_{xy} = 0$ . Thus, from Equation 3.98, we obtain

$$\begin{aligned} \varepsilon_{xx}^{\circ} &= \frac{A_{22}}{A_{11}A_{22} - A_{12}^2} h\sigma_{xx}, \\ \varepsilon_{yy}^{\circ} &= -\frac{A_{12}}{A_{11}A_{22} - A_{12}^2} h\sigma_{xx}, \\ \gamma_{xy}^{\circ} &= 0, \end{aligned}$$

which give

$$E_{xx} = \frac{\sigma_{xx}}{\varepsilon_{xx}^{\circ}} = \frac{A_{11}A_{22} - A_{12}^2}{hA_{22}}, \quad (3.99)$$

$$\nu_{xy} = -\frac{\varepsilon_{yy}^{\circ}}{\varepsilon_{xx}^{\circ}} = \frac{A_{12}}{A_{22}}. \quad (3.100)$$

In turn, applying  $N_{yy}$  and  $N_{xy}$  separately, we can determine

$$E_{yy} = \frac{A_{11}A_{22} - A_{12}^2}{hA_{11}}, \quad (3.101)$$

$$\nu_{yx} = \frac{A_{12}}{A_{11}} \left( \text{which is the same as } \nu_{xy} \frac{E_{yy}}{E_{xx}} \right), \quad (3.102)$$

and

$$G_{xy} = \frac{A_{66}}{h}. \quad (3.103)$$

### EXAMPLE 3.10

Elastic properties of a symmetric quasi-isotropic laminate: For a symmetric quasi-isotropic laminate,

$$[A] = \begin{bmatrix} A_{11} & A_{12} & 0 \\ A_{12} & A_{22} = A_{11} & 0 \\ 0 & 0 & A_{66} = \frac{A_{11} - A_{12}}{2} \end{bmatrix}$$

and  $[B] = [0]$

Now using the results of [Example 3.9](#), we obtain

$$E_{xx} = E_{yy} = \frac{A_{11}^2 - A_{12}^2}{hA_{11}},$$

$$\nu_{xy} = \frac{A_{12}}{A_{11}},$$

$$G_{xy} = \frac{A_{11} - A_{12}}{2h},$$

where  $h$  is the laminate thickness.

Note that for a quasi-isotropic laminate,  $E_{xx} = E_{yy}$  and, from the previous equations, it can be easily shown that

$$G_{xy} = \frac{E_{xx}}{2(1 + \nu_{xy})}.$$

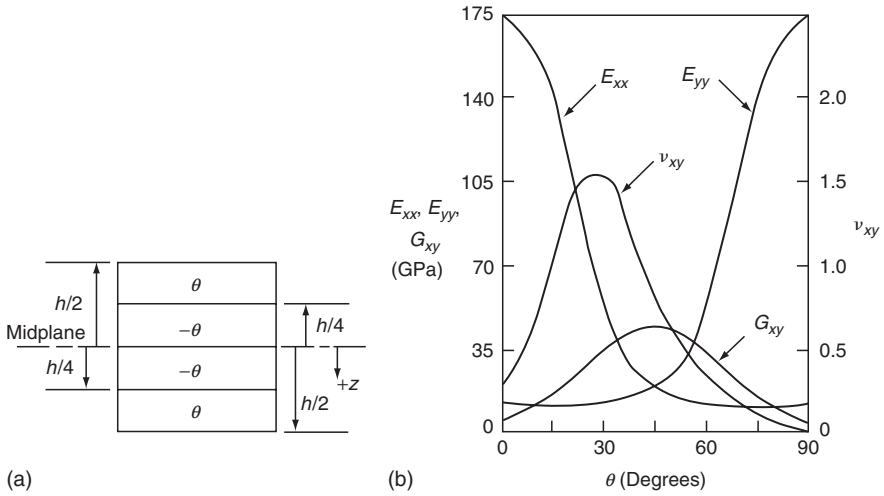
However,  $E_{xx} = E_{yy}$  does not necessarily mean quasi-isotropy. For example,  $E_{xx}$  and  $E_{yy}$  are equal for a  $[0/90]_S$  laminate, but it is not a quasi-isotropic laminate. For a quasi-isotropic laminate, elastic modulus at any arbitrary angle in the plane of the laminate is the same as  $E_{xx}$  or  $E_{yy}$ . That will not be the case with the  $[0/90]_S$  laminate.

### EXAMPLE 3.11

Elastic properties of symmetric angle-ply laminates: For angled plies with  $\theta$  and  $-\theta$  fiber orientation angles,

$$\begin{aligned}\bar{Q}_{11}(\theta) &= \bar{Q}_{11}(-\theta), \\ \bar{Q}_{22}(\theta) &= \bar{Q}_{22}(-\theta), \\ \bar{Q}_{12}(\theta) &= \bar{Q}_{12}(-\theta), \\ \bar{Q}_{66}(\theta) &= \bar{Q}_{66}(-\theta), \\ \bar{Q}_{16}(\theta) &= -\bar{Q}_{16}(-\theta), \\ \bar{Q}_{26}(\theta) &= -\bar{Q}_{26}(-\theta).\end{aligned}$$

Referring to the four-layer angle-ply laminate shown in the left side of the figure, we can write the elements in the extensional stiffness matrix  $[A]$  of the  $[\theta/-\theta]_S$  as



$$\begin{aligned}
 A_{ij} &= (\bar{Q}_{ij})_{\theta} \left( -\frac{h}{4} + \frac{h}{2} \right) + (\bar{Q}_{ij})_{-\theta} \left( 0 + \frac{h}{4} \right) \\
 &\quad + (\bar{Q}_{ij})_{-\theta} \left( \frac{h}{4} - 0 \right) + (\bar{Q}_{ij})_{\theta} \left( \frac{h}{2} - \frac{h}{4} \right) \\
 &= \frac{h}{2} [(\bar{Q}_{ij})_{\theta} + (\bar{Q}_{ij})_{-\theta}].
 \end{aligned}$$

Thus,

$$[A] = \begin{bmatrix} h\bar{Q}_{11} & h\bar{Q}_{12} & 0 \\ h\bar{Q}_{12} & h\bar{Q}_{22} & 0 \\ 0 & 0 & h\bar{Q}_{66} \end{bmatrix}.$$

Now, using [Equations 3.99](#) through [3.103](#), we can write

$$\begin{aligned}
 E_{xx} &= \frac{\bar{Q}_{11}\bar{Q}_{22} - \bar{Q}_{12}^2}{\bar{Q}_{22}}, \\
 E_{yy} &= \frac{\bar{Q}_{11}\bar{Q}_{22} - \bar{Q}_{12}^2}{\bar{Q}_{11}}, \\
 \nu_{xy} &= \frac{\bar{Q}_{12}}{\bar{Q}_{22}}, \\
 G_{xy} &= \bar{Q}_{66}.
 \end{aligned}$$

Since  $\bar{Q}_{11}$ ,  $\bar{Q}_{22}$ ,  $\bar{Q}_{12}$ , and  $\bar{Q}_{66}$  are functions of the fiber orientation angle  $\theta$ , the elastic properties of the angle-ply laminate will also be functions of  $\theta$ . This

is illustrated in the right side of the figure. Note that the shear modulus is maximum at  $\theta = 45^\circ$ , that is, for a  $[\pm 45]_S$  laminate. In addition, note the variation in the Poisson's ratio, which has values greater than unity for a range of fiber orientation angles. In an isotropic material, the Poisson's ratio cannot exceed a value of 0.5.

### EXAMPLE 3.12

Bending of a balanced symmetric laminate beam specimen: For a balanced symmetric laminate,  $[B] = [0]$ .

$$[D] = \begin{bmatrix} D_{11} & D_{12} & D_{16} \\ D_{12} & D_{22} & D_{26} \\ D_{16} & D_{26} & D_{66} \end{bmatrix},$$

$$[D^{-1}] = \frac{1}{D_0} \begin{bmatrix} D_{11}^\circ & D_{12}^\circ & D_{16}^\circ \\ D_{12}^\circ & D_{22}^\circ & D_{26}^\circ \\ D_{16}^\circ & D_{26}^\circ & D_{66}^\circ \end{bmatrix},$$

where

$$D_0 = D_{11}(D_{22}D_{66} - D_{26}^2) - D_{12}(D_{12}D_{66} - D_{16}D_{26}) + D_{16}(D_{12}D_{26} - D_{22}D_{16})$$

$$D_{11}^\circ = (D_{22}D_{66} - D_{26}^2)$$

$$D_{12}^\circ = -(D_{12}D_{66} - D_{16}D_{26})$$

$$D_{16}^\circ = (D_{12}D_{26} - D_{22}D_{16})$$

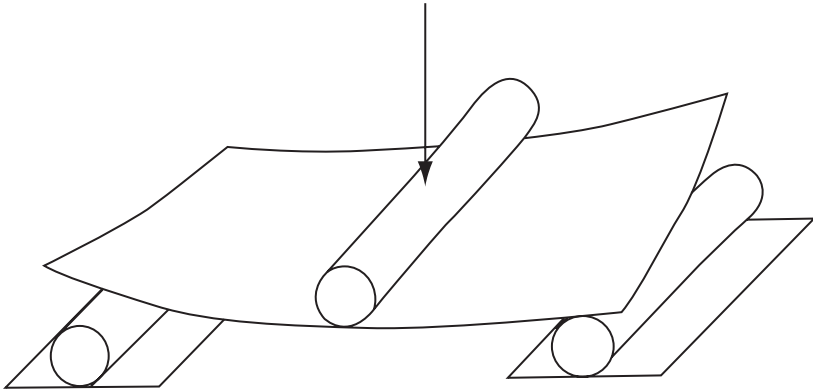
$$D_{22}^\circ = (D_{11}D_{66} - D_{16}^2)$$

$$D_{26}^\circ = -(D_{11}D_{26} - D_{12}D_{16})$$

$$D_{66}^\circ = (D_{11}D_{12} - D_{12}^2)$$

If a bending moment is applied in the  $yz$  plane so that  $M_{xx}$  is present and  $M_{yy} = M_{xy} = 0$ , the specimen curvatures can be obtained from [Equation 3.97](#):

$$\begin{aligned} k_{xx} &= \frac{D_{11}^\circ}{D_0} M_{xx}, \\ k_{yy} &= \frac{D_{12}^\circ}{D_0} M_{xx}, \\ k_{xy} &= \frac{D_{16}^\circ}{D_0} M_{xx}. \end{aligned} \tag{3.104}$$



Thus, even though no twisting moment is applied, the specimen would tend to twist unless  $D_{16}^{\circ} = (D_{12}D_{26} - D_{22}D_{16}) = 0$ . This is possible only if the balanced symmetric laminate contains fibers in the  $0^{\circ}$  and  $90^{\circ}$  directions. The twisting phenomenon can be easily demonstrated in a three-point flexural test in which the specimen lifts off the support on opposite corners of its span, as shown in the figure.

### 3.3.2.6 Lamina Strains and Stresses Due to Applied Loads

Knowing the midplane strains and curvatures for the laminate, strains at the midplane of each lamina can be calculated using the following linear relationships:

$$\begin{bmatrix} \varepsilon_{xx} \\ \varepsilon_{yy} \\ \gamma_{xy} \end{bmatrix}_j = \begin{bmatrix} \varepsilon_{xx}^{\circ} \\ \varepsilon_{yy}^{\circ} \\ \gamma_{xy}^{\circ} \end{bmatrix} + z_j \begin{bmatrix} k_{xx} \\ k_{yy} \\ k_{xy} \end{bmatrix}, \quad (3.105)$$

where  $z_j$  is the distance from the laminate midplane to the midplane of the  $j$ th lamina.

In turn, stresses in the  $j$ th lamina can be calculated using its stiffness matrix. Thus,

$$\begin{bmatrix} \sigma_{xx} \\ \sigma_{yy} \\ \tau_{xy} \end{bmatrix}_j = [\bar{Q}_{mn}]_j \begin{bmatrix} \varepsilon_{xx} \\ \varepsilon_{yy} \\ \gamma_{xy} \end{bmatrix}_j = [\bar{Q}_{mn}]_j \begin{bmatrix} \varepsilon_{xx}^{\circ} \\ \varepsilon_{yy}^{\circ} \\ \gamma_{xy}^{\circ} \end{bmatrix} + z_j [\bar{Q}_{mn}]_j \begin{bmatrix} k_{xx} \\ k_{yy} \\ k_{xy} \end{bmatrix}. \quad (3.106)$$

Figure 3.51 demonstrates schematically the strain and stress distributions in a laminate. Note that the strain distribution is continuous and linearly varies with the distance  $z$  from the laminate midplane. The stress distribution is not continuous, although it varies linearly across each lamina thickness. For thin laminas, the strain and stress variation across the thickness of each lamina is small. Therefore, their average values are calculated using the center distance  $z_j$ , as shown in Equations 3.105 and 3.106.

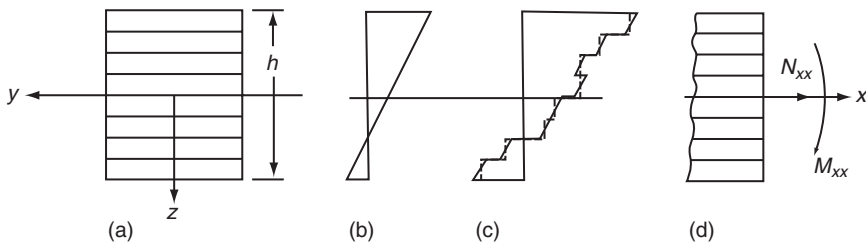


**FIGURE 3.51** Strain and stress distributions in a laminate. (a) Laminate; (b) Strain distribution; (c) Stress distribution; and (d) Normal force and bending moment resultants.

### EXAMPLE 3.13

Calculate lamina stresses at the midplane of each lamina in the  $[+45/-45]$  laminate in [Example 3.7](#) due to  $N_{xx} = 100 \text{ kN/m}$ .

#### SOLUTION

Step 1: From the laminate stiffness matrices  $[A]$ ,  $[B]$ , and  $[D]$ , determine  $[A^{-1}]$ ,  $[D^*]$ ,  $[A_1]$ ,  $[B_1]$ ,  $[C_1]$ , and  $[D_1]$ .

$$[A^{-1}] = \begin{bmatrix} 0.697 & -0.584 & 0 \\ -0.584 & 0.697 & 0 \\ 0 & 0 & 0.241 \end{bmatrix} \times 10^{-8} \text{ m/N},$$

$$[B][A^{-1}][B] = \begin{bmatrix} 3.06 & 3.06 & 0 \\ 3.06 & 3.06 & 0 \\ 0 & 0 & 2.87 \end{bmatrix} \times 10^3 \text{ N m},$$

$$[D^*] = [D] - [B][A^{-1}][B] = \begin{bmatrix} 2715.84 & 1779.84 & 0 \\ 1779.84 & 2715.84 & 0 \\ 0 & 0 & 2108.08 \end{bmatrix} \text{ N m},$$

$$[D_1] = [(D^*)^{-1}] = \begin{bmatrix} 6.45 & -4.23 & 0 \\ -4.23 & 6.45 & 0 \\ 0 & 0 & 4.74 \end{bmatrix} \times 10^{-4} \frac{1}{\text{N m}},$$

$$[B_1] = -[A^{-1}][B][(D^*)^{-1}] = \begin{bmatrix} 0 & 0 & 603.54 \\ 0 & 0 & 603.54 \\ 602.74 & 602.74 & 0 \end{bmatrix} \times 10^{-9} \frac{1}{\text{N}},$$

$$[C_1] = -[(D^*)^{-1}][B][A^{-1}] = \begin{bmatrix} 0 & 0 & 602.74 \\ 0 & 0 & 602.74 \\ 603.54 & 603.54 & 0 \end{bmatrix} \times 10^{-9} \frac{1}{\text{N}},$$

$$[A_1] = [A^{-1}] + [A^{-1}][B][(D^*)^{-1}][B][A^{-1}] = \begin{bmatrix} 7.7385 & -5.0715 & 0 \\ -5.0715 & 7.7385 & 0 \\ 0 & 0 & 5.683 \end{bmatrix} \times 10^{-9} \text{ m/N.}$$

Step 2: Using [Equations 3.93](#) and [3.94](#), calculate the  $[\varepsilon^\circ]$  and  $[k]$  matrices.

$$[\varepsilon^\circ] = \begin{bmatrix} \varepsilon_{xx}^\circ \\ \varepsilon_{yy}^\circ \\ \gamma_{xy}^\circ \end{bmatrix} = [A_1] \begin{bmatrix} 100 \times 10^3 \text{ N/m} \\ 0 \\ 0 \end{bmatrix}.$$

Therefore,

$$\begin{aligned} \varepsilon_{xx}^\circ &= 77.385 \times 10^{-5} \text{ m/m}, \\ \varepsilon_{yy}^\circ &= -50.715 \times 10^{-5} \text{ m/m}, \\ \gamma_{xy}^\circ &= 0. \end{aligned}$$

$$[k] = \begin{bmatrix} k_{xx} \\ k_{yy} \\ k_{xy} \end{bmatrix} = [C_1] \begin{bmatrix} 100 \times 10^3 \text{ N/m} \\ 0 \\ 0 \end{bmatrix},$$

Therefore,

$$\begin{aligned} k_{xx} &= 0 \\ k_{yy} &= 0 \\ k_{xy} &= 0.060354 \text{ per m} \end{aligned}$$

Step 3: Using [Equation 3.105](#), calculate  $\varepsilon_{xx}^\circ$ ,  $\varepsilon_{yy}^\circ$ , and  $\gamma_{xy}$  at the midplane of  $+45^\circ$  and  $-45^\circ$  laminas.

$$\begin{aligned} \begin{bmatrix} \varepsilon_{xx} \\ \varepsilon_{yy} \\ \gamma_{xy} \end{bmatrix}_{+45^\circ} &= \begin{bmatrix} 77.385 \times 10^{-5} \\ -50.715 \times 10^{-5} \\ 0 \end{bmatrix} + (-3 \times 10^{-3}) \begin{bmatrix} 0 \\ 0 \\ 0.060354 \end{bmatrix} \\ &= \begin{bmatrix} 77.385 \\ -50.715 \\ -18.106 \end{bmatrix} \times 10^{-5}. \end{aligned}$$

Similarly,

$$\begin{bmatrix} \varepsilon_{xx} \\ \varepsilon_{yy} \\ \gamma_{xy} \end{bmatrix}_{-45^\circ} = \begin{bmatrix} 77.385 \\ -50.715 \\ 18.106 \end{bmatrix} \times 10^{-5}.$$

Step 4: Using [Equation 3.106](#), calculate  $\sigma_{xx}$ ,  $\sigma_{yy}$ , and  $\tau_{xy}$  at the midplanes of  $+45^\circ$  and  $-45^\circ$  laminas.

$$\begin{bmatrix} \sigma_{xx} \\ \sigma_{yy} \\ \tau_{xy} \end{bmatrix}_{+45^\circ} = \begin{bmatrix} 40.11 & 33.61 & 31.3 \\ 33.61 & 40.11 & 31.3 \\ 31.3 & 31.3 & 34.57 \end{bmatrix} \text{GPa} \begin{bmatrix} 77.385 \times 10^{-5} \\ -50.715 \times 10^{-5} \\ -18.106 \times 10^{-5} \end{bmatrix} = \begin{bmatrix} 8.33 \\ 0 \\ 2.09 \end{bmatrix} \text{MPa}.$$

Similarly,

$$\begin{bmatrix} \sigma_{xx} \\ \sigma_{yy} \\ \tau_{xy} \end{bmatrix}_{-45^\circ} = \begin{bmatrix} 8.33 \\ 0 \\ -2.09 \end{bmatrix} \text{MPa}.$$

Using the stress transformation [Equation 3.30](#), we may compute the longitudinal, transverse, and shear stresses in the 1–2 directions, which give the following results:

	45° Layer (MPa)	–45° Layer (MPa)
$\sigma_{11}$	6.255	6.255
$\sigma_{22}$	2.075	2.075
$\tau_{12}$	–4.165	4.165

### 3.3.2.7 Thermal Strains and Stresses

If a temperature variation  $\Delta T$  is involved, lamina strains will be

$$\begin{aligned} \varepsilon_{xx} &= \varepsilon_{xx}^M + \varepsilon_{xx}^T = \varepsilon_{xx}^\circ + z k_{xx}, \\ \varepsilon_{yy} &= \varepsilon_{yy}^M + \varepsilon_{yy}^T = \varepsilon_{yy}^\circ + z k_{yy}, \\ \gamma_{xy} &= \gamma_{xy}^M + \gamma_{xy}^T = \gamma_{xy}^\circ + z k_{xy}, \end{aligned} \quad (3.107)$$

where the superscripts M and T denote the mechanical and thermal strains, respectively.

Thermal strains are due to free expansions (or contractions) caused by temperature variations, but mechanical strains are due to both applied loads and thermal loads. Thermal loads appear due to restrictions imposed by various layers against their free thermal expansion. In many applications involving polymer matrix composites, moisture can also influence the laminate strains owing to volumetric expansion (swelling) or contraction of the matrix caused by moisture absorption or desorption [24]. In such cases, a third term representing hygroscopic strains must be added in the middle column of [Equation 3.107](#).

Modifying [Equations 3.85](#) and [3.86](#) for thermal effects, we can write

$$\begin{bmatrix} N_{xx} \\ N_{yy} \\ N_{xy} \end{bmatrix} = [A] \begin{bmatrix} \varepsilon_{xx}^{\circ} \\ \varepsilon_{yy}^{\circ} \\ \gamma_{xy}^{\circ} \end{bmatrix} + [B] \begin{bmatrix} k_{xx} \\ k_{yy} \\ k_{xy} \end{bmatrix} - [T^*] \Delta T \quad (3.108)$$

and

$$\begin{bmatrix} M_{xx} \\ M_{yy} \\ M_{xy} \end{bmatrix} = [B] \begin{bmatrix} \varepsilon_{xx}^{\circ} \\ \varepsilon_{yy}^{\circ} \\ \gamma_{xy}^{\circ} \end{bmatrix} + [D] \begin{bmatrix} k_{xx} \\ k_{yy} \\ k_{xy} \end{bmatrix} - [T^{**}] \Delta T, \quad (3.109)$$

where

$$[T^*] = \begin{bmatrix} \sum_{j=1}^N [(\bar{Q}_{11})_j(\alpha_{xx})_j + (\bar{Q}_{12})_j(\alpha_{yy})_j + (\bar{Q}_{16})_j(\alpha_{xy})_j](h_j - h_{j-1}) \\ \sum_{j=1}^N [(\bar{Q}_{12})_j(\alpha_{xx})_j + (\bar{Q}_{22})_j(\alpha_{yy})_j + (\bar{Q}_{26})_j(\alpha_{xy})_j](h_j - h_{j-1}) \\ \sum_{j=1}^N [(\bar{Q}_{16})_j(\alpha_{xx})_j + (\bar{Q}_{26})_j(\alpha_{yy})_j + (\bar{Q}_{66})_j(\alpha_{xy})_j](h_j - h_{j-1}) \end{bmatrix} \quad (3.110)$$

$$[T^{**}] = \frac{1}{2} \begin{bmatrix} \sum_{j=1}^N [(\bar{Q}_{11})_j(\alpha_{xx})_j + (\bar{Q}_{12})_j(\alpha_{yy})_j + (\bar{Q}_{16})_j(\alpha_{xy})_j](h_j^2 - h_{j-1}^2) \\ \sum_{j=1}^N [(\bar{Q}_{12})_j(\alpha_{xx})_j + (\bar{Q}_{22})_j(\alpha_{yy})_j + (\bar{Q}_{26})_j(\alpha_{xy})_j](h_j^2 - h_{j-1}^2) \\ \sum_{j=1}^N [(\bar{Q}_{16})_j(\alpha_{xx})_j + (\bar{Q}_{26})_j(\alpha_{yy})_j + (\bar{Q}_{66})_j(\alpha_{xy})_j](h_j^2 - h_{j-1}^2) \end{bmatrix}$$

Note that even if no external loads are applied, that is, if  $[N] = [M] = [0]$ , there may be midplane strains and curvatures due to thermal effects, which in turn will create thermal stresses in various laminas. These stresses can be calculated using midplane strains and curvatures due to thermal effects in [Equation 3.106](#).

When a composite laminate is cooled from the curing temperature to room temperature, significant curing (residual) stresses may develop owing to the thermal mismatch of various laminas. In some cases, these curing stresses may be sufficiently high to cause intralaminar cracks [25]. Therefore, it may be prudent to consider them in the analysis of composite laminates.

For example, consider a  $[0/90]_S$  laminate being cooled from the curing temperature to room temperature. If the plies were not joined and could contract freely, the  $0^\circ$  ply will contract much less in the  $x$  direction than the  $90^\circ$  ply, while the reverse is true in the  $y$  direction. Since the plies are joined and must deform together, internal residual stresses are generated to maintain the geometric compatibility between the plies. In  $[0/90]_S$  laminate, residual stresses

are compressive in the fiber direction, but tensile in the transverse direction in both  $0^\circ$  and  $90^\circ$  plies (see Example 3.16). Thus, when such a laminate is loaded in tension in the  $x$  direction, residual tensile stress added to the applied tensile stress can initiate transverse cracks in the  $90^\circ$  plies at relatively low loads.

Equations 3.108 and 3.109 are also useful for calculating the coefficients of thermal expansion and the cured shapes of a laminate. This is demonstrated in the following two examples.

### EXAMPLE 3.14

Coefficients of thermal expansion for a balanced symmetric laminate

#### SOLUTION

For a balanced symmetric laminate,  $A_{16} = A_{26} = 0$  and  $[B] = [0]$ . In a thermal experiment,  $[M] = [M] = [0]$ . Therefore, from Equation 3.108,

$$\begin{bmatrix} 0 \\ 0 \\ 0 \end{bmatrix} = \begin{bmatrix} A_{11} & A_{12} & 0 \\ A_{12} & A_{22} & 0 \\ 0 & 0 & A_{66} \end{bmatrix} \begin{bmatrix} \varepsilon_{xx}^\circ \\ \varepsilon_{yy}^\circ \\ \gamma_{xy}^\circ \end{bmatrix} - \begin{bmatrix} T_1^* \\ T_2^* \\ T_3^* \end{bmatrix} \Delta T,$$

which gives

$$\begin{aligned} A_{11}\varepsilon_{xx}^\circ + A_{12}\varepsilon_{yy}^\circ &= T_1^*\Delta T, \\ A_{12}\varepsilon_{xx}^\circ + A_{22}\varepsilon_{yy}^\circ &= T_2^*\Delta T, \end{aligned}$$

and

$$A_{66}\gamma_{xy}^\circ = T_3^*\Delta T.$$

From the first two of these equations, we calculate  $\varepsilon_{xx}^\circ$  and  $\varepsilon_{yy}^\circ$  as

$$\begin{aligned} \varepsilon_{xx}^\circ &= \frac{A_{22}T_1^* - A_{12}T_2^*}{A_{11}A_{22} - A_{12}^2} \Delta T, \\ \varepsilon_{yy}^\circ &= \frac{A_{11}T_2^* - A_{12}T_1^*}{A_{11}A_{22} - A_{12}^2} \Delta T. \end{aligned}$$

Following the definitions of thermal expansion coefficients, we write

$$\begin{aligned} \alpha_{xx} &= \frac{\varepsilon_{xx}^\circ}{\Delta T} = \frac{A_{22}T_1^* - A_{12}T_2^*}{A_{11}A_{22} - A_{12}^2}, \\ \alpha_{yy} &= \frac{\varepsilon_{yy}^\circ}{\Delta T} = \frac{A_{11}T_2^* - A_{12}T_1^*}{A_{11}A_{22} - A_{12}^2}, \\ \alpha_{xy} &= \frac{\gamma_{xy}^\circ}{\Delta T} = \frac{T_3^*}{A_{66}}. \end{aligned}$$

For a balanced symmetric laminate, elements in the  $[T^{**}]$  matrix are zero. Therefore, there will be no curvatures due to temperature variation. However, the same is not true for unsymmetric laminates.

### EXAMPLE 3.15

Determine the curvatures of a two-layer unsymmetric  $[0/90]$  laminate after it is cooled from the curing temperature to the room temperature. The material is T-300 carbon fiber in an epoxy matrix for which  $\alpha_{11} = -0.5 \times 10^{-6}$  m/m per  $^{\circ}\text{C}$  and  $\alpha_{22} = 12 \times 10^{-6}$  m/m per  $^{\circ}\text{C}$ . Other material properties are the same as those in [Example 3.6](#). The thickness of each layer is  $t$ , and the temperature drop is  $\Delta T$ .

#### SOLUTION

From [Example 3.6](#), the stiffness matrices for the  $0^{\circ}$  and  $90^{\circ}$  layers are

$$[Q]_{0^{\circ}} = \begin{bmatrix} 134.03 & 2.29 & 0 \\ 2.29 & 8.82 & 0 \\ 0 & 0 & 3.254 \end{bmatrix} \times 10^9 \text{ N/m}^2,$$

$$[Q]_{90^{\circ}} = \begin{bmatrix} 8.82 & 2.29 & 0 \\ 2.29 & 134.03 & 0 \\ 0 & 0 & 3.254 \end{bmatrix} \times 10^9 \text{ N/m}^2.$$

Step 1: Determine the  $[A]$ ,  $[B]$ , and  $[D]$  matrices for the laminate.

Referring to the figure (top), we note that  $h_0 = -t$ ,  $h_1 = 0$ , and  $h_2 = t$ . Following [Equations 3.90](#) through [3.92](#), the  $[A]$ ,  $[B]$ , and  $[D]$  matrices for the  $[0/90]$  laminate can be written.

$$[A] = \begin{bmatrix} 142.85 & 4.58 & 0 \\ 4.58 & 142.85 & 0 \\ 0 & 0 & 6.508 \end{bmatrix} \times 10^9 t \text{ N/m},$$

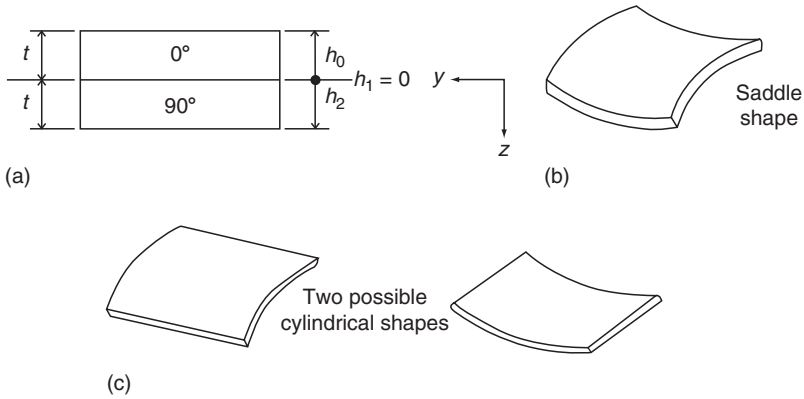
$$[B] = \begin{bmatrix} -62.605 & 0 & 0 \\ 0 & 62.605 & 0 \\ 0 & 0 & 0 \end{bmatrix} \times 10^9 t^2 \text{ N},$$

$$[D] = \begin{bmatrix} 47.62 & 1.53 & 0 \\ 1.53 & 47.62 & 0 \\ 0 & 0 & 2.17 \end{bmatrix} \times 10^9 t^3 \text{ N m}.$$

Step 2: Determine the  $[T^*]$  and  $[T^{**}]$  matrices for the laminate.

The first element in the  $[T^*]$  matrix is

$$T_1^* = [(\bar{Q}_{11})_1(\alpha_{xx})_1 + (\bar{Q}_{12})_1(\alpha_{yy})_1](0 + t) \\ + [(\bar{Q}_{11})_2(\alpha_{xx})_2 + (\bar{Q}_{12})_2(\alpha_{yy})_2](t - 0).$$



Since  $(\alpha_{xx})_1 = (\alpha_{yy})_2 = \alpha_{11} = -0.5 \times 10^{-6}$  m/m per  $^\circ\text{C}$  and  $(\alpha_{xx})_2 = (\alpha_{yy})_1 = 12 \times 10^{-6}$  m/m per  $^\circ\text{C}$ , we obtain

$$\begin{aligned} T_1^* &= [(134.03)(-0.5) + (2.29)(12)](10^9)(10^{-6})t \\ &\quad + [(8.82)(12) + (2.29)(-0.5)](10^9)(10^{-6})t \\ &= 65.16 \times 10^3 t \text{ N/m}^\circ\text{C}. \end{aligned}$$

Using appropriate expressions for other elements in  $[T^*]$  and  $[T^{**}]$ , we obtain

$$\begin{aligned} [T^*] &= \begin{bmatrix} 65.16 \\ 65.16 \\ 0 \end{bmatrix} \times 10^3 t \text{ N/m}^\circ\text{C}, \\ [T^{**}] &= \begin{bmatrix} 72.12 \\ -72.12 \\ 0 \end{bmatrix} \times 10^3 t^2 \text{ N/}^\circ\text{C}. \end{aligned}$$

Step 3: Determine the laminate curvature matrix.

Substitution of  $[T^*]$  and  $[T^{**}]$  in [Equations 3.108](#) and [3.109](#) gives

$$\begin{aligned} \begin{bmatrix} 0 \\ 0 \\ 0 \end{bmatrix} &= [A] \begin{bmatrix} \varepsilon_{xx}^\circ \\ \varepsilon_{yy}^\circ \\ \gamma_{xy}^\circ \end{bmatrix} + [B] \begin{bmatrix} k_{xx} \\ k_{yy} \\ k_{xy} \end{bmatrix} - \begin{bmatrix} 65.16 \\ 65.16 \\ 0 \end{bmatrix} \times 10^3 t \Delta T, \\ \begin{bmatrix} 0 \\ 0 \\ 0 \end{bmatrix} &= [B] \begin{bmatrix} \varepsilon_{xx}^\circ \\ \varepsilon_{yy}^\circ \\ \gamma_{xy}^\circ \end{bmatrix} + [D] \begin{bmatrix} k_{xx} \\ k_{yy} \\ k_{xy} \end{bmatrix} - \begin{bmatrix} 72.12 \\ -72.12 \\ 0 \end{bmatrix} \times 10^3 t^2 \Delta T, \end{aligned}$$

where  $[A]$ ,  $[B]$ , and  $[D]$  are laminate stiffness matrices.

Eliminating the midplane strain matrix from the previous equations, we obtain the following expression relating the laminate curvature matrix to temperature variation  $\Delta T$ :

$$[k] = [C_1][T^*] + [D_1][T^{**}],$$

where  $[C_1]$  and  $[D_1]$  are given in Equation 3.95.

In this example,

$$[C_1] = \begin{bmatrix} 0.0218 & 0 & 0 \\ 0 & -0.0218 & 0 \\ 0 & 0 & 0 \end{bmatrix} 10^{-9} t^{-2} \frac{1}{\text{N}},$$

$$[D_1] = \begin{bmatrix} 0.0497 & -0.0016 & 0 \\ -0.0016 & 0.0497 & 0 \\ 0 & 0 & 0.4608 \end{bmatrix} 10^{-9} t^{-3} \frac{1}{\text{Nm}}.$$

Therefore, solving for  $[k]$ , we obtain

$$k_{xx} = -k_{yy} = 5.119 \times 10^{-6} t^{-1} \Delta T \text{ per m,}$$

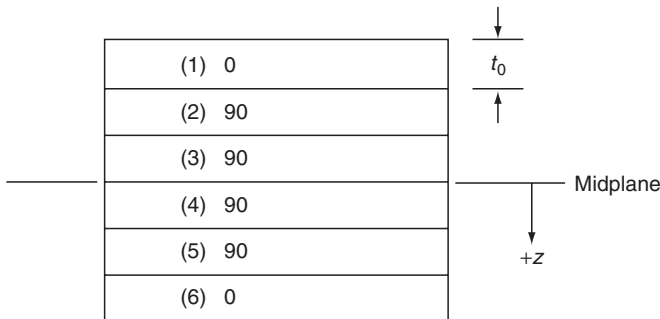
$$k_{xy} = 0.$$

From the expressions for  $k_{xx}$  and  $k_{yy}$ , we note that both curvatures decrease with increasing layer thickness as well as decreasing temperature variation. Furthermore, since  $k_{yy} = -k_{xx}$ , the laminate will assume a saddle shape at room temperature, as shown in the figure ((b) on page 207).

Classical lamination theory, such as that used here, predicts the room temperature shapes of all unsymmetric laminates to be a saddle. However, Hyer [26,27] has shown that both cylindrical and saddle shapes are possible, as shown in the figure ((c) on page 207). The cured shape of the laminate depends on the thickness-width ratio as well as the thickness-length ratio. Saddle shapes are obtained for thick laminates, but depending on the relative values of length and width, two different cylindrical shapes (with either  $k_{xx}$  or  $k_{yy} = 0$ ) are obtained for thin laminates in which the thickness-length or thickness-width ratios are small. It should be noted that symmetric laminates do not curve (warp) on curing since  $[B] = [0]$  as well as  $[T^{**}] = [0]$ .

### EXAMPLE 3.16

Residual stresses generated because of cooling from high curing temperatures: A  $[0/90_2]_S$  laminate of AS-4 carbon fiber-epoxy is cured at temperature  $T_i = 190^\circ\text{C}$  and slowly cooled down to room temperature,  $T_f = 23^\circ\text{C}$ . Determine the residual stresses generated in each layer because of cooling from the curing temperature. Assume each layer in the laminate has a thickness  $t_0$ .



Following material properties are known:

$$\begin{aligned}
 E_{11} &= 142 \text{ GPa}, \\
 E_{22} &= 10.3 \text{ GPa}, \\
 \nu_{12} &= 0.27, \\
 G_{12} &= 7.6 \text{ GPa}, \\
 \alpha_{11} &= -1.8 \times 10^{-6} \text{ per } ^\circ\text{C}, \\
 \alpha_{22} &= 27 \times 10^{-6} \text{ per } ^\circ\text{C}.
 \end{aligned}$$

### SOLUTION

Step 1: Using Equation 3.80, determine stiffness matrices for the  $0^\circ$  and  $90^\circ$  layers.

$$\begin{aligned}
 [\bar{Q}]_{0^\circ} &= \begin{bmatrix} 142.77 & 2.796 & 0 \\ 2.796 & 10.356 & 0 \\ 0 & 0 & 7.6 \end{bmatrix} \times 10^9 \text{ N/m}^2, \\
 [\bar{Q}]_{90^\circ} &= \begin{bmatrix} 10.356 & 2.796 & 0 \\ 2.796 & 142.77 & 0 \\ 0 & 0 & 7.6 \end{bmatrix} \times 10^9 \text{ N/m}^2.
 \end{aligned}$$

Step 2: Determine the  $[A]$  matrix for the laminate.

Note that because of symmetry,  $[B]=[0]$  and, since  $[k]=[0]$ , we need not determine the  $[D]$  matrix.

For a  $[0/90_2]_S$  laminate,  $A_{mn} = 2t_0 [(\bar{Q}_{mn})_0 + 2(\bar{Q}_{mn})_{90}]$ . Therefore,

$$[A] = 2t_0 \begin{bmatrix} 163.48 & 8.39 & 0 \\ 8.39 & 295.90 & 0 \\ 0 & 0 & 22.8 \end{bmatrix} \times 10^9 \text{ N/m}.$$

Step 3: Determine the  $[T^*]$  matrix for the laminate.

$$\begin{aligned}
 T_1^* &= 2\{[(\bar{Q}_{11})_0(\alpha_{xx})_0 + (\bar{Q}_{12})_0(\alpha_{yy})_0 + 0](-2t_0 + 3t_0) \\
 &\quad + [(\bar{Q}_{11})_{90}(\alpha_{xx})_{90} + (\bar{Q}_{12})_{90}(\alpha_{yy})_{90} + 0](-t_0 + 2t_0) \\
 &\quad + [(\bar{Q}_{11})_{90}(\alpha_{xx})_{90} + (\bar{Q}_{12})_{90}(\alpha_{yy})_{90} + 0](0 + t_0)\}.
 \end{aligned}$$

Since  $(\alpha_{xx})_0 = (\alpha_{yy})_{90} = \alpha_{11} = -1.8 \times 10^{-6}$  per  $^\circ\text{C}$  and  $(\alpha_{yy})_0 = (\alpha_{xx})_{90} = \alpha_{22} = 27 \times 10^{-6}$  per  $^\circ\text{C}$ , we obtain

$$T_1^* = 735.32t_0 \times 10^3 \text{ N/m}^\circ\text{C}.$$

Similarly,  $T_2^* = -176.82 t_0 \times 10^3 \text{ N/m } ^\circ\text{C}$  and  $T_3^* = 0$ .

Therefore,

$$[T^*] = \begin{bmatrix} 735.32t_0 \\ -176.82t_0 \\ 0 \end{bmatrix} \times 10^3 \text{ N/m}^\circ\text{C}.$$

Step 4: Using Equation 3.108, determine the midplane strains.

Since there are no external forces,  $[N] = [0]$ . Since  $[B] = [0]$ , we can write Equation 3.108 as

$$[0] = [A] \begin{bmatrix} \varepsilon_{xx}^\circ \\ \varepsilon_{yy}^\circ \\ \gamma_{xy}^\circ \end{bmatrix} + [0] - \begin{bmatrix} T_1^* \\ T_2^* \\ T_3^* \end{bmatrix} \Delta T,$$

where  $\Delta T = T_f - T_i$  (which, in this case, has a negative value).

Solving for the strain components gives

$$\begin{bmatrix} \varepsilon_{xx}^\circ \\ \varepsilon_{yy}^\circ \\ \gamma_{xy}^\circ \end{bmatrix} = \begin{bmatrix} 2.267 \\ -0.352 \\ 0 \end{bmatrix} \times 10^{-6} \Delta T \text{ m/m}.$$

Step 5: Determine strains in each layer.

Since  $[k] = [0]$ , strains in each layer are the same as the midplane strains.

Step 6: Determine the free thermal contraction strains in each layer.

$$\begin{bmatrix} \varepsilon_{xxf} \\ \varepsilon_{yjf} \\ \gamma_{xyf} \end{bmatrix}_{0^\circ} = \begin{bmatrix} -1.8 \\ 27 \\ 0 \end{bmatrix} \times 10^{-6} \Delta T \text{ m/m}$$

and

$$\begin{bmatrix} \varepsilon_{xxf} \\ \varepsilon_{yjf} \\ \gamma_{xyf} \end{bmatrix}_{90^\circ} = \begin{bmatrix} 27 \\ -1.8 \\ 0 \end{bmatrix} \times 10^{-6} \Delta T \text{ m/m}.$$

Step 7: Subtract free thermal contraction strains from strains determined in Step 5 to obtain residual strains in each layer.

$$\begin{bmatrix} \varepsilon_{xxr} \\ \varepsilon_{yyr} \\ \gamma_{xyr} \end{bmatrix}_{0^\circ} = \begin{bmatrix} (2.267 - (-1.8)) \times 10^{-6} \Delta T \\ (-0.352 - 27) \times 10^{-6} \Delta T \\ 0 \end{bmatrix} = \begin{bmatrix} 4.067 \\ -27.352 \\ 0 \end{bmatrix} \times 10^{-6} \Delta T \text{ m/m}$$

and

$$\begin{bmatrix} \varepsilon_{xxr} \\ \varepsilon_{yyr} \\ \gamma_{xyr} \end{bmatrix}_{90^\circ} = \begin{bmatrix} (2.267 - 27) \times 10^{-6} \Delta T \\ (-0.352 - (-1.8)) \times 10^{-6} \Delta T \\ 0 \end{bmatrix} = \begin{bmatrix} -24.733 \\ 1.448 \\ 0 \end{bmatrix} \times 10^{-6} \Delta T \text{ m/m}.$$

Step 8: Calculate the residual stresses in each layer

$$\begin{bmatrix} \sigma_{xxr} \\ \sigma_{yyr} \\ \tau_{xyr} \end{bmatrix}_{0^\circ} = [\bar{Q}]_{0^\circ} \begin{bmatrix} \varepsilon_{xxr} \\ \varepsilon_{yyr} \\ \gamma_{xyr} \end{bmatrix}_{0^\circ} = \begin{bmatrix} 504.17 \\ -271.89 \\ 0 \end{bmatrix} \times 10^3 \Delta T \text{ N/m}^2$$

and

$$\begin{bmatrix} \sigma_{xxr} \\ \sigma_{yyr} \\ \tau_{xyr} \end{bmatrix}_{90^\circ} = [\bar{Q}]_{90^\circ} \begin{bmatrix} \varepsilon_{xxr} \\ \varepsilon_{yyr} \\ \gamma_{xyr} \end{bmatrix}_{90^\circ} = \begin{bmatrix} -252.087 \\ 137.550 \\ 0 \end{bmatrix} \times 10^3 \Delta T \text{ N/m}^2.$$

Since, in this case,  $\Delta T = 23^\circ\text{C} - 190^\circ\text{C} = -167^\circ\text{C}$ , the residual stresses are as follows:

	0° Layer	90° Layer
In the fiber direction	-84.2 MPa	-22.97 MPa
In the transverse direction	45.40 MPa	42.10 MPa

### 3.4 INTERLAMINAR STRESSES

Load transfer between adjacent layers in a fiber-reinforced laminate takes place by means of interlaminar stresses, such as  $\sigma_{zz}$ ,  $\tau_{xz}$ , and  $\tau_{yz}$ . To visualize the mechanism of load transfer, let us consider a balanced symmetric  $[\pm 45]_S$  laminate under uniaxial tensile load  $N_{xx}$  (Figure 3.52). Since  $A_{16} = A_{26} = 0$  and  $[B] = [0]$  for this laminate, the midplane strains are given by

$$\begin{aligned} \varepsilon_{xx}^\circ &= \frac{A_{22}}{A_{11}A_{22} - A_{12}^2} N_{xx}, \\ \varepsilon_{yy}^\circ &= -\frac{A_{12}}{A_{11}A_{22} - A_{12}^2} N_{xx}, \\ \gamma_{xy}^\circ &= 0. \end{aligned}$$

The state of stress in the  $j$ th layer is

$$\begin{bmatrix} \sigma_{xx} \\ \sigma_{yy} \\ \tau_{xy} \end{bmatrix}_j = \begin{bmatrix} \bar{Q}_{11} & \bar{Q}_{12} & \bar{Q}_{16} \\ \bar{Q}_{12} & \bar{Q}_{22} & \bar{Q}_{26} \\ \bar{Q}_{16} & \bar{Q}_{26} & \bar{Q}_{66} \end{bmatrix}_j \begin{bmatrix} \varepsilon_{xx}^\circ \\ \varepsilon_{yy}^\circ \\ 0 \end{bmatrix}.$$

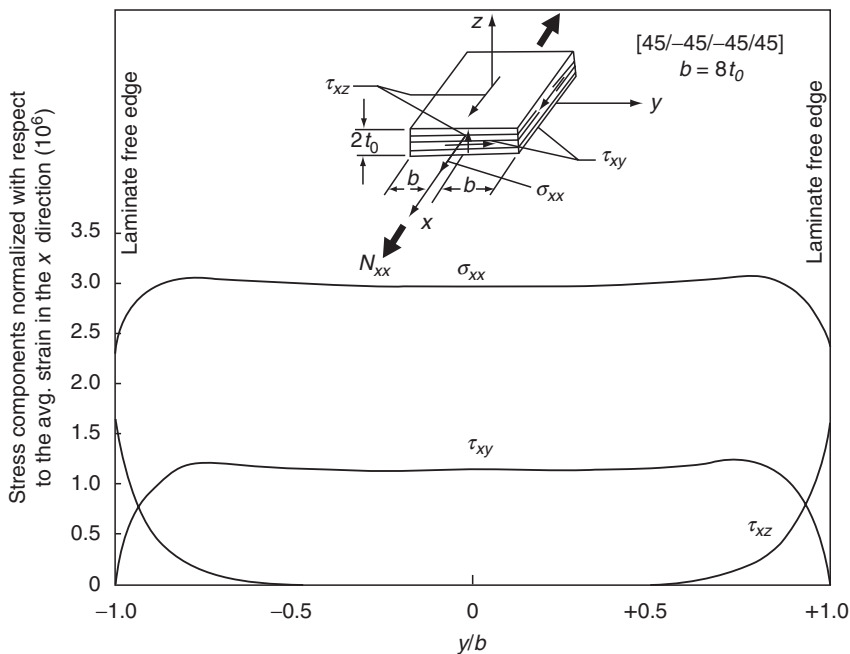


**FIGURE 3.52** Interlaminar shear stress  $\tau_{xz}$  between the  $+45^\circ$  and  $-45^\circ$  plies at the free edges of a  $[\pm 45]_S$  laminate. (After Pipes, R.B. and Pagano, N.J., *J. Compos. Mater.*, 4, 538, 1970.)

Thus, although the shear stress resultant  $N_{xy}$  on the laminate is zero, each layer experiences an in-plane shear stress  $\tau_{xy}$ . Since there is no applied shear stress at the laminate boundary, the in-plane shear stress must diminish from a finite value in the laminate interior to zero at its free edges. The large shear stress gradient at the ends of the laminate width is equilibrated by the development of the interlaminar shear stress  $\tau_{xz}$  near the free edges, as shown in Figure 3.52. Similar equilibrium arguments can be made to demonstrate the presence of  $\tau_{yz}$  and  $\sigma_{zz}$  in other laminates.

The principal reason for the existence of interlaminar stresses is the mismatch of Poisson's ratios  $\nu_{xy}$  and coefficients of mutual influence  $m_x$  and  $m_y$  between adjacent laminas. If the laminas were not bonded and could deform freely, an axial loading in the  $x$  direction would create dissimilar transverse strains  $\epsilon_{yy}$  in various laminas because of the difference in their Poisson's ratios. However, in perfect bonding, transverse strains must be identical throughout the laminate. The constraint against free transverse deformations produces normal stress  $\sigma_{yy}$  in each lamina and interlaminar shear stress  $\tau_{yz}$  at the lamina

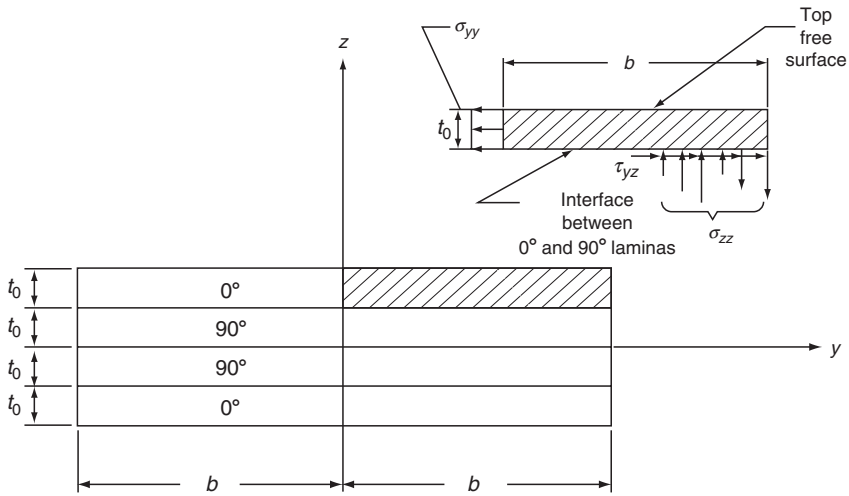


**FIGURE 3.53** Source of interlaminar shear stress  $\tau_{yz}$  and interlaminar normal stress  $\sigma_{zz}$  in a [0/90/90/0] laminate.

interfaces (Figure 3.53). Similarly, the difference in the coefficients of mutual influence  $m_x$  would create dissimilar shear strains  $\gamma_{xy}$  in various laminas only if they were not bonded. For a bonded laminate, equal shear strains for all laminas require the development of interlaminar shear stress  $\tau_{zx}$ . Although the force equilibrium in the  $y$  direction is maintained by the action of  $\sigma_{yy}$  and  $\tau_{yz}$ , the force resultants associated with  $\sigma_{yy}$  and  $\tau_{yz}$  are not collinear. The moment equilibrium about the  $x$  axis is satisfied by the action of the interlaminar normal stress  $\sigma_{zz}$ .

Interlaminar stresses  $\sigma_{zz}$ ,  $\tau_{xz}$ , and  $\tau_{yz}$  are determined by numerical methods (e.g., finite difference [28] or finite element methods [29,30]), which are beyond the scope of this book. A few approximate methods have also been developed [31,32]. For practical purposes, it may be sufficient to note the following.

1. Interlaminar stresses in laminated composites develop owing to mismatch in the Poisson's ratios and coefficients of mutual influence between various layers. If there is no mismatch of these two engineering properties, there are no interlaminar stresses regardless of the mismatch in elastic and shear moduli.
2. Interlaminar stresses can be significantly high over a region equal to the laminate thickness near the free edges of a laminate. The free edges may be at the boundaries of a laminated plate, around a cutout or hole, or at the ends of a laminated tube. As a result of high interlaminar stresses,

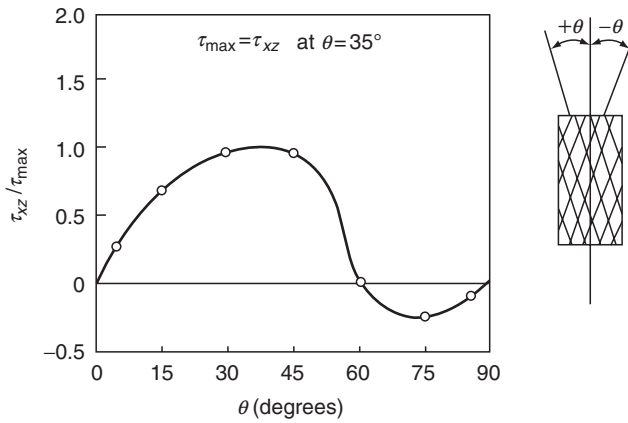


**FIGURE 3.54** Variation of interlaminar shear stress  $\tau_{xz}$  in a  $[\pm\theta]_s$  laminate with fiber orientation angle  $\theta$ . (Adapted from Pipes, R.B. and Pagano, N.J., *J. Compos. Mater.*, 4, 538, 1970.)

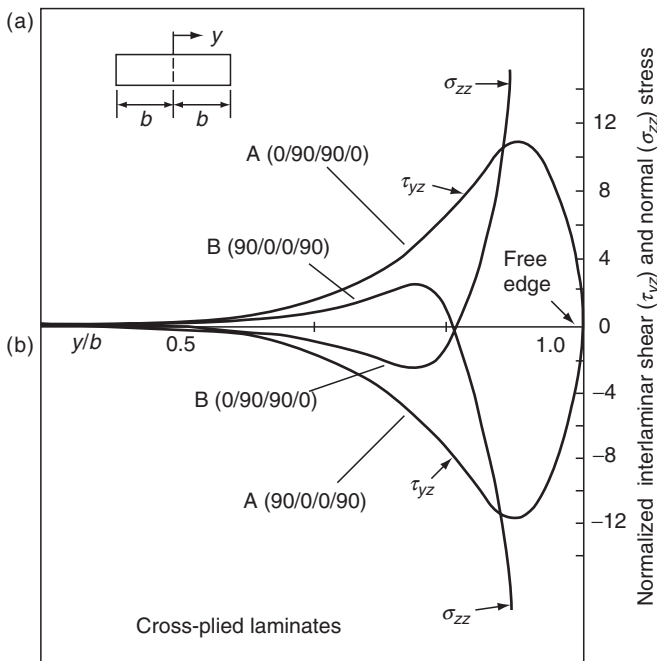


**FIGURE 3.55** Distribution of (a) interlaminar shear stress  $\tau_{yz}$  and (b) interlaminar normal stress  $\sigma_{zz}$  along the width of cross-plyed laminates. (Note that the interlaminar stresses are normalized with respect to the average normal strain in the  $x$  direction.) (Adapted from Pipes, R.B., *Fibre Sci. Technol.*, 13, 49, 1980.)

*delamination* (i.e., separation between various laminas) may initiate at the free edges.

3. For an  $[\theta/-\theta]$  angle-ply laminate in uniaxial tension,  $\tau_{xz}$  is the most significant interlaminar stress at the interfaces of the  $\theta$  and  $-\theta$  laminas. Its magnitude and direction depend strongly on the fiber orientation angle  $\theta$  (Figure 3.54). Furthermore,  $\tau_{xz}$  has a higher value at the  $(\theta/-\theta)$  interfaces in a clustered  $[\theta_n/-\theta_n]_S$  laminate than in an alternating  $[(\theta/-\theta)_n]_S$  laminate.
4. For a  $[0/90]$  type laminate in uniaxial tension, the significant interlaminar stresses are  $\sigma_{zz}$  and  $\tau_{yz}$ . Their magnitude, locations, and directions depend strongly on the stacking sequence (Figure 3.55). For example, the maximum  $\sigma_{zz}$  at the midplane of a  $[0/90/90/0]$  laminate is tensile, but maximum  $\sigma_{zz}$  at the midplane of a  $[90/0/0/90]$  laminate is compressive. Thus, delamination is likely in the  $[0/90/90/0]$  laminate.
5. For a general laminate, different combinations of  $\tau_{xz}$ ,  $\tau_{yz}$ , and  $\sigma_{zz}$  may be present between various laminas. For example, consider a  $[45/-45/0/0/-45/45]$  laminate in uniaxial tension. In this case, all

**TABLE 3.4**  
**Effect of Stacking Sequence on the Critical Interlaminar Stresses**  
**in Quasi-Isotropic  $[0/90/\pm 45]_S$  T-300 Carbon-Epoxy**  
**Laminates under Uniaxial Tension<sup>a</sup>**

Laminate	Max $\sigma_{zz}$		Max $\tau_{xz}$	
	Value	Location	Value	Location
$[90/45/0/-45]_S$	-6.8	Midplane	-6.9	$0^\circ/-45^\circ$
$[0/-45/90/45]_S$	6.2	$90^\circ$ layer	-6.6	$90^\circ/45^\circ$
$[45/90/0/-45]_S$	6.6	$90^\circ$ layer	5.9	$0^\circ/-45^\circ$
$[45/90/-45/0]_S$	6.9	$90^\circ$ layer	-6.5	$45^\circ/90^\circ$
$[45/0/90/-45]_S$	7.6	$90^\circ$ layer	-5.8	$90^\circ/-45^\circ$
$[45/0/-45/90]_S$	10.4	Midplane	-6.0	$0^\circ/-45^\circ$
$[90/0/-45/45]_S$	-8.2	$-45^\circ/45^\circ$	9.0	$-45^\circ/45^\circ$
$[90/45/-45/0]_S$	-7.4	$45^\circ/-45^\circ$	-9.2	$45^\circ/-45^\circ$
$[0/90/45/-45]_S$	-7.6	$45^\circ$ layer	-9.2	$45^\circ/-45^\circ$
$[0/45/-45/90]_S$	10.0	Midplane	-8.3	$45^\circ/-45^\circ$
$[45/-45/90/0]_S$	9.0	$0^\circ$ layer	-7.7	$45^\circ/-45^\circ$
$[45/-45/0/90]_S$	10.9	Midplane	-7.2	$45^\circ/-45^\circ$

Source: Adapted from Herakovich, C.T., *J. Compos. Mater.*, 15, 336, 1981.

<sup>a</sup> The stress magnitudes are in ksi. To transform to MPa, multiply by 6.89. The (/) indicates interface between adjacent layers.

three interlaminar stress components are present between the 45/−45 layers as well as the 0/−45 layers. However, the interlaminar shear stress  $\tau_{xz}$  between adjacent 45/−45 laminae is higher than that between adjacent 0/−45 laminae. On the other hand, the interlaminar shear stress  $\tau_{yz}$  between 0/−45 laminae is higher than that between 45/−45 laminae. However, the maximum  $\sigma_{zz}$  occurs at the laminate midplane.

- Stacking sequence has a strong influence on the nature, magnitude, and location of interlaminar stresses. This is demonstrated in Table 3.4. Note that laminates with interspersed  $\pm 45^\circ$  layers (separated by  $0^\circ$  or  $90^\circ$  layers) have lower  $\tau_{xz}$  than those with adjacent  $\pm 45^\circ$  layers, and, therefore, are less likely to delaminate. Among the laminates with

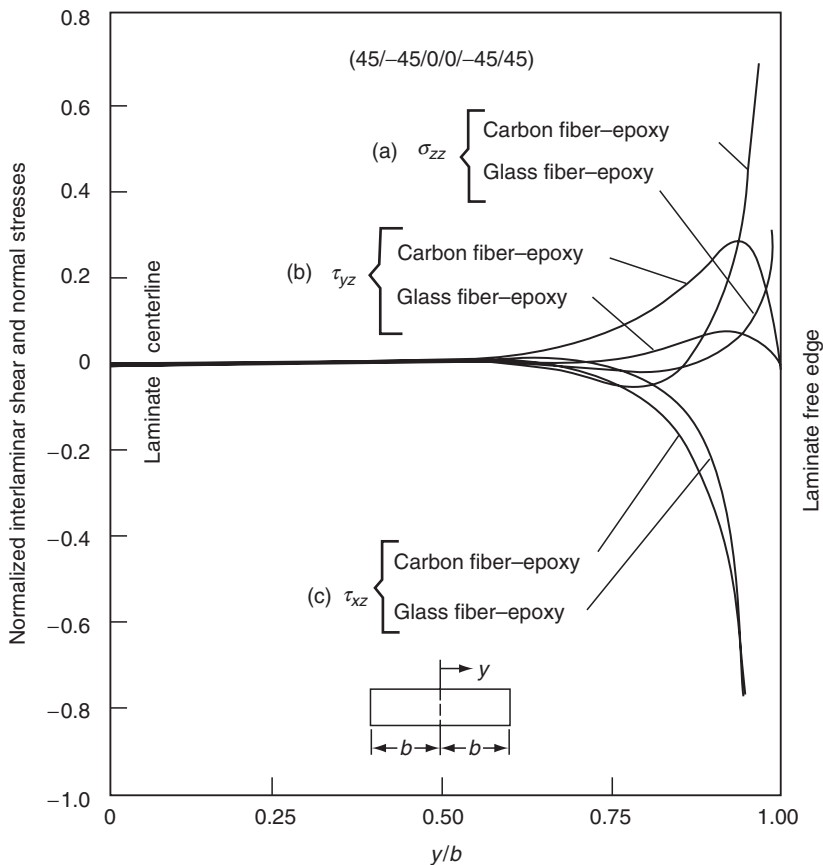


**FIGURE 3.56** Distribution of interlaminar stresses in  $[\pm 45/0]_S$  laminates with carbon and glass fibers in an epoxy matrix. (Adapted from Pipes, R.B., *Fibre Sci. Technol.*, 13, 49, 1980.)

interspersed  $\pm 45^\circ$  layers,  $[90/45/0/-45]_S$  has the most favorable  $\sigma_{zz}$  under a uniaxial tensile load applied on the laminates.

7. Material properties also have a strong influence on the interlaminar shear stresses of a laminate, as shown in [Figure 3.56](#).

## REFERENCES

1. G.S. Holister and C. Thomas, *Fibre Reinforced Materials*, Elsevier Publishing Co., London (1966).
2. C.C. Chamis, Micromechanics strength theories, *Composite Materials, Vol. 5, Fracture and Fatigue* (L.J. Broutman, ed.), Academic Press, New York, p. 93 (1974).
3. A.N. Netravali, P. Schwartz, and S.L. Phoenix, Study of interfaces of high performance glass fibers and DGEBA-based epoxy resins using single-fiber-composite test, *Polym. Compos.*, 6:385 (1989).
4. H.L. Cox, The elasticity and strength of paper and other fibrous materials, *Br. J. Appl. Phys.*, 3:72 (1952).
5. J. Cook and J.E. Gordon, A mechanism for the control of crack propagation in all brittle systems, *Proc. R. Soc. Lond., A*, 282:508 (1964).
6. D.C. Phillips, The fracture energy of carbon fibre reinforced glass, *J. Mater. Sci.*, 7 (1972).
7. J.O. Outwater and M.C. Murphy, The fracture energy of unidirectional laminates, Proc. 24th Annual Technical Conference, Society of the Plastics Industry (1969).
8. A. Kelly, Interface effects and the work of fracture of a fibrous composite, *Proc. R. Soc. Lond., A*, 319:95 (1970).
9. G.A. Cooper, Micromechanics aspects of fracture and toughness, *Composite Materials, Vol. 5, Fracture and Fatigue* (L.J. Broutman, ed.), Academic Press, New York, p. 415 (1974).
10. D.F. Adams and D.R. Doner, Transverse normal loading of a unidirectional composite, *J. Compos. Mater.*, 1:152 (1967).
11. L.B. Greszczuk, Theoretical and experimental studies on properties and behavior of filamentary composites, Proc. 21st Annual Technical Conference, Society of the Plastics Industry (1966).
12. B.W. Rosen, Mechanics of composite strengthening, *Fiber Composite Materials*, American Society for Metals, Metals Park, OH, p. 37 (1965).
13. C.R. Schultheisz and A.M. Waas, Compressive failure of composites, Part I: Testing and micromechanical theories, *Prog. Aerospace Sci.*, 32:1 (1996).
14. B. Budiansky and N.A. Fleck, Compressive failure of fibre composites, *J. Mech. Phys. Solids.*, 41:183 (1993).
15. T.A. Collings, Transverse compressive behavior of unidirectional carbon fibre reinforced plastics, *Composites*, 5:108 (1974).
16. R.M. Jones, *Mechanics of Composite Materials*, 2nd Ed., Taylor & Francis, Philadelphia (1999).
17. R.M. Christensen, The numbers of elastic properties and failure parameters for fiber composites, *J. Eng. Mater. Technol.*, 120:110 (1998).

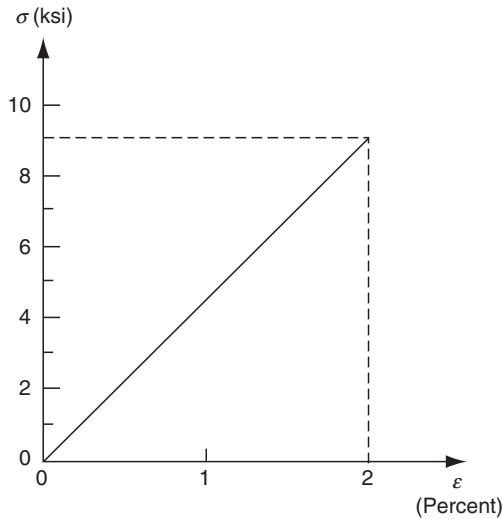
18. N.J. Pagano and P.C. Chou, The importance of signs of shear stress and shear strain in composites, *J. Compos. Mater.*, 3:166 (1969).
19. C.C. Chamis and G.P. Sendeckyj, Critique on theories predicting thermoelastic properties of fibrous composites, *J. Compos. Mater.*, 2:332 (1968).
20. R.M. Jones, Stiffness of orthotropic materials and laminated fiber-reinforced composites, *AIAA J.*, 12:112 (1974).
21. R.A. Schapery, Thermal expansion coefficients of composite materials based on energy principles, *J. Compos. Mater.*, 2:280 (1968).
22. L.B. Greszczuk, Effect of material orthotropy on the directions of principal stresses and strains, *Orientation Effects in the Mechanical Behavior of Anisotropic Structural Materials, ASTM STP*, 405:1 (1966).
23. S.W. Tsai and N.J. Pagano, Invariant properties of composite materials, *Composite Materials Workshop* (S.W. Tsai, J.C. Halpin, and N.J. Pagano, eds.), Technomic Publishing Co., Stamford, CT, p. 233 (1968).
24. R.B. Pipes, J.R. Vinson, and T.W. Chou, On the hygrothermal response of laminated composite systems, *J. Compos. Mater.*, 10:129 (1976).
25. H.T. Hahn, Residual stresses in polymer matrix composite laminates, *J. Compos. Mater.*, 10:266 (1976).
26. M.W. Hyer, Some observations on the cured shape of thin unsymmetric laminates, *J. Compos. Mater.*, 15:175 (1981).
27. M.W. Hyer, Calculations of room-temperature shapes of unsymmetric laminates, *J. Compos. Mater.*, 15:295 (1981).
28. R.B. Pipes and N.J. Pagano, Interlaminar stresses in composite laminates under uniform axial extension, *J. Compos. Mater.*, 4:538 (1970).
29. G. Isakson and A. Levy, Finite-element analysis of interlaminar shear in fibrous composites, *J. Compos. Mater.*, 5:273 (1971).
30. E.F. Rybicki, Approximate three-dimensional solutions for symmetric laminates under inplane loading, *J. Compos. Mater.*, 5:354 (1971).
31. J.M. Whitney, Free-edge effects in the characterization of composite materials, *Analysis of the Test Methods for High Modulus Fibers and Composites, ASTM STP*, 521:167 (1973).
32. P. Conti and A.D. Paulis, A simple model to simulate the interlaminar stresses generated near the free edge of a composite laminate, *Delamination and Debonding of Materials, ASTM STP*, 876:35 (1985).

## PROBLEMS

- P3.1. Calculate the longitudinal modulus, tensile strength, and failure strain of a unidirectional continuous fiber composite containing 60 vol% of T-800 carbon fibers ( $E_f = 294$  GPa and  $\sigma_{fu} = 5.6$  GPa) in an epoxy matrix ( $E_m = 3.6$  GPa,  $\sigma_{mu} = 105$  MPa, and  $\varepsilon_{mu} = 3.1\%$ ). Compare these values with the experimentally determined values of  $E_L = 162$  GPa,  $\sigma_{Ltu} = 2.94$  GPa, and  $\varepsilon_{Ltu} = 1.7\%$ . Suggest three possible reasons for the differences. What fraction of load is carried by the fibers in this composite?

P3.2. The material of a tension link is changed from a Ti-6Al-4V (aged) titanium alloy to a unidirectional continuous GY-70 carbon fiber–epoxy. The stress–strain curve of the epoxy resin is shown in the following figure. Calculate the volume fraction of GY-70 fibers required in the composite link to match the modulus of the titanium alloy.

In addition, estimate the tensile strength of the composite link and compare its strength–weight ratio with that of the titanium alloy.

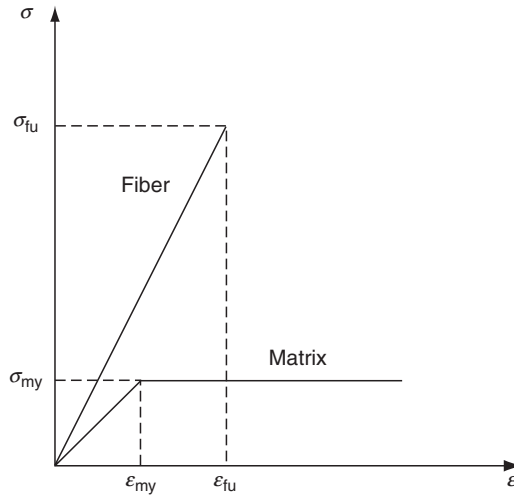


P3.3. To increase the longitudinal tensile modulus of a unidirectional continuous E-glass fiber-reinforced epoxy, some of the E-glass fibers are replaced with T-300 carbon fibers. The total fiber volume fraction is kept unchanged at 60%. Assume that the E-glass and T-300 carbon fibers in the new composite are uniformly distributed.

1. Calculate the volume fraction of T-300 carbon fibers needed in the new composite to double the longitudinal tensile modulus
2. Compare the longitudinal tensile strength of the new composite with that of the original composite
3. Schematically compare the stress–strain diagrams of the fibers, the matrix, and the composite

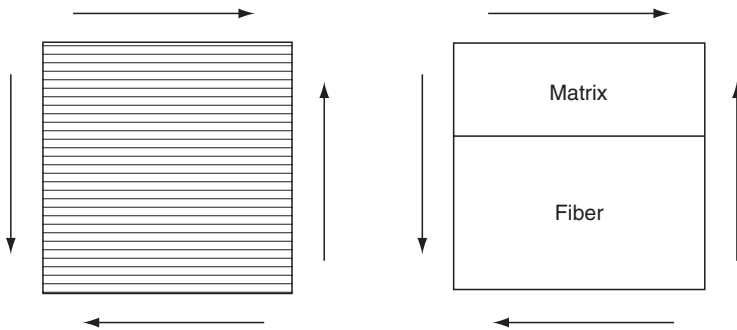
The tensile modulus and strength of the epoxy are 5 GPa and 50 MPa, respectively. Assume that the tensile stress–strain diagram of the epoxy is linear up to the point of failure.

P3.4. Consider a unidirectional continuous fiber lamina containing brittle, elastic fibers in an elastic-perfectly plastic matrix. The stress–strain diagrams for the fibers and the matrix are shown as follows:



1. Calculate the longitudinal modulus of the composite lamina before and after the matrix yielding
  2. Calculate the failure stress for the lamina
  3. Draw the stress–strain diagram for the lamina, and explain how it may change if the matrix has the capacity for strain hardening
  4. Compare the loads carried by the fibers before and after the matrix yields
- P3.5. Compare  $E_T/E_L$  vs.  $v_f$  of a unidirectional continuous IM-7 carbon fiber-reinforced epoxy and a unidirectional continuous fiber E-glass-reinforced epoxy. Assume  $E_m = 2.8$  GPa. What observations will you make from this comparison?
- P3.6. A unidirectional continuous fiber lamina is subjected to shear stress as shown in the following figure. Using the “slab” model, show that the shear modulus  $G_{LT}$  of the lamina can be represented by the following equation.

$$\frac{1}{G_{LT}} = \frac{v_f}{G_f} + \frac{(1 - v_f)}{G_m}.$$



Unidirectional continuous fiber-reinforced composite and the equivalent slab model in in-plane shear loading

- P3.7. Compare the minimum critical fiber aspect ratios for E-glass, T-300 carbon, P-100 carbon, and Kevlar 49 fibers in an epoxy matrix. Assume that the epoxy matrix behaves as an elastic, perfectly plastic material with a tensile yield strength of 10,000 psi.
- P3.8. Compare the failure strength of a unidirectional alumina whisker ( $l_f/d_f=200$ )-reinforced epoxy with that of a unidirectional continuous alumina fiber-reinforced epoxy. The tensile strength of alumina whiskers is 1,000,000 psi, but that of continuous alumina fibers is 275,000 psi. Assume  $v_f=0.5$  and  $\tau_{my}=4,800$  psi.
- P3.9. A unidirectional discontinuous E-glass fiber-reinforced vinyl ester composite is required to have a longitudinal tensile strength of 1000 MPa. The fiber volume fraction is 60%. Fiber length and fiber bundle diameter are 12 and 1 mm, respectively. Determine the fiber–matrix interfacial shear strength needed to achieve the required longitudinal tensile strength. The fiber and matrix properties are as follows:  
 Fiber: Modulus = 72.4 GPa, tensile strength = 2500 MPa  
 Matrix: Modulus = 2.8 GPa, tensile strength = 110 MPa.
- P3.10. Derive an expression for the critical fiber volume fraction in a unidirectional discontinuous fiber composite. On a plot of the composite tensile strength vs. fiber volume fraction, indicate how the critical fiber volume fraction depends on the fiber length.
- P3.11. In deriving Equation 3.13, the interfacial shear stress has been assumed constant. Instead, assume that

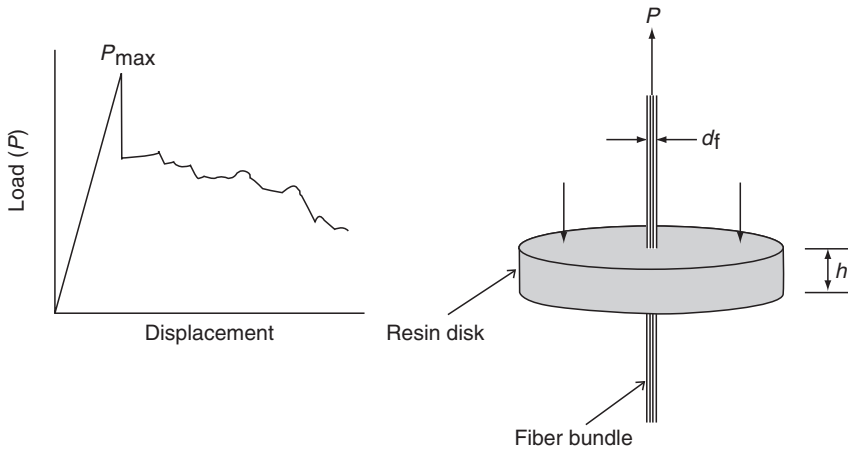
$$\begin{aligned} \tau_i &= 3000 - 6000 \frac{x}{l_f} \text{ psi for } 0 \leq x \leq \frac{1}{2} l_f \\ &= 0 \quad \text{for } \frac{1}{2} l_f \leq x \leq \frac{1}{2} l_f \end{aligned}$$

(a) Show how the fiber stress varies with  $x$ , (b) Calculate the critical fiber length, and (c) Calculate the average fiber stress.

P3.12. Using Equation 3.20, derive an expression for the average longitudinal stress in a discontinuous fiber. Assuming a simple square array of AS-1 carbon fibers in an epoxy matrix ( $G_m = 1.01$  GPa), plot the average longitudinal fiber stress as a function of  $l_f/d_f$  for  $v_f = 0.2, 0.4,$  and  $0.6$ .

P3.13. The interfacial shear strength of a fiber–matrix joint is often measured by a pullout test. This involves pulling a fiber bundle out of a resin disk cast around a small length of the bundle. A typical load–displacement curve obtained in a pullout test is shown.

1. Calculate the average interfacial shear strength of the joint
2. What must the maximum thickness of the resin disk be so that the fiber bundle pulls out before it breaks within the disk?



P3.14. Using the equations for the fiber pullout energies (Table 3.2) show that the maximum energy dissipation by fiber pullout occurs at  $l_f = l_c$ . How do the fiber tensile strength and fiber–matrix interfacial strength affect the pullout energy?

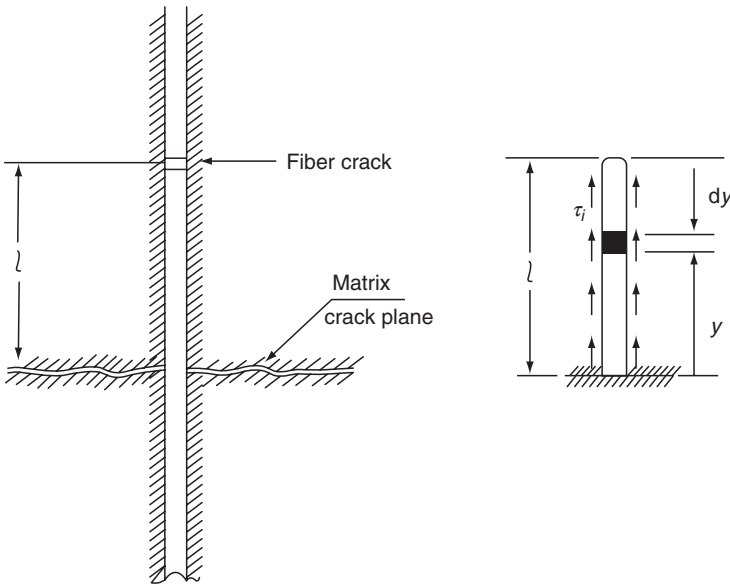
P3.15. Longitudinal tensile tests of single-fiber specimens containing AS-1 carbon fiber in epoxy and HMS-4 carbon fiber in epoxy produce cleavage cracks (normal to the fiber direction) in the matrix adjacent to the fiber rupture. However, the cleavage crack in the AS specimen is longer than in the HMS specimen. Furthermore, the longitudinal tensile strength of the AS specimen increases significantly with increasing matrix ductility, but that of the HMS carbon specimen remains

unaffected. Explain both phenomena in terms of the energy released on fiber fracture.

- P3.16. A fiber breaks at a location away from the matrix crack plane and pulls out from the matrix with the opening of the matrix crack. Assuming that the embedded fiber length  $l$  in the figure is less than half the critical length  $l_c$ , show that the work required to pull out the fiber is

$$W_{po} = \frac{\pi}{2} d_f l^2 \tau_i,$$

where  $\tau_i$  is the interfacial shear stress (assumed constant). What might be expected if the embedded fiber length  $l$  is greater than  $\frac{1}{2}l_c$ ?



- P3.17. Using the rule of mixture approach as was done for longitudinal tensile loading, derive equations for the longitudinal compressive modulus and strength of a unidirectional continuous fiber composite for the following cases:

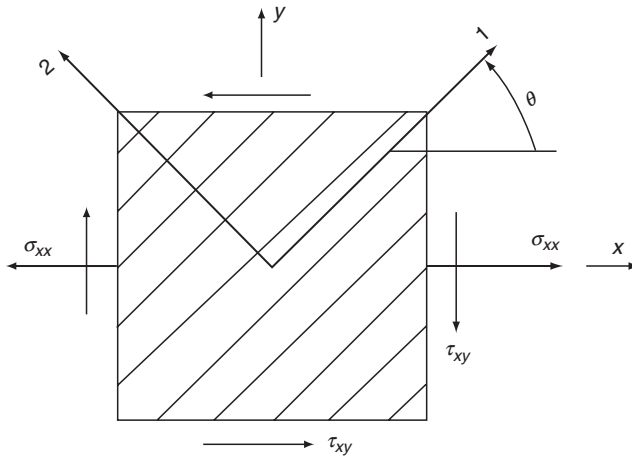
1.  $\varepsilon_{fc} < \varepsilon_{myc}$
2.  $\varepsilon_{fc} > \varepsilon_{myc}$

where

- $\varepsilon_{fc}$  = fiber “fracture” strain in compression
- $\varepsilon_{myc}$  = matrix yield strain in compression

Compare the rule of mixtures approach with Rosen's microbuckling approach for a carbon fiber-reinforced epoxy composite using the following information:  $E_{fc} = 517 \text{ GPa}$ ,  $\varepsilon_{fc} = 0.25\%$ ,  $E_{mc} = 2.1 \text{ GPa}$ ,  $\varepsilon_{myc} = 2.85\%$ ,  $\nu_m = 0.39$ , and  $\nu_f = 0.4, 0.5, 0.6$ .

- P3.18. Under longitudinal compressive loads, a unidirectional continuous fiber-reinforced brittle matrix composite often fails by longitudinal matrix cracks running parallel to the fibers. Explain this failure mode in terms of the stress and strain states in the matrix, and, derive an equation for the longitudinal compressive strength of the composite for this failure mode.
- P3.19. A 500 mm long  $\times$  25 mm wide  $\times$  3 mm thick composite plate contains 55% by weight of unidirectional continuous T-300 carbon fibers in an epoxy matrix parallel to its length.
1. Calculate the change in length, width, and thickness of the plate if it is subjected to an axial tensile force of 75 kN in the length direction
  2. Calculate the change in length, width, and thickness of the plate if it is subjected to an axial tensile force of 75 kN in the width direction
- Assume that the density, modulus, and Poisson's ratio of the epoxy matrix are  $1.25 \text{ g/cm}^3$ ,  $3.2 \text{ GPa}$ , and  $0.3$ , respectively.
- P3.20. A round tube (outside diameter = 25 mm, wall thickness = 2.5 mm, and length = 0.5 m) is made by wrapping continuous AS-4 carbon fiber-reinforced epoxy layers, all in the hoop direction. The fiber volume fraction is 60%.
1. Determine the change in length and diameter of the tube if it is subjected to an axial tensile load of 2 kN
  2. Determine the maximum axial tensile load that can be applied on the tube?
  3. Suppose the tube is used in a torsional application. What will be its torsional stiffness (torque per unit angle of twist)?
- The modulus, tensile strength, and Poisson's ratio of the epoxy matrix are  $5 \text{ GPa}$ ,  $90 \text{ MPa}$ , and  $0.34$ , respectively.
- P3.21. The normal stress  $\sigma_{xx}$  of 100 MPa and shear stress  $\tau_{xy}$  of 25 MPa are applied on a unidirectional angle-ply lamina containing fibers at an angle  $\theta$  as shown in the figure. Determine the stresses in the principal material directions for  $\theta = 0^\circ, 15^\circ, 30^\circ, 45^\circ, 60^\circ, 75^\circ$ , and  $90^\circ$ . Do these stresses remain the same (a) if the direction for the shear stress  $\tau_{xy}$  is reversed and (b) if the fiber orientation angles are reversed?



P3.22. A tubular specimen containing fibers at a helix angle  $\alpha$  with the tube axis is tested in a combined tension–torsion test. Determine the ratio of  $\sigma_{xx}$  and  $\tau_{xy}$  as well as the required helix angle  $\alpha$  that will create biaxial principal stresses  $\sigma_{11}$  and  $\sigma_{22}$  of ratio  $m$ . Note that the shear stress  $\tau_{12}$  in the principal stress directions is zero.

P3.23. A cylindrical oxygen tank made of an E-glass fiber-reinforced epoxy contains oxygen at a pressure of 10 MPa. The tank has a mean diameter of 300 mm and a wall thickness of 8.9 mm. The fiber orientation angles in various layers of the tank wall are  $\pm 55^\circ$  with its longitudinal axis. Neglecting the interaction between the layers, calculate the stresses in the principal material directions for both fiber orientation angles.

P3.24. The following tensile modulus values were experimentally determined for a unidirectional carbon fiber-reinforced PEEK composite ( $\nu_f = 0.62$ ):

Fiber orientation angle (degrees)	0	5	10	30	45	60	75	90
Modulus (GPa)	135.2	113.4	72	25.4	11.5	9.65	8.36	9.20

Plot the data as a function of the fiber orientation angle and compare them with the theoretical predictions assuming  $E_f = 230$  GPa,  $\nu_f = 0.28$ ,  $E_m = 3.45$  GPa, and  $\nu_m = 0.4$ . Verify the validity of [Equation 3.36](#).

P3.25. Calculate the elastic constants  $E_{xx}$ ,  $E_{yy}$ ,  $\nu_{xy}$ ,  $\nu_{yx}$ , and  $G_{xy}$  for a T-300 carbon fiber-reinforced epoxy lamina. The fiber orientation angle is  $30^\circ$ ,

and the fiber volume fraction is 0.6. For the epoxy matrix, use  $E_m = 2.07$  GPa and  $\nu_m = 0.45$ .

P3.26. A unidirectional discontinuous fiber lamina contains T-300 carbon fiber in an epoxy matrix. The fiber aspect ratio ( $l_f/d_f$ ) is 50, and the fiber volume fraction is 0.5. Determine the elastic constants  $E_{11}$ ,  $E_{22}$ ,  $\nu_{12}$ ,  $\nu_{21}$ , and  $G_{12}$  for the lamina. For the matrix, use  $E_m = 2.07$  GPa and  $\nu_m = 0.45$ . If the fibers are misaligned by  $10^\circ$  with the uniaxial loading direction, how would these elastic constants change?

P3.27. The material used in the transmission gears of an automobile is an injection-molded nylon 6,6 containing 20 wt% of chopped randomly oriented E-glass fibers. The tensile modulus of this material is  $1.25 \times 10^6$  psi.

In a more demanding application for the transmission gears, the modulus of the material must be 50% higher. An engineer wants to accomplish this by replacing the E-glass fibers with carbon fibers. If the fiber weight fraction remains the same, calculate the length of carbon fibers that must be used to obtain the desired modulus.

Use the following information in your calculations. (a) For the carbon fiber,  $\rho_f = 1.8$  g/cm<sup>3</sup>,  $E_f = 30 \times 10^6$  psi, and  $d_f = 0.0006$  in. and (b) for nylon 6,6,  $\rho_m = 1.14$  g/cm<sup>3</sup> and  $E_m = 0.4 \times 10^6$  psi.

P3.28. A unidirectional discontinuous E-glass fiber-reinforced polyphenylene sulfide (PPS) composite needs to be developed so that its longitudinal tensile modulus is at least 25 GPa and its longitudinal tensile strength is at least 950 MPa. Through the use of proper coupling agent on the glass fiber surface, it would be possible to control the interfacial shear strength between 10 and 30 MPa. The fiber bundle diameter is 0.30 mm and the fiber weight fraction is 60%. Determine the fiber length required for this composite.

The matrix properties are:  $\rho_m = 1.36$  g/cm<sup>3</sup>,  $E_m = 3.5$  GPa, and  $S_{mu} = 165$  MPa.

P3.29. A unidirectional continuous fiber lamina contains carbon fibers in an epoxy matrix. The fiber volume fraction is 0.55. The coefficient of longitudinal thermal expansion for the lamina is measured as  $-0.61 \times 10^{-6}$  per  $^\circ\text{C}$ , and that for the matrix at the same temperature is  $54 \times 10^{-6}$  per  $^\circ\text{C}$ . Estimate the coefficient of thermal expansion for the fiber. The longitudinal modulus of the lamina is 163.3 GPa and the matrix modulus is 3.5 GPa.

P3.30. Coefficients of axial and transverse thermal expansion of  $0^\circ$  unidirectional Spectra 900 fiber-reinforced epoxy composite ( $v_f = 60\%$ ) are

$-9 \times 10^{-6}$  and  $100 \times 10^{-6}$  per  $^{\circ}\text{C}$ , respectively. For the same composite, the major Poisson's ratio is 0.32. The matrix properties are  $E_m = 2.8$  GPa,  $\nu_m = 0.38$ , and  $\alpha_m = 60 \times 10^{-6}$  per  $^{\circ}\text{C}$ . Using these values, estimate (a) the Poisson's ratio of the fiber, (b) coefficients of thermal expansion of the fiber in longitudinal and radial directions, and (c) the fiber volume fraction at which the composite has a zero CTE.

P3.31. A 1 m long thin-walled composite tube has a mean diameter of 25 mm and its wall thickness is 2 mm. It contains 60 vol% E-glass fibers in a vinyl ester matrix. Determine the change in length and diameter of the tube if the temperature is increased by  $50^{\circ}\text{C}$ . The matrix properties are  $E_m = 3.5$  GPa,  $\nu_m = 0.35$ ,  $\alpha_m = 70 \times 10^{-6}$  per  $^{\circ}\text{C}$ .

P3.32. An E-glass fiber–epoxy laminate has the following construction:

$$[0/30/-30/45/-45/90/-45/45/-30/30/0].$$

The following are known:  $\nu_f = 0.60$ ,  $E_f = 10 \times 10^6$  psi,  $E_m = 0.34 \times 10^6$  psi,  $\nu_f = 0.2$ ,  $\nu_m = 0.35$ ,  $\alpha_f = 5 \times 10^{-6}$  per  $^{\circ}\text{C}$ , and  $\alpha_m = 60 \times 10^{-6}$  per  $^{\circ}\text{C}$ . Determine the coefficients of thermal expansion in the  $x$  and  $y$  directions for each lamina.

P3.33. Consider a unidirectional continuous fiber lamina. Applying  $\sigma_{11}$ ,  $\sigma_{22}$ , and  $\tau_{12}$  separately, show that the engineering elastic constants  $E_{11}$ ,  $E_{22}$ ,  $\nu_{12}$ ,  $\nu_{21}$ , and  $G_{12}$  can be expressed in terms of the elements in the lamina stiffness matrix as

$$E_{11} = Q_{11} - \frac{Q_{12}^2}{Q_{22}},$$

$$E_{22} = Q_{22} - \frac{Q_{12}^2}{Q_{11}},$$

$$\nu_{12} = \frac{Q_{12}}{Q_{22}},$$

$$\nu_{21} = \frac{Q_{12}}{Q_{11}},$$

$$G_{12} = Q_{66}.$$

P3.34. A T-300 carbon fiber–epoxy lamina ( $\nu_f = 0.60$ ) with a fiber orientation angle of  $45^{\circ}$  is subjected to a biaxial stress state of  $\sigma_{xx} = 100$  MPa and  $\sigma_{yy} = -50$  MPa. Determine (a) the strains in the  $x$ – $y$  directions, (b) the strains in the 1–2 directions, and (c) the stresses in the 1–2 directions. Use the material property data of [Example 3.6](#).

- P3.35. Plot and compare the coefficients of mutual influence as functions of fiber orientation angle  $\theta$  in T-300 carbon fiber–epoxy laminas containing fibers at the  $+\theta$  and  $-\theta$  orientations. For what fiber orientation angle  $\theta$  do the coefficients of mutual influence have the maximum values? Use the material property data of [Example 3.6](#).
- P3.36. The elastic constants of a  $0^\circ$  unidirectional carbon fiber-reinforced PEEK lamina are  $E_{11}=132.2$  GPa,  $E_{22}=9.2$  GPa,  $G_{12}=4.90$  GPa, and  $\nu_{12}=0.35$ . Write the compliance and stiffness matrices for the same material if the fiber orientation angle is (a)  $30^\circ$ , (b)  $-30^\circ$ , (c)  $60^\circ$ , and (d)  $90^\circ$ .
- P3.37. A T-300 carbon fiber–epoxy lamina ( $\nu_f=0.6$ ) is subjected to a uniaxial normal stress  $\sigma_{xx}$ . Compare the strains in the  $x$ – $y$  directions as well as in the 1–2 directions for  $\theta=0^\circ$ ,  $+45^\circ$ ,  $-45^\circ$ , and  $90^\circ$ . Use the material property data of [Example 3.6](#) and [Problem P3.35](#).
- P3.38. Compare the stiffness matrices of three-layered  $[0/60/-60]$ ,  $[-60/0/60]$ , and  $[-60/60/-60]$  laminates. Which of these laminates can be considered quasi-isotropic, and why? Assume that each layer has the same thickness  $t_0$ .
- P3.39. Compare the stiffness matrices of two-layered, three-layered, and four-layered angle-ply laminates containing alternating  $\theta$  and  $-\theta$  laminas. Assume that each layer has the same thickness  $t_0$ .
- P3.40. Show that the extensional stiffness matrices for quasi-isotropic  $[0/\pm 60]_S$ ,  $[\pm 60/0]_S$ , and  $[60/0/-60]_S$  laminates are identical, while their bending stiffness matrices are different.
- P3.41. The modulus of a  $[0_m/90_n]$  laminate can be calculated using the following “averaging” equation.

$$E_{xx} = \frac{m}{m+n} E_{11} + \frac{n}{m+n} E_{22}.$$

Suppose a  $[0/90/0]_{3S}$  laminate is constructed using continuous T-300 fibers in an epoxy matrix. Verify that the modulus of the laminate calculated by the averaging equation is the same as calculated by the lamination theory. Use the material properties given in [Example 3.6](#).

- P3.42. The  $[A]$  matrix for a boron fiber–epoxy  $[\pm 45]_S$  laminate of thickness  $h$  is

$$[A] = \begin{bmatrix} 0.99h & 0.68h & 0 \\ 0.68h & 0.99h & 0 \\ 0 & 0 & 0.72h \end{bmatrix} \times 10^7 \text{ lb/in.}$$

1. Calculate the engineering elastic constants for the laminate
2. Calculate the strains in the  $+45^\circ$  and  $-45^\circ$  laminas owing to average laminate stresses  $N_{xx}/h = N_{yy}/h = p$  and  $N_{xy}/h = 0$ . Assume that each lamina has a thickness of  $h/4$

P3.43. The elastic properties of unidirectional carbon fiber–epoxy lamina are  $E_{11} = 181.3$  GPa,  $E_{22} = 10.27$  GPa,  $G_{12} = 7.17$  GPa, and  $\nu_{12} = 0.28$ . Compare the engineering elastic constants of the  $[\pm 45/0]_S$  and  $[\pm 45/0/90]_S$  laminates manufactured from this carbon fiber–epoxy material.

P3.44. Show that the shear modulus of a thin  $[\pm 45]_{nS}$  plate is given by

$$G_{xy} = \frac{1}{4} \left[ \frac{E_{11} + E_{22} - 2\nu_{12}E_{22}}{1 - \nu_{12}\nu_{21}} \right].$$

P3.45. Show that the elements in the bending stiffness matrix of  $[0/-60/60]_S$  and  $[0/90/45/-45]_S$  laminates are given by

$$D_{ij} = \frac{h^3}{12} \left[ \frac{(\bar{Q}_{ij})_{60^\circ} + 7(\bar{Q}_{ij})_{-60^\circ} + 19(\bar{Q}_{ij})_{0^\circ}}{27} \right]$$

and

$$D_{ij} = \frac{h^3}{12} \left[ \frac{(\bar{Q}_{ij})_{-45^\circ} + 7(\bar{Q}_{ij})_{45^\circ} + 19(\bar{Q}_{ij})_{90^\circ} + 37(\bar{Q}_{ij})_{0^\circ}}{64} \right],$$

respectively. Here,  $h$  represents the laminate thickness.

P3.46. A torsional moment  $M_{xy}$  applied to a symmetric laminated plate creates a bending curvature as well as a twisting curvature. Find an expression for the additional bending moment  $M_{xx}$  that must be applied to the plate to create a pure twisting curvature  $k_{xy}$ .

P3.47. An ARALL-4 laminate contains three layers of 2024-T8 aluminum alloy sheet (each 0.3 mm thick) and two layers of  $0^\circ$  unidirectional Kevlar 49-epoxy in an alternate sequence,  $[A1/0_K/A1/0_K/A1]$ . Elastic properties of the aluminum alloy are  $E = 73$  GPa and  $\nu = 0.32$ , whereas

those for the Kevlar layers are  $E_{11} = 56.2$  GPa,  $E_{22} = 4.55$  GPa,  $\nu_{12} = 0.456$ , and  $G_{12} = 1.85$  GPa. The nominal thickness of the laminate is 1.3 mm. Calculate the elastic properties of the ARALL-4 laminate.

- P3.48. Using the basic ply level properties of [Example 3.6](#), determine the stresses in each layer of a  $[\pm 45]_{32S}$  laminate subjected to  $N_{xx} = 0.1$  N/mm. The ply thickness is 0.013 mm.
- P3.49. Using the material properties in [Example 3.16](#), determine the residual thermal stresses in each lamina of (i) a  $[90_2/0]_S$  and (ii) a  $[0/90/0]_S$  laminate. Both laminates are slowly cooled down from a curing temperature of 190°C to 23°C.
- P3.50. The following thermomechanical properties are known for a carbon fiber–epoxy composite:  $E_{11} = 145$  GPa,  $E_{22} = 9$  GPa,  $G_{12} = 4.5$  GPa,  $\nu_{12} = 0.246$ ,  $\alpha_{11} = -0.25 \times 10^{-6}$  per °C, and  $\alpha_{22} = 34.1 \times 10^{-6}$  per °C. Determine the coefficients of thermal expansion of a  $[45/-45]_S$  laminate of this material.
- P3.51. Using the ply level thermomechanical properties given in Problem 3.49, determine the coefficients of thermal expansion of a  $[0/45/-45/90]_S$  laminate of this material.
- P3.52. An approximate expression for the maximum interlaminar shear stress  $\tau_{xz}$  in a  $[\theta/-\theta]_{nS}$  class of laminates\* is

$$\text{Max } \tau_{xz} = \frac{1}{2n} \left[ \frac{A_{22}\bar{Q}_{16} - A_{12}\bar{Q}_{26}}{A_{11}A_{22} - A_{12}^2} \right] \frac{N_{xx}}{h},$$

where  $N_{xx}/h$  is the average tensile stress on the laminate in the  $x$  direction.

Using this expression, compare the maximum interlaminar shear stress  $\tau_{xz}$  in  $[15/-15]_{8S}$  and  $[45/-45]_{8S}$  T-300 carbon–epoxy laminates. Use [Example 3.6](#) for the basic material property data.

- P3.53. Following is an approximate expression\* for the maximum interlaminar normal stress,  $\sigma_{zz}$ , at an interface position  $z$  from the midplane of a symmetric  $[0/90]_S$  type laminate:

---

\* J.M. Whitney, I.M. Daniel, and R.B. Pipes, *Experimental Mechanics of Fiber Reinforced Composite Materials*, Society for Experimental Mechanics, Brookfield Center, CT (1984).

$$\text{Max } \sigma_{zz}(z) = \frac{90\bar{\sigma}_{xx}}{7Ah} \sum_j \left[ A_{22}(\bar{Q}_{12})_j - A_{12}(\bar{Q}_{22})_j \right] t_j(\eta_j - z),$$

where

$\sigma_{xx}$  = applied normal stress in the  $x$  direction

$A = A_{11}A_{22} - A_{12}^2$

$h$  = laminate thickness

$\eta_j$  = distance from the midplane of the laminate to the midplane of the  $j$ th lamina

$t_j$  = thickness of the  $j$ th lamina

and the summation extends over all the laminas above the interface position  $z$ . This equation is valid for thin laminas in which the variation of in-plane stresses is assumed to be negligible over the thickness of each lamina.

Using this approximate expression, compare the maximum inter-laminar normal stresses at the midplanes of [0/90/90/0] and [90/0/0/90] laminates.

